



universität  
wien

## DIPLOMARBEIT

### ANALYSIS OF THE FUNCTION AND TRANSLATIONAL REGULATION OF ILEI, AN ESSENTIAL CYTOKINE IN TUMORPROGRESSION

eingereicht von

**Susanne Sölch**

Zur Erlangung des akademischen Grades  
Magister der Naturwissenschaften  
An der Formal- und Naturwissenschaftlichen Fakultät  
der Universität Wien

Wien, September 2008

Studienkennzahl lt. Studienblatt:

A 419

Studienrichtung lt. Studienblatt:

Diplom Chemie

Betreuer:

Prof. Dr. Hartmut Beug

There is a theory which states that if ever anyone discovers exactly what the Universe is for and why it is here, it will instantly disappear and be replaced by something even more bizarre and inexplicable.

There is another which states that this has already happened.

Douglas Adams

**ACKNOWLEDGEMENTS**

Initially I want to thank **Prof. Dr. Hautmut Beug** for giving me the opportunity to work on such a challenging project in his great lab.

My biggest thank goes to **Agnes Csiszar** who supervised me in an ideal fashion. She always encouraged and supported me and I appreciate very much her patience with me and my experiments without her this diploma thesis would not be what it is today. She was the best boss I could have had and a great friend.

In addition I want to thank **Gabi Litos** for her incredible commitment in keeping the lab running, and lending me a hand every time I needed one. She also always cheered me up when my karma was wrecked and converted work into real fun.

**Evi Wiedemann** I want to thank for her help with the huge amount of cell culture work and accompany me to lunch when nobody else was hungry.

Furthermore I want to thank all the **members of the Beug lab especially Memo** for constructive advice, helpful suggestions and a great working atmosphere.

I would like to thank my **parents** for the financial support they have given me during all my studies.

I also want to thank **all my friends** who helped me with solicitousness, encouragement and their friendship to overcome some difficult moments and to appreciate the good times.

I finally - but very specially - want to thank **Oliver Czeizner**, for his love, encouragement and all the really good times he given me throughout the last years.

**ACRONYMS AND ABBREVIATIONS**

1''	1 seconds
2'	2 minutes
3'-UTR	3 prime untranslated region
5'-UTR	5 prime untranslated region
60S	large ribosomal subunit
80S	translation-competent ribosome
Amp	Ampecillin
bp	Base pair
BPE	Bovine pituitary gland extract
BSA	Bovine Serum Albumine
cDNA	Complementary deoxyribonucleic acid
Cp	Ceruloplasmin
cpm	Counts per minute
DAPI	4',6-Diamidino-2-phenylindol
DEX	Dexamethasone
DMEM-F12	Dulbecco's Modified Eagle Medium F12
DMSO	Dimethylsulfoxid
DNA	Deoxyribonucleic acid
Dox	Doxicycline hyclate
DTT	1,4-Dithiothreitol
ECM	Extracellular matrix
EDTA	ethylenediaminetetraacetic acid
eIF	Eukaryotic initiation factor
EMT	Epithelial to Mesenchymal Transition
EpC40	EpH4 cells transformed with oncogenic Ras bearing in addition the effector loop mutation C40
EpH4	Mouse mammary epithelial cells
EpRas	Oncogenic Ras transformed EpH4 cells
EPRS	Glutamyl-prolyl-tRNA synthase
ER	Endoplasmic reticulum
ERK	Extracellular signal regulated kinase
EST	Expressed sequence tag
FACS	Fluorescence activated cell sorting
FCS	Foetal calf serum
FFL	Firefly Luciferase
GAIT	IFN $\gamma$ activated inhibitor of translation
GAPDH	Glyceraldehyde 3-phosphate dehydrogenase
GCN4	General control protein N4
GFP	Green fluorescing protein
Hepes	2-(4-(2-Hydroxyethyl)- 1-piperazinyl)-ethansulfonacid
IFN $\gamma$	Interferon $\gamma$
IgG	Immunoglobulin G
IHC	Immunohistochemistry
ILEI	Interleukin-like EMT inducer
IP	Isopropterinol
IRES	Internal ribosome entry site
kb	Kilo base
LB	Lysogeny broth



---

MAPK	Mitogen-activated protein kinase
MCS	Multi cloning site
MEK	
MET	Mesenchymal to Epithelial Transition
miRNA	Micro ribonucleic acid
MOPS	3 ( N-Morpholino )-propansulfonacid
mRNA	Messenger ribonucleic Acid
NASAP1	NS1-associated protein-1
NP40	Nonylphenylpolyethylenglykol 40
OD <sub>260</sub>	Optical density at 260nm
ORF	Open reading frame
PABP	Poly-A-binding protein
PAGE	Polyacrylamid-Gelelektrophoresis
PBS	Phosphate Buffered Saline
PBST	Phosphate Buffered Saline with Tween 20
PCR	Polymerase chain reaction
PDK1	Pyruvate dehydrogenase kinase 1
PFA	Paraformaldehyd
PH	Pleckstrinno nolosy
PI3K	Phosphatidyl-Inositol-3-Kinase
PIP2	Phosphatidylinositol biphosphate
PIP3	Phosphatidylinositol (3,4,5)-trisphosphate
PMSF	Phenylmethysulfonylfluorid
poly(A)	Poly adenylation site
Raf	Rapidly growing fibrosarcoma
rcf	Relative centrifugation force
RNA	Ribonucleic acid
rpm	Rounds per minute
RTK	Receptor tyrosin kinase
SD	Standard deviation
SDS	Sodium dodecylsulfate
SEM	Standard error of means
TAE	Tris-acetat-EDTA
TBS	Tris buffered saline
TBST	Tris buffered saline with Tween 20
TE	Tris-EDTA
Tet-On-ILEI	pcDNA4™/TO-ILEI
TetR	pcDNA6/TR®
TGF $\alpha$	Transforming Growth Factor $\alpha$
TGF $\beta$	Transforming Growth Factor $\beta$
TGF $\beta$ RI	Transforming Growth Factor $\beta$ receptor I
TGF $\beta$ RII	Transforming Growth Factor $\beta$ receptor II
TOP	Terminal oligo-pyrimidine
U	Units
uORF	Upstream open reading frame
UV	Ultra violet
w/v	Weight per volume
XT	Ex Tumor cells from EpRas Tumors or TGF $\beta$ treated EpRas cells in collagen gels
ZO	Zona occludens

---

## ZUSAMMENFASSUNG

Das Einwandern in fremde Gewebe ist ein entscheidender Schritt in der Entwicklung eines Tumors. Am Anfang dieser Entwicklung steht, dass die Zellen sich aus dem primären Tumor auswandern, und mit dem Blutstrom in entfernte Organe gelangen, wo sie auswandern und Metastasen bilden. Ein wichtiger Schritt in diesem Prozess ist, dass epitheliale sesshafte Krebszellen sich in fibroblastoide bewegliche Zellen umwandeln. Diese Transformation ist als epithelial zu mesenchymaler transformation - kurz EMT - bekannt. In diesem Zusammenhang spielt TGF $\beta$  eine wichtige Rolle, denn es reguliert die Expression vieler EMT Gene. ILEI wird von TGF $\beta$  auf translationaler Ebene hochreguliert. ILEI ist ein neu gefundenes Cytokin ähnliches Protein das selbstständig in der Lage ist EMT, tumorigenese und Metastasenbildung in epithelialen Zellen einzuleiten. Allerdings ist noch nicht viel über die Funktion von ILEI bekannt.

Der übliche Weg, die Funktion von Genen *in vitro* zu studieren ist es, stabile Zelllinien mit veränderten Levels der Genexpression zu generieren. Allerdings birgt diese Vorgehensweise die Gefahr für clonale Effekte zu selektieren. Außerdem können primäre Effekte oft nicht von nachfolgenden Ereignissen unterschieden werden, da diese durch kompensatorische Mechanismen verdeckt werden. Die Klonierung von induzierbaren Systemen zur Manipulation der Genexpressions Levels kann all diese Probleme vermeiden. Zusätzlich kann man auch die zeitliche Abfolge zellulärer Reaktionen untersuchen nach dem An- oder Abschalten des gewünschten Gens.

Das Ziel meiner Diplomarbeit was es, die Generierung eines induzierbaren tumorbiologischen Werkzeuges, um Genfunktionen *in vitro* zu studieren. Anschließend sollten die Auswirkungen von induzierter ILEI Überexpression in dem bereits sehr bekanntem EpH4 Zellsystem untersucht werden. Ein weiteres Ziel meiner Arbeit ist es, zu untersuchen, wie ILEI translationell von TGF $\beta$  reguliert wird.

Das EpH4 Zellsystem war die Grundlage meiner Untersuchungen. Ich habe einen Tet-ON Klon aus EpH4 (nicht tumorigen), EpRas (mit Ras-V12 transformierte, tumorigene EpH4 Zellen) und EpC40 (mit Ras-V12-C40 Mutante, welche eine weitere Punktmutation an dem effector loop C40 trägt, transformierte EpH4 Zellen), hergestellt. Dadurch hat man eine Serie von Zelllinien die nicht tumorigene (EpH4), die tumorigen aber nicht metastatisierend (EpC40) und die metastatisierend (EpRas) Zellen, in denen es uns gelang, Tet-induzierbares ILEI zu exprimieren.

---

**ABSTRACT**

Invasion and metastasis are crucial steps in tumor progression in which tumor cells disengage from their primary tumor site, enter the bloodstream and migrate from there into distant organs to form secondary tumors. An essential step in this process is that epithelial, sessile cancer cells transform into fibroblastic, more mobile mesenchymal cells, termed epithelial to mesenchymal transition (EMT). In this context, TGF $\beta$  plays an important role. By regulating the expression of many genes involved in EMT. It up regulates ILEI (Interleukin-like EMT Inducer) acting exclusively at the level of translational control. ILEI is a novel cytokine-like protein that is sufficient to induce EMT, tumorigenesis and metastasis formation in epithelial cells. However, not much is known about its function.

The common way to study gene function *in vitro* is to generate stable cell lines with altered levels of gene expression. However, these systems have the risk to select for clonal effects and primary effects, while primary effects of the introduced genes can not be distinguished from downstream events or might be masked by compensatory mechanisms.

Choosing inducible systems for the manipulation of gene expression levels can avoid all this problems. In addition, this approach makes it possible to investigate the kinetics of cellular responses after the induction of gene over-expression or knock down.

Although there are some inducible tumor cell lines available to study EMT, a comprehensive, inducible model system which would allow studying several aspects of tumor formation and progression.

The aim of this diploma thesis is to generate a general tool for tumor biology to study gene function *in vitro* in an inducible manner. Subsequently, the ramifications of inducible ILEI in the established EpH4 system is to study. A second aim of this thesis is to dissect how ILEI is translationally regulated by TGF $\beta$ .

The EpH4 cell system, was the choice of our studies. I generated Tet-ON inducible EpH4 (mouse mammary epithelial cells), EpRas (oncogenic Ras transformed EpH4 cells) and EpC40 (Eph4 cells transformed with oncogenic Ras bearing in addition the effector loop mutation C40) cell lines. Through this, there is a series of cell lines representing non-tumorigenic (Eph4), tumorigenic but non-metastatic (EpC40) and metastatic (EpRas) stages. We obtained cell lines from all three cell types, in which ILEI could be induced by Dox and started to analyse their phenotype.

## TABLE OF CONTENTS

<b>ACKNOWLEDGEMENTS</b> .....	<b>3</b>
<b>ACRONYMES AND ABBREVIATIONS</b> .....	<b>4</b>
<b>ZUSAMMENFASSUNG</b> .....	<b>6</b>
<b>ABSTRACT</b> .....	<b>7</b>
<b>1 INTRODUCTION</b> .....	<b>11</b>
<b>1.1 Cancer as a multistep process</b> .....	<b>11</b>
1.1.1 EMT (Epithelial to Mesenchymal Transition) .....	13
1.1.2 TGF $\beta$ effects on cancer progression .....	15
1.1.3 TGF $\beta$ signalling pathways .....	16
1.1.4 Ras effector pathways.....	17
1.1.5 Cooperative interaction of Ras and TGF $\beta$ via the ERK/MAPK and PI3K pathways .....	19
1.1.6 The EMT model system .....	20
1.1.7 Screen for EMT specific genes .....	22
1.1.8 ILEI .....	23
1.1.9 Principle and strategy of the T-REx™ inducible system .....	24
<b>1.2 Translational regulation of gene expression</b> .....	<b>25</b>
1.2.1 Regulatory elements of the 5' -UTR .....	25
1.2.1.1 Cap dependent translation initiation:.....	25
1.2.1.2 Cap independent translation initiation: .....	26
1.2.1.3 Upstream open reading frames (uORFs):.....	27
1.2.1.4 Terminal oligo-pyrimidine tract (TOP) as translational regulator: .....	28
1.2.2 Regulatory elements of the 3' -UTR .....	29
1.2.2.1 Micro RNAs as translational regulator:.....	29
1.2.2.2 Poly(A) tail as translational regulator: .....	30
1.2.2.3 GAIT as translational regulator:.....	30
<b>1.3 The ILEI mRNA</b> .....	<b>32</b>
<b>1.3 Aim of this work</b> .....	<b>33</b>
<b>2 MATERIALS AND METHODS</b> .....	<b>34</b>
<b>2.1 DNA techniques</b> .....	<b>34</b>
2.1.1 Design of oligonucleotides .....	34
2.1.2 PCR (Polymerase Chain Reaction).....	34
2.1.3 Determination of the concentration of nucleic acids .....	35
2.1.4 Recovery of DNA from agarose gels.....	35
2.1.5 Purification of DNA from a PCR reaction .....	35
2.1.6 Restriction digestion of DNA.....	35
2.1.7 Ligation of DNA .....	35
2.1.8 Heat-Shock transformation of DNA into competent bacteria.....	36
2.1.9 Transformation of DNA into competent bacteria by electroporation .....	36
2.1.10 Small scale plasmid preparation (Mini-Prep) .....	36
2.1.11 Large scale plasmid preparation (Maxi-Prep) .....	36
2.1.12 Bac clone DNA isolation .....	36

<b>2.2 Cloning strategies</b>	<b>38</b>
2.2.1 The inducible Tet-On system	38
2.2.2 The UTR constructs	38
<b>2.3 RNA techniques</b>	<b>40</b>
2.3.1 Isolation of RNA	40
2.3.1.1 TRIZOL Reagent Invitrogen	40
2.3.1.2 Quiagen RNeasy® Mini Kit	40
2.3.2 RNA clean up	40
2.3.3 RNA nano chip	41
2.3.4 Isolation of polysome bound RNA on Sucrose-Gradient	41
2.3.5 Northern blot	42
2.3.6 Northern blot probe labelling	42
2.3.7 Reverse transcription of RNA into cDNA	43
<b>2.4 Protein chemistry</b>	<b>44</b>
2.4.1 Determination of protein concentration (Bradford assay)	44
2.4.2 Cell lysis for SDS-PAGE	44
2.4.3 Supernatant preparation for SDS-PAGE	44
2.4.4 SDS-PAGE	44
2.4.5 Western blot analysis (semi dry)	44
<b>2.5 Cell culture</b>	<b>45</b>
2.5.1 Cultivation of adherent mammalian cells	45
2.5.2 Freezing of adherent cells	45
2.5.3 Thawing of adherent cells	45
2.5.4 Liposome based transfection of adherent mammalian cells	45
2.5.5 Subcloning of cell lines via single cell sort	45
2.5.6 Establishing stable transfected cell lines	46
2.5.7 Dox induction (Tet-ON system)	46
2.5.8 TGFβ induction	46
2.5.9 Renilla FFL reporter assays	46
2.5.10 <i>In vitro</i> cell assays in collagen gels	46
2.5.11 <i>In vitro</i> cell assays on filters	47
2.5.12 Proliferation curve	47
<b>2.6 Mouse work</b>	<b>48</b>
2.6.1 Mammary gland fat pad injection of tumor cells	48
2.6.2 Tail vein injection of tumor cells	48
<b>2.7 Histology</b>	<b>49</b>
2.7.1 Preparation of frozen tissue samples	49
2.7.2 Preparation of PFA-fixed and paraffin embedded tissue sections	49
<b>2.8 Immunocyto- and Immunohistochemistry</b>	<b>50</b>
2.8.1 Staining of Collagen gels	50
2.8.2 Staining of PFA-fixed paraffin-embedded tissue sections	50
2.8.2.1 Hematoxylin and Eosin staining	50
2.8.2.2 Cleaved caspase 3 staining	50
2.8.2.3 Ki67 staining	50
2.8.2.4 ILEI staining	51
<b>2.9 Microscopy</b>	<b>52</b>
2.9.1 Light and fluorescence microscopy	52

---

2.9.2 Confocal microscopy .....	52
<b>3 RESULTS .....</b>	<b>53</b>
3.1 Generating the TetR clones .....	53
3.1.1 <i>In vitro</i> characterisation of the TetR-clones .....	55
3.1.2 <i>In vivo</i> characterisation .....	60
3.2 Tet-On-ILEI overexpressing clones .....	62
3.2.1 <i>In vitro</i> characterisation of the Tet-On clones .....	62
3.2.1.1 Western blot analysis for inducibility .....	62
3.2.1.2 Proliferation curves .....	64
3.2.1.3 Morphology of the Tet-On clones .....	67
3.2.2 <i>In vivo</i> characterisation of the EpRas-Tet-On-ILEI and EpC40-Tet-On-ILEI clones .....	69
3.2.3 Histological analysis of exgrafted tumors .....	73
3.3 Translational control of ILEI .....	76
3.3.1 Regulatory motives in the 5'-UTR of ILEI .....	76
3.3.2 Regulatory motives in the 3'-UTR of ILEI .....	78
3.3.3 Characterisation of the translation rate of the two ILEI 3'-UTR isoforms ...	79
3.3.4 Evaluation of the importance of different UTR regions .....	82
<b>4 DISCUSSION .....</b>	<b>84</b>
4.1 TetR clones .....	85
4.2 ILEI inducible clones .....	87
4.3 Translational control of ILEI .....	89
<b>APPENDIX .....</b>	<b>91</b>
<b>REFERENCES .....</b>	<b>93</b>
<b>CURRICULUM VITAE .....</b>	<b>96</b>

# 1 INTRODUCTION

## 1.1 Cancer as a multistep process

Tumor progression associated with metastasis formation accounts for 90% of cancer deaths, and represents one of the prime causes of human mortality (Sporn MB, 1969). In general, cancer arises from a stepwise accumulation of genetic changes and progressive alterations in gene expression. Extensive cancer research has generated a rich and complex body of knowledge, revealing cancer to be a disease involving dynamic changes in the genome. This has been achieved by the discovery of mutations that produce oncogenes with dominant gain of function and tumor suppressor genes with recessive loss of function; both classes of cancer genes have been identified through their alteration in human and animal cancer cells.

Several lines of evidence indicate that tumorigenesis in humans is a multistep process and that these steps reflect successive genetic alterations that drive the progressive transformation of normal human cells into highly malignant derivatives. It has been proposed that most and perhaps all types of human tumors share six altered capabilities of tumor cells (FIGURE 1). These are: self-sufficiency in growth signals, insensitivity to growth-inhibitory signals, evasion of apoptosis, unlimited replicative potential, constitutive angiogenesis, and tissue invasion and metastasis.

(i) tumor cells show a greatly reduced dependence on exogenous growth factors, through generation of autocrine growth signals and constitutively active, mutated receptors, thereby becoming independent of their microenvironment.

(ii) antigrwth signals can block proliferation by two mechanisms. Cells can be forced out of the active proliferative cycle into quiescence ( $G_0$ ) or cells can be introduced to permanently relinquish their proliferative potential by being induced to enter into postmitotic states. Incipient cancer cells must evade this signals if they are to prosper.

(iii) the ability of tumor cells to expand is not only determent by the rate of cell proliferation but also by evading programmed cell death, a program that is latently present in all types of cells. Most cancer cells, perhaps all, are resistant to apoptotic signals.

(iv) the uncoupling of a cell's growth program from its environment, alone does not ensure limitless growth. The limited multiplication capacity of many, perhaps all cell types, an intrinsic cell-autonomous program relying on telomere shortening during consecutive divisions must be also disrupted, e.g. by constitutive expression of telomerase.

(v) proliferating cells per se have no intrinsic ability to attract blood vessels and stimulating their growth. In order to progress to larger tumor sizes cancer cells must develop angiogenic abilities.

(vi) at some point during development of most types of human cancer, primary tumors spawn pioneer cells that move out and travel to distant sites were they may found new colonies. This distant settlements are the cause for most cancer deaths in humans. Successful invasion and metastasis depends upon all five other acquired hallmarks described earlier. Invasion and metastasis formation utilize similar operational strategies, involving changes in the physical coupling of cells to their microenvironment, activation of extracellular proteases as well as changes in integrin expression and increase of epithelial carcinoma cells, loss of epithelial polarity.

Each of these physiological changes is a novel capability acquired during tumor development and represents the successful breaching of multiple anticancer defence mechanism (Hanahan D, 2000; Hahn WC, 2002).

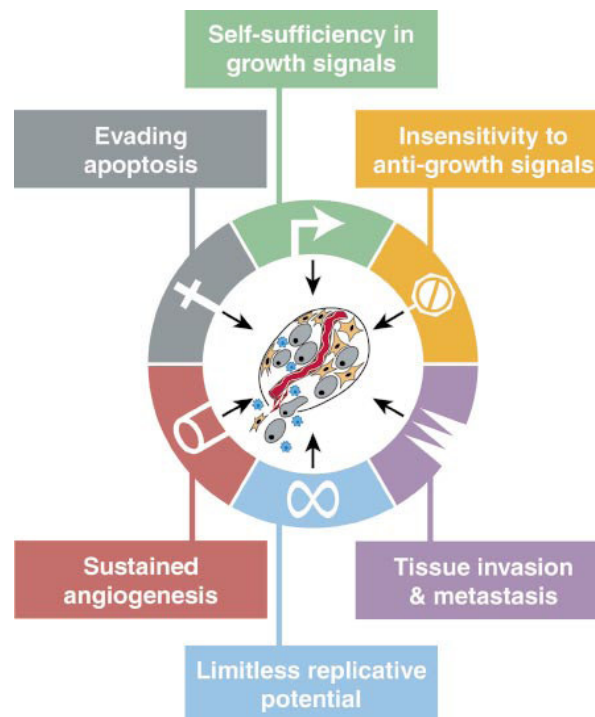


**FIGURE 1 |** **Acquired Capabilities of Cancer** (Hanahan D, 2000)  
Most of the cancers develop a similar set of functional capabilities during their development but through various mechanisms.



### 1.1.1 EMT (Epithelial to Mesenchymal Transition)

Epithelial cells adhere to each other by specialized membrane structures in form of a tight monolayer and are strongly connected to the extracellular matrix (ECM). The core elements of the cell-cell interactions are tight junctions built up by claudin and occludin, adherens junctions formed by cadherins and gap junctions made from connexins. The main way that cells both bind to and respond to the ECM are integrins. They are part of a large family of cell adhesion receptors which are involved in cell-extracellular matrix and cell-cell interactions. Integrins are composed of long extracellular domains which adhere to their ligands, and short cytoplasmic domains that link the receptors to the cytoskeleton of the cell. The organization of the junctions as a lateral belt with localized distribution of adhesion molecules and the polarized organization of the actin cytoskeleton apical of the ECM defines the polarity of the epithelium. Based on these defined parameters, epithelial cells can only move in their plane (Berx G, 2007; Hugo H, 2007).

Mesenchymal cells, as an opposite, form irregular structures with focal adhesions that are less strong than their counterparts with tight junctions. The mesenchyme has no apical-basolateral polarisation, but some polar organisation of their leading and tailing and during motility generated by a dynamic polarisation of the actin cytoskeleton along the axis of migration. Thus, these cells can move in all three dimensions by reorganising the actin cytoskeleton according the changes in the direction of migration. EMT describes the process in which epithelial cells lose their sessile phenotype and gain migrant features (FIGURE 2).

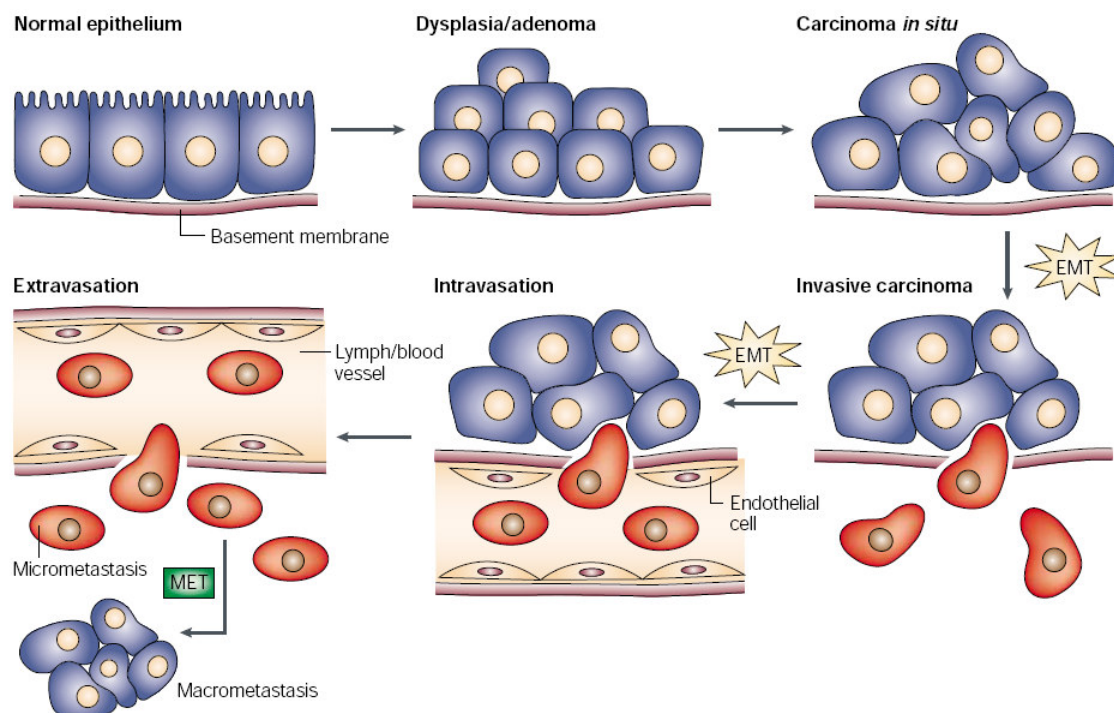


FIGURE 2 | EMT, an essential process in tumor formation. (Thiery JP, 2002)

Epithelial carcinoma cells undergo EMT to escape the mass and to intravasate lymph or blood vessels. After intravasation, the cancer cells must survive the shear forces of the circulation allowing their passive transport to distant organs. To create a new malignancy the cells undergo MET, after extravasating from the blood stream.

EMT is associated with early embryogenesis in mammals when mesoderm and endoderm are formed (Thiery JP, 2006). Later in development EMT is responsible for organ and tissue formation. It plays an important role in the regeneration process during wound healing. In a pathological context EMT is the reason for fibrosis and metastasis formation.

Epithelial versus mesenchymal cells - beside their prominent structural morphological differences - have big differences in their gene expression profile as well. Some of the differently expressed genes can be used as good biomarkers to distinguish these two cell fates. One example, a typical marker for epithelial cells is E-cadherin. It is localized, as a transmembrane protein that is responsible for cell-cell contact in a  $\text{Ca}^{2+}$  dependent manner, to adherent junctions at the basal membrane and mediates cell-cell adhesions. E-cadherin is not (or only weakly) expressed in mesenchymal cells.

Another marker for epithelial cells is ZO-1. ZO-1 is a protein which is only present on the cytoplasmic side of tight junctions, where it interacts with claudin, occludin as well as with the actin cytoskeleton provides a linkage between the actin cytoskeleton and the tight junction.

Vimentin, a typical marker for mesenchymal cells, forms intermediate filaments and offers the cell with its dynamic nature flexibility. Vimentin plays a significant role in positioning and anchoring the organelles in the cytosol. Therefore, vimentin is the cytoskeletal component responsible for maintaining cell integrity under mechanical stress *in vivo*.

The destruction of strong cell-cell contacts of epithelial cells has devastating consequences for the whole tissue. The loss of E-cadherin, is one very important step towards EMT. E-cadherin is a strong tumor suppressor and E-cadherin reintroduction is sufficient to partially or even completely revert EMT in certain cell types (Christofori G, 1999; Arias AM, 2001).

EMT requires alterations in morphology, cellular architecture, adhesion and migration capacity. This complexity of changes might explain why EMT is controlled by at least six pathways (Wnt, TGF $\beta$ , Hedgehog, Notch, RTK and NF- $\kappa$ B (Huber MA, 2004)). In the situation of cancer these pathways and their cross talk are often deregulated and so become able to drive cells into EMT (Grünert S, 2003; Gotzmann J, 2004; Huber MA, 2005; Berx G, 2007; Lee JM, 2007).

### 1.1.2 TGF $\beta$ effects on cancer progression

Transforming growth factor  $\beta$  (TGF $\beta$ ) is an important pathway in tumor progression which can have both tumor suppressive and pro-oncogenic effects on tumorigenesis (FIGURE 3). It acts in early stages of cancer development as a tumor suppressor, but later on as a stimulant for invasion and tumor progression. The pro oncogenic effects of TGF $\beta$  are so significant because many human tumors overexpress TGF $\beta$ . In breast cancer for example, high levels of TGF $\beta$  correlate with the rate of disease progression (Gorsch SM, 1992; Akhurst RJ, 1999; Fujimoto K, 2001). The TGF $\beta$  protein has been shown to induce apoptosis in several normal cell types. The initial events that follow receptor activation and result in growth inhibition and cell death are not fully understood yet (Derynck R, 2001). The cancer cells must find a way around the growth inhibition and cell death. One way is to decapitate the pathway with receptor-inactivating mutations and therefore silence autocrine TGF $\beta$  signalling. The other way is to selectively amputate the tumor-suppressive arm of the pathway either by mutations within the cascade or by inhibition caused by other altered or mutated pathways. This second mode allows cancer cells to extract additional benefits by embracing the TGF $\beta$  response for pro-tumorigenic purpose, enabling autocrine action of TGF $\beta$  to enhance EMT and metastasis. In both cases, cancer cells can use TGF $\beta$  to modulate the microenvironment to avert immune surveillance or to induce the production of protumorigenic cytokines. In the EpH4 model, (see chapter 1.6) TGF $\beta$  acts in autocrine fashion (Zhao J, 1995; de Caestecker MP, 2000; Elenbaas B, 2001; Joan Massagué, 2008). Of the three TGF $\beta$ s, TGF $\beta$ 1 is most frequently upregulated in tumor cells and is the focus of most studies on the role of TGF $\beta$  in tumorigenesis (Derynck R, 2001). It also has been suggested that TGF $\beta$ 1 elicits an epithelial to mesenchymal transition *in vivo* and that TGF $\beta$ 3 might be involved in maintenance of the spindle cell phenotype. The action of TGF $\beta$ 1 in enhancing malignant progression may mimic its proposed function in modulating epithelial cell plasticity during embryonic development (Cui, 1996).

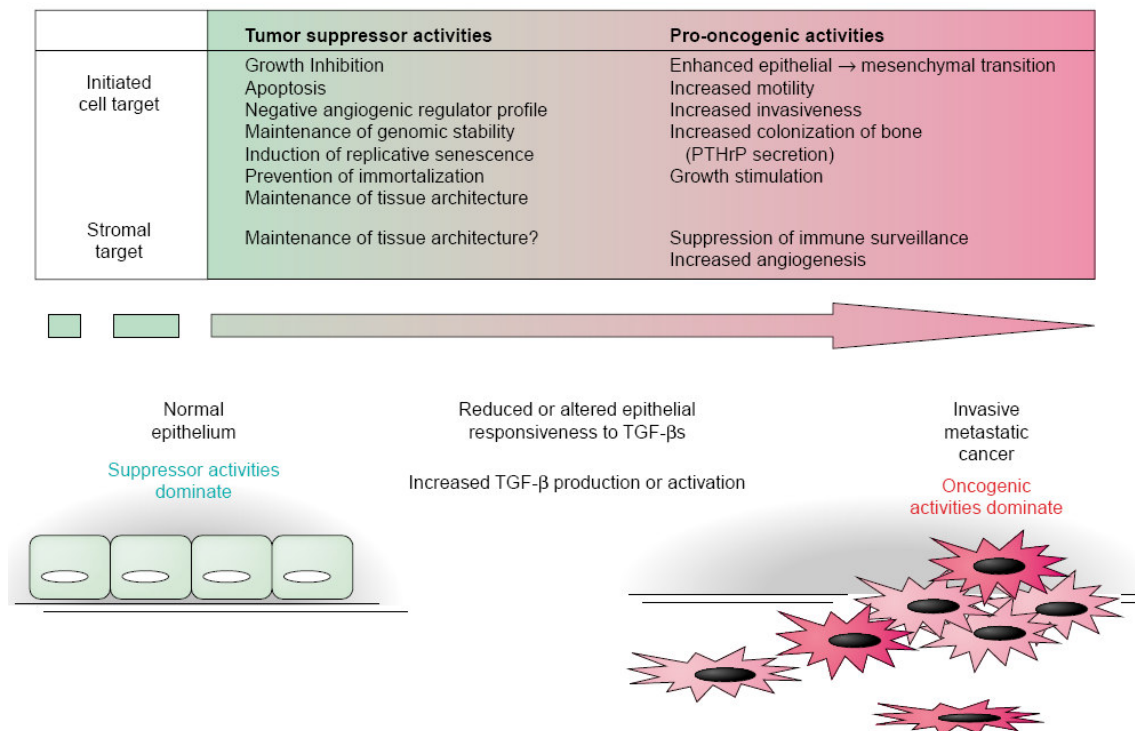


FIGURE 3 | Alternative roles of TGF $\beta$  signalling in tumor suppression and cancer progression (Wakefield LM, 2001)

### 1.1.3 TGF $\beta$ signalling pathways

There are three different TGF $\beta$  isoforms, TGF $\beta$ 1, TGF $\beta$ 2 and TGF $\beta$ 3, which are encoded by different genes and which all function through the similar receptor signalling systems. TGF $\beta$  is secreted in a latent form, which must be activated for binding to the signalling receptors (Wakefield LM, 2001). The signalling mechanism of TGF $\beta$  precursor through the ligand induced activation of a heteromeric cell-surface complex of two types of transmembrane serine/threonine kinase receptors, named TGF $\beta$  Receptor I (TGF $\beta$ RI) and TGF $\beta$  Receptor II (TGF $\beta$ RII). TGF $\beta$ RI has been shown to transduce most known signals induced by TGF $\beta$ . TGF $\beta$ RI binds and phosphorylates the transcription factor. Smad2 or, alternatively, its close homolog Smad3. In their phosphorylated form Smad2 and Smad3 associate with Smad4, enter the nucleus and modulate transcription of TGF $\beta$  responsive genes (Massague J, 2000; Derynck R, 2001). Besides the Smad pathway there are several Smad independent ways how TGF $\beta$  can activate gene expression (FIGURE 4).

Please note that "TGF $\beta$ " refers to TGF $\beta$ 1 in my thesis.

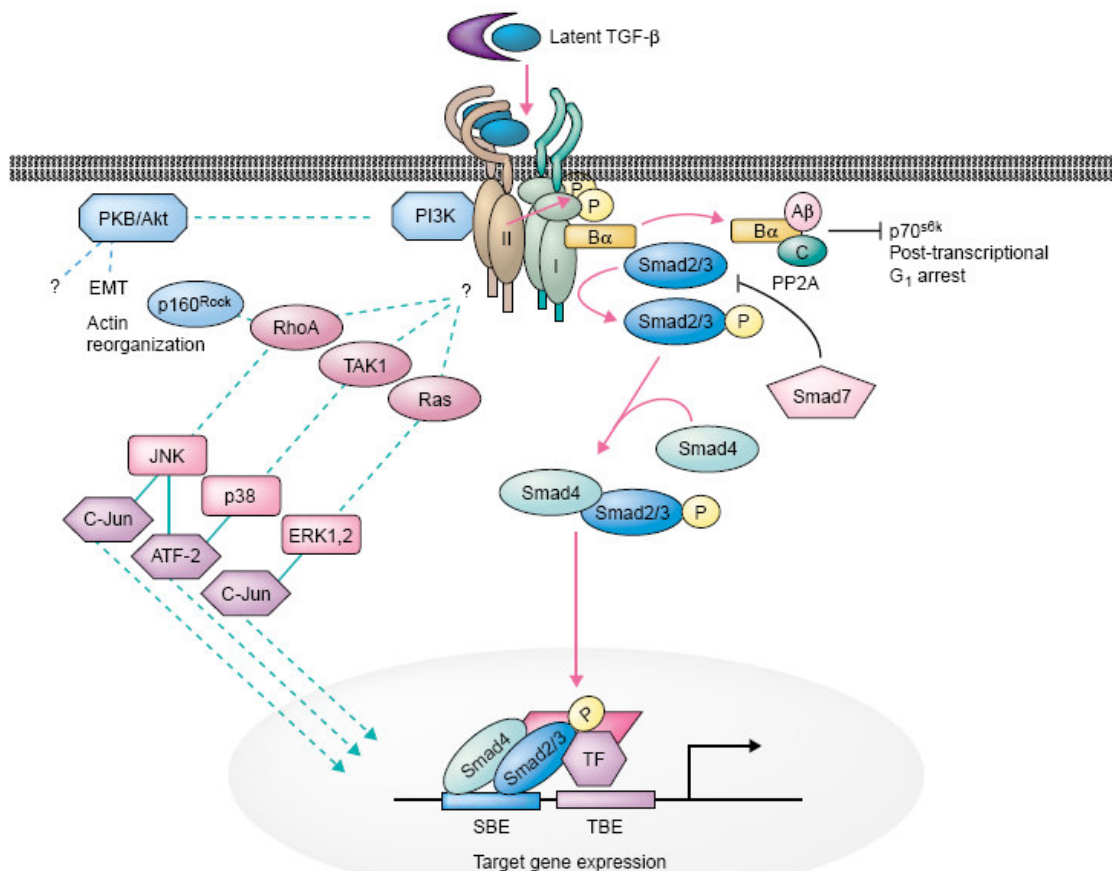
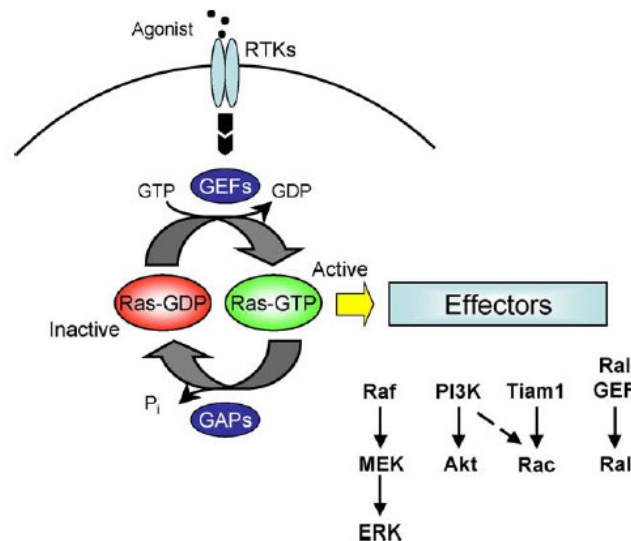


FIGURE 4 | Various TGF $\beta$  signalling pathways. (Wakefield LM, 2001)

#### 1.1.4 Ras effector pathways

Ras proteins regulate cell fates by coupling receptor activation to more than 20 downstream effector pathways that control diverse cellular responses including proliferation, differentiation and survival (Repasky GA, 2004; Rajalingam K, 2006; Karnoub AE, 2008). Ras proteins are small GTPases that cycle between inactive, guanosine diphosphate (GDP)-bound and active, guanosine triphosphate (GTP)-bound conformations (FIGURE 5) (Schubbert S, 2007). In the active form Ras binds to the many downstream effectors and stimulates their signalling pathways.



**FIGURE 5 | Upstream and downstream of Ras signalling.** (Campbell PM, 2004)  
Stimuli from outside of the cell activate e.g. through TGF $\beta$  and other adaptor proteins guanine nucleotide exchange factors (GEF). GEF replaces Ras bound GDP with GTP and renders Ras therefore active. GTPase activating protein (GAP) triggers the hydrolysis of GTP back to GDP and so into an inactive form. The active GTP-bound Ras binds to the many downstream effectors and stimulates their signalling pathways.

The PI3K cascade:

PI3K is a heterodimer comprised of the p85 regulatory and p110 catalytic subunits (Cantley LC, 2002). Ras can recruit and activate PI3K direct by binding to the p110 unit. At the membrane, PI3K phosphorylates phosphatidylinositol-4,5-bisphosphate (PIP<sub>2</sub>) and converts PIP<sub>2</sub> into PIP<sub>3</sub>. Then PIP<sub>3</sub> recruits other downstream molecules—particularly the serine-threonine kinases Akt and PDK1—via binding to their pleckstrin homology (PH) domains. Akt is activated through phosphorylation by PDK1 at the membrane. Akt in turn regulates a wide range of target proteins that control cell proliferation, survival, growth, and other processes (Lawlor MA, 2003).

The Ras/MEK/ERK cascade:

Activated Ras proteins interact directly with the Raf family kinases (comprised of A-Raf, B-Raf and C-Raf). This interaction is the first step required for Raf activation. Strikingly, converting the Raf kinases from inactive into active enzymes is a highly complex process, involving membrane localization, cycles of phosphorylation/dephosphorylation and protein interactions. Once activated, all Raf family members are capable of initiating the phosphorylation cascade, whereby Raf activates MEK by phosphorylation, and MEK activates ERK again by phosphorylation. When ERK activation is achieved it phosphorylates critical targets in the cytoplasm and nucleus required to carry out the cellular response (McKay MM, 2007).

Replacing glycine 12 of Ras with any other amino acid except proline it biochemically activates Ras by rendering it into a constitutive GTP bound state. This constitutive active Ras-V12 mutant activates all the Ras effector pathways simultaneously. Additional point mutations in the core effector domain of Ras (residues 32 to 40) can selectively activate specific pathways. For example, the T35S mutation causes loss of PI3K and Ral effector binding, but maintains the capability of Raf activation. In contrast, the E37G mutation causes the loss of Raf and PI3K, but not of Ral activation. Finally, the Y40C substitution does not impair PI3K activation, but causes the loss of Raf and Ral activation (FIGURE 6) (Campbell PM, 2004). Thus, the combination of the V12 mutation with one of the effector loop mutations in the Ras protein enables the selective study of the necessity of effects of different Ras effector pathways.

There are several known Ras effector pathways: Tiam1, PI3K, ERK/MAPK, Ral/GEF, PLC $\epsilon$ , RASSF1 and others. The ERK/MAPK and PI3K pathway were extensively studied in the Eph4 system and were the most relevant for my studies. Therefore, these will be the ones I introduce in more detail.

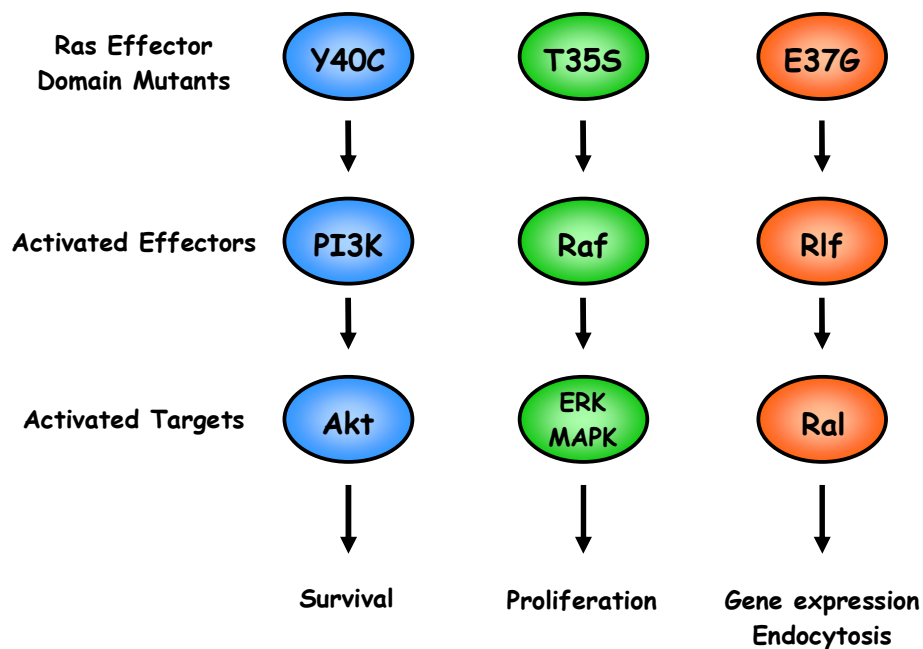


FIGURE 6 | Ras effector mutations. (Campbell PM, 2004)



### 1.1.5 Cooperative interaction of Ras and TGF $\beta$ via the ERK/MAPK and PI3K pathways

TGF $\beta$  can activate MAPK pathways directly, and interact with the pathway when it is activated via other routes. There is data that suggest an activation of MAPK pathways plays an important role in diverting the TGF $\beta$  response towards a pro-oncogenic outcome. TGF $\beta$  and activated Ras cooperate to promote invasive, metastatic behaviour and induction of EMT in epithelial cells. This behaviour is dependent on the presence both of activated Ras and of a functional TGF $\beta$  autocrine loop that is enhanced by Ras (Chen RH, 1993; Oft M, 1996; Wakefield LM, 2001).

The importance of the PI3K pathway for tumor cell hyperproliferation is also evident *in vivo*. EpC40 cells caused rapidly growing tumors, while ERK/MAPK-activating EpRas-V12-S35 (EpS35) cells caused only slow tumor growth. Nevertheless, EpS35, but not EpC40 tumor cells underwent TGF $\beta$  induced EMT *in vivo*, showed an EMT phenotype after recultivation of tumor cells and induced lung metastases upon tail vein injection. These results indicate that tumor cell dedifferentiation during EMT and tumor cell hyperproliferation are separable events, caused by different signal transduction pathways (Jechlinger M, 2002). A hyperactive Raf/MAPK pathway is required for TGF $\beta$  induced EMT, tumorigenesis, and metastasis formation. In contrast, activation of the PI3K pathway is required for protection from TGF $\beta$  induced apoptosis, allowing scattering but not EMT and causing tumors but not metastasis. Thus, EMT and metastasis are closely linked processes, both relying on the synergism between constitutive hyperactivation of the Raf/MAPK signalling module and TGF $\beta$  -R signalling (Janda E, 2002b).

1.1.6 The EMT model system

In this diploma thesis all the work has been done in the EpH4 model system (FIGURE 7).

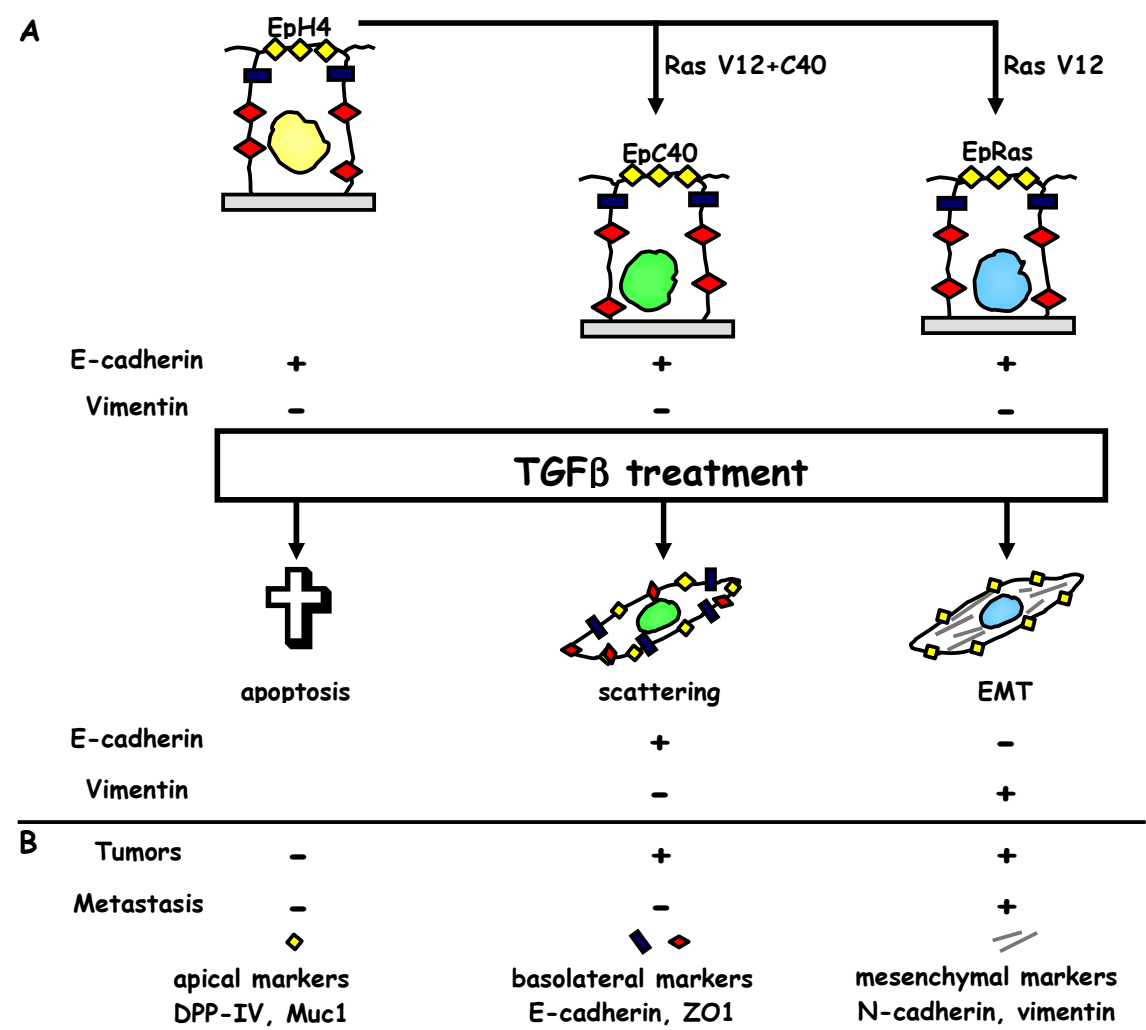


FIGURE 7 | The model cell system A) *in vitro* and B) *in vivo*.

The EpH4 cells are well-polarized, nontumorigenic mammary epithelial cells and they are used to establish a model system of EMT *in vitro* and *in vivo* (Janda E, 2002b; Janda E, 2002a). In type I collagen gels, they form organotypic tubular structures requiring minute amounts of TGFβ whereas higher TGFβ concentrations induce cell cycle arrest and apoptosis (Oft M, 1996). EpH4 cells were derived from primary mammary gland tissue of mid-pregnant BALB/c mice by spontaneous immortalization (Reichmann E, 1989; Reichmann E, 1992; Fialka I, 1996).

EpRas are derivatives of EpH4 cells. They were generated by the transformation of EpH4 cells with oncogenic Ha-Ras-V12 (FIGURE 7). They form rapidly growing tumors in mice and undergo EMT in response to TGFβ both in tumors and in collagen gels. Thus, Ha-Ras oncoprotein cooperates with endogenous TGFβ to cause EMT of mammary epithelial cells, both *in vitro* and upon tumor formation in mice. Along with the morphological changes of EpRas cells during EMT changes in marker expression occur as well. E-cadherin is down regulated and vimentin is up regulated. When cultured in type I collagen matrices in the complete absence of TGFβ, both nontumorigenic EpH4 cells and their counterparts EpRas develop into lumenforming, organotypic structures consisting of monolayers of polarized epithelial cells. In the presence of TGFβ,



however, EpRas cells form lumenless cords and cell strands that consist of cells exhibiting fibroblastoid properties. This is in contrast to EpH4 cells, which upon TGF $\beta$  treatment stop proliferating and undergo apoptosis. The converted, the fibroblastoid cells themselves produce high levels of TGF $\beta$ , but they revert to an epithelial phenotype in sparse cultures upon exposure to neutralizing TGF $\beta$  antibodies or TGF $\beta$ R inhibitors, indicating that an autocrine TGF $\beta$  loop is required for the maintenance of the mesenchymal phenotype (Oft M, 1996).

Exgrafted EpRas cells can be recultivated and are called from then on EpRasXT (ex tumor) cells. These EpRasXT cells are characterized by a spindle-like morphology, loss of epithelial and gain of mesenchymal marker proteins, a phenotype stabilized by an autocrine TGF $\beta$  loop *in vitro* and *in vivo* (Oft M, 1996).

The third cell line is called EpC40 (FIGURE 7). They represent EpH4 cells transformed by mutated oncogenic Ha-Ras-V12-C40, which only signals along the PI3K pathway. They form strictly nonmetastatic tumors in mice and undergo scattering upon TGF $\beta$  treatment, a phenotype resembling partial EMT: E-cadherin still expressed at the plasma membrane, vimentin not induced.

### 1.1.7 Screen for EMT specific genes

A screen to identify molecular players involved in EMT and metastasis formation has been performed in the laboratory of Hartmut Beug. For the Expression profiling a set of *in vitro* and *in vivo* model cell systems has been chosen. The basis of this screen were fully polarised mammary epithelial cells (EpH4) and eight closely related cell pairs (FIGURE 8). This pairs were modified by defined oncogenes (e.g. Ras) and/or external factors (e.g. TGF $\beta$ ) so that specific aspects of migration, local invasion and metastasis formation could be studied. Since mRNA levels do not necessarily reflect protein levels in cells, an improved expression profiling method based on polysome-bound RNA has been used (Mikulits W, 2000). This setup was suitable to analyse global gene expression on Affymetrix chips. A substantial fraction of all regulated genes was found to be exclusively controlled at the translational level. Furthermore, profiling of the above multiple cell pairs allowed one to identify small numbers of genes by cluster analysis, specifically correlating gene expression with EMT, metastasis, scattering and/or oncogene function. For complete EMT and metastasis >30 genes have been found. A small set of genes specifically regulated during EMT was identified, including key regulators and signalling pathways involved in cell proliferation, epithelial polarity, survival and transdifferentiation to mesenchymal-like cells with invasive behaviour (Jechlinger M, 2003). In this screen, a novel gene was found, belonging to a small gene family (FAM3A-D) with no sequence homology to any known genes. It was translationally controlled in cells undergoing EMT and methastasis formation. It was named ILEI , Interleucin Like EMT Inducer.

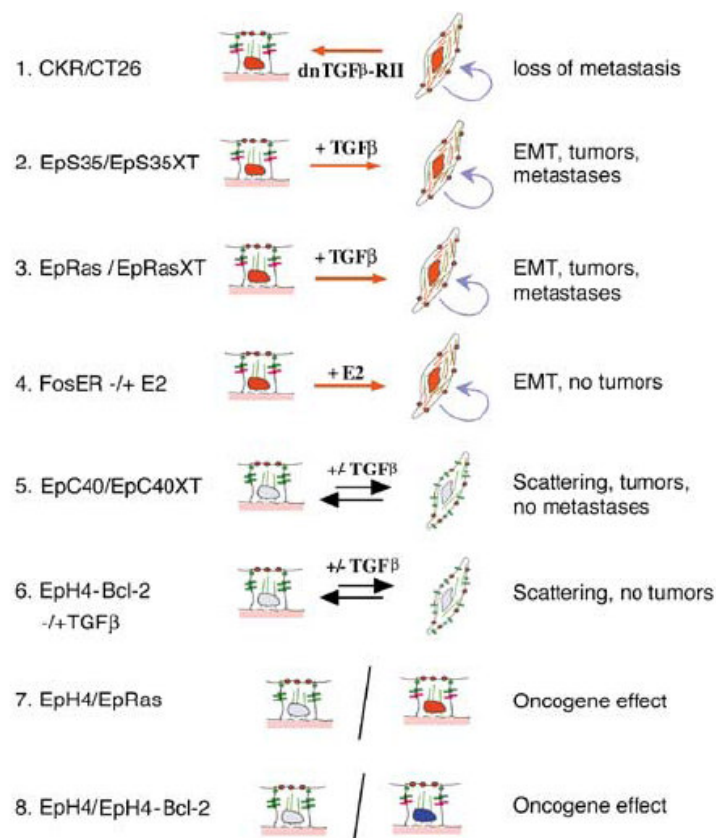


FIGURE 8 | Cell pairs in the expression profiling screen. (Jechlinger M, 2003)

The cell pairs employed in this screen are depicted schematically. Apical markers: red dots, basolateral markers: green/pink square, mesenchymal markers: red fibrils, the pictograms show also the *in vitro* observed phenotypical changes in this cells. Tumorigenic and metastatic potential was tested by injection in nude mice.

### 1.1.8 ILEI

ILEI is part of a novel gene family, FAM3 (Family with sequence similarity 3). There are four genes in this family, *FAM3A*, *FAM3B*, *FAM3C*, and *FAM3D*, each encoding a protein of 224-235 amino acids. The family was identified by a genome-wide screen for the identification of novel genes encoding proteins with a four-helix-bundle cytokine fold. Northern analysis indicates that *FAM3B* is highly expressed in pancreas, *FAM3D* in placenta, and *FAM3A* and *FAM3C* in almost all tissues (Zhu Y, 2002), for example in the developing inner ear of the mouse (Pilipenko VV, 2004). ILEI is equivalent with *FAM3C*. The four  $\alpha$ -helices within *FAM3C*, however, do not structurally resemble the 4 helix bundle of interleukins.

Ectopic expression of ILEI is able to induce complete EMT as determined by the loss of the epithelial marker E-cadherin and the gain of vimentin expression (TABLE 1). The induction of EMT by ILEI is independent of TGF $\beta$  but depends on Ras signalling. If Ras signalling is totally abolished through a specific inhibitor, EMT is blocked, despite of ILEI overexpression. It is possible to mimic ILEI effects with recombinant ILEI. Consistent with this findings, EMT is fully reversed upon ILEI depletion using an anti-ILEI antibody. The way, how ILEI exactly works is unknown but it is sufficient to induce EMT. ILEI does not need TGF $\beta$  signalling for EMT. ILEI induced EMT can not be reversed by TGF $\beta$ -receptor blockage, unlike TGF $\beta$  induced EMT (Waerner T, 2006).

In normal tissues, ILEI localisation shows a granular patterning which might represent storage vesicles. In biopsies of cancer patients show that ILEI there is expressed in varying levels with a cytoplasmic localisation. The switch between granular and cytoplasmic ILEI localisation correlates with the disease free and overall survival of the patients, suggesting that ILEI might serve as a new diagnostic marker.

Cell Line	Ras Activity	ILEI Expression	EMT <sup>§</sup>	Tumorigenesis	Metastasis
EpH4	low	low	-	-	-
	low	over-expressed	+	+	+
	inhibited by L739749 <sup>%</sup>	over-expressed	-	-	-
EpC40 + TGF $\beta$	constitutive active <sup>&amp;</sup>	low	-	+	-
	constitutive active <sup>&amp;</sup>	low	scattering	+	-
	constitutive active <sup>&amp;</sup>	over-expressed	+	+	+
EpRas + TGF $\beta$ + TGF $\beta$	constitutive active	low	-		
	constitutive active	low	+	+	+
	constitutive active	inhibited by siRNA	-	-	-
	constitutive active	over-expressed	+	+	+

<sup>§</sup> As assayed by decreased E-cadherin and increased vimentin expression.

<sup>%</sup> Specific nontoxic inhibitor of Ras-farnesylation

<sup>&</sup> Activation only of the PI3K pathway

TABLE 1 | ILEI effects in the model system regarding EMT. Modified (Mackenzie NC, 2006)

### 1.1.9 Principle and strategy of the T-REx™ inducible system

The expression of the gene of interest (ILEI) is repressed in the T-REx™ system when tetracycline is absent and induced in the presence of tetracycline or its derivate (doxycyclin short Dox) (Yao F, 1998). The T-REx™ system uses only regulatory elements from the native Tet operon so that the tetracycline-regulated gene expression resembles closely the regulation of the native bacterial *tet* operon (Hillen W, 1983; Hillen W, 1994) and avoids the potentially toxic effects of viral transactivation domains observed in some mammalian cell lines.

The two components of the T-REx™ system are the inducible expression plasmid pcDNA4/TO® (called Tet-On-ILEI vector) and the Tet-Repressor expression vector pcDNA6/TR® (called TetR vector).

The gene of interest in the expression plasmid is controlled by a CMV promoter (Boshart M, 1985; Nelson JA, 1987; Andersson S, 1989) into which 2 copies of the *tet* operator 2 (TetO<sub>2</sub>) sequence have been inserted in tandem. The TetO<sub>2</sub> sequences consist of 2 copies of a 19 nucleotide sequence separated by a 2bp spacer (Hillen W, 1983; Hillen W, 1994). Each of this 19bp TetO<sub>2</sub> sequence serves as a binding site for the Tet Repressor homodimer.

The second vector, the pcDNA6/TR® regulatory vector expresses high levels of the TetR gene (Postle K, 1984) under the control of the human CMV promoter. In the absence of Dox, the Tet Repressor binds with high affinity to the TetO<sub>2</sub> sequence in the promoter of the expression vector and so the expression of the gene of interest is off (FIGURE 9). When doxycycline is added, it binds with high affinity to the TetR dimmers. This binding cause a conformational change and the TetR is no longer able to bind the TetO<sub>2</sub> operator which allows the transcription of the gene of interest.

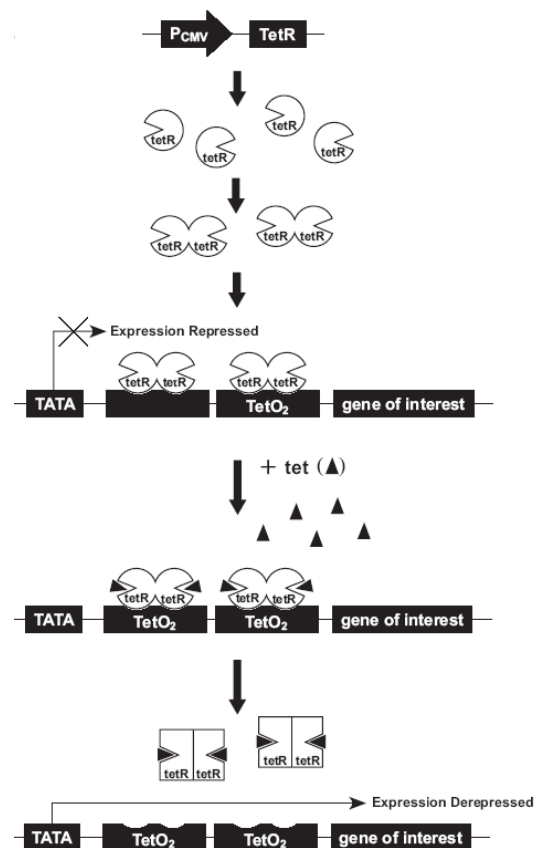


FIGURE 9 | Mechanism of the T-REx™ system.

## 1.2 Translational regulation of gene expression

Control of gene expression is achieved at various levels, such as transcription, post-transcriptional processing, mRNA stability, translation, post-translational modifications and protein degradation. (Meijer HA, 2002). In most cases, translational control mechanisms result from the interaction of RNA-binding proteins with 5'- or 3'-untranslated regions (UTRs) of mRNA. In organisms ranging from viruses to humans, protein-mediated interactions between transcript termini result in the formation of an RNA loop. Such RNA 'circularization' is thought to increase translational efficiency and, in addition, permits regulation (Mazumder B, 2003).

### 1.2.1 Regulatory elements of the 5'-UTR

The 5'-UTR is a particular section of DNA and mRNA in front of the coding sequence. It starts at the +1 position, and ends before the start codon (usually AUG) of the coding region. It usually contains a ribosome binding site and can be hundreds or more nucleotides long (FIGURE 10) (Lodish H, 2004).

During protein synthesis the translational control has two major mechanisms for initiating translation: cap-dependent initiation and cap-independent initiation using the so called internal ribosome entry site (IRES).

#### 1.2.1.1 Cap dependent translation initiation:

The 5' cap is a distinctive feature of eukaryotic mRNA. The cap consists of 7-methyl guanosine linked via an inverted 5'-5' triphosphate bridge to the initiating nucleoside of the transcript. A binary complex of eukaryotic translation initiation factor 2 (eIF2) and GTP binds to methionyl-transfer RNA (Met-tRNA<sup>i</sup>-Met), and the ternary complex associates with the 40S ribosomal subunit. The association of additional factors, such as eIF3 and eIF1A, with the 40S subunit promotes ternary complex binding and generates a 43S pre-initiation complex. The cap-binding complex, which consists of eIF4E, eIF4G and eIF4A, binds to the 7-methyl-GTP (m<sup>7</sup>GTP) cap structure at the 5' end of a messenger RNA (mRNA). eIF4G also binds to the poly(A)-binding protein (PABP), thereby bridging the 5'- and 3'-UTRs of the mRNA. This mRNA circularization and the ATP-dependent helicase activity of eIF4A are thought to promote the binding of the 43S pre-initiation complex to the mRNA, which produces a 48S pre-initiation complex. Following scanning of the ribosome to the AUG start codon, GTP is hydrolysed by eIF2, which triggers the dissociation of factors from the 48S complex and allows the eIF5B- and GTP-dependent binding of the large, 60S ribosomal subunit. Although the precise timing and requirements for the release of factors from the pre-initiation complexes are not clear, the 80S product of the pathway is competent for translation elongation and protein synthesis (FIGURE 10 and 11a) (Klann E, 2004).

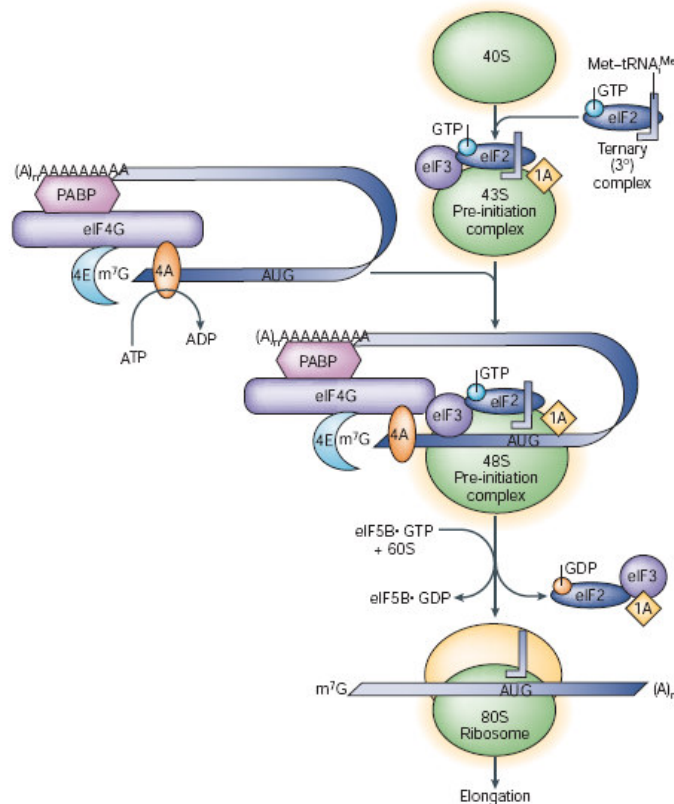


FIGURE 10 | Pathway of cap dependent translation initiation in eukaryotes (Klann E, 2004).

#### 1.2.1.2 Cap independent translation initiation:

IRES is a nucleotide sequence that forms strong secondary or tertiary structures (or both) and allows translation initiation in the middle of a mRNA sequence. The first IRES was discovered for cytoplasmic RNA viruses but has also been identified for DNA viruses and cellular mRNAs. IRES directs internal binding of ribosomes and nucleates the formation of a translation initiation complex (FIGURE 11b) (Semler BL, 2007). IRES mediated, cap independent, translations make 3-5% of all translated cellular mRNAs. Interestingly, many mRNAs that contain IRES encode proteins that have important roles in cell growth and proliferation, differentiation and the regulation of apoptosis. This is, perhaps, not surprising given that these cellular processes require the strict control of gene expression. IRES-mediated translation provides a means for escaping the global decline in protein synthesis and allows the selective translation of specific mRNAs. This led to the idea that the selective regulation of IRES mediated translation is important for the regulation of cell death and survival. As mentioned, IRES continue to function when cap-dependent translation is compromised. This is because IRES translation is independent of the presence or integrity of several canonical initiation factors (primarily eIF4E). Efficient IRES-dependent translation requires auxiliary cellular proteins that are known as IRES *trans*-acting factors (ITAFs). Several ITAFs have been implicated in IRES-mediated translation, although the requirement for these proteins is not absolute and seems to be IRES specific (Holcik M, 2005).

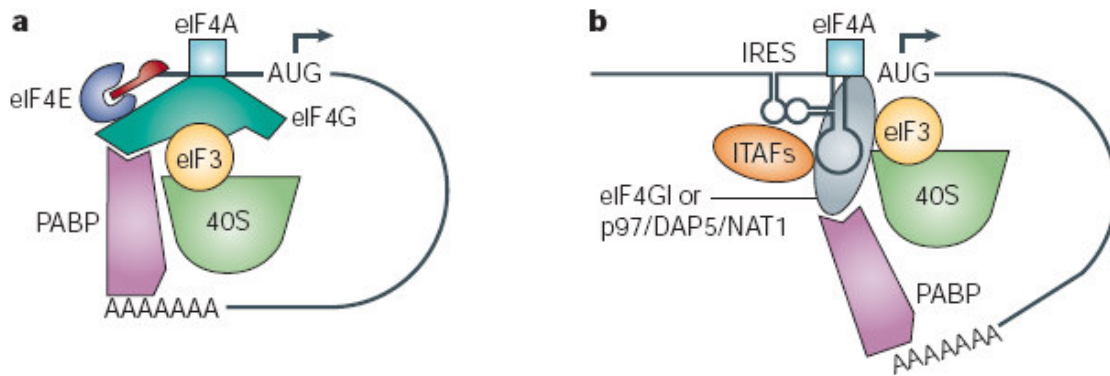


FIGURE 11 | Cap-dependent versus internal ribosome-entry site-dependent translation initiation (Holcik M, 2005).

a) The cap-binding protein eIF4E; (blue), binds to the 5' m7GpppN cap structure (red). The capped end of the mRNA is bridged to the 40S ribosomal subunit (green) by an adapter molecule eIF4G (dark green), which binds to eIF3 (yellow). eIF4A (cyan) is an RNA-dependent ATPase and RNA helicase, which is thought to be involved in the unwinding of the secondary structure of the mRNA 5'-UTR. PABP; (pink) circularizes the mRNA through its interaction with both the 3'-UTR (through the poly(A) tail) and the 5' UTR (through the interaction with eIF4G).

b) IRES *trans*-acting factors (ITAFs; orange) and proteolytic fragments of eIF4G1 or p97/DAP5/NAT1, a distant homologue of eIF4G, (light grey) stimulate IRES translation. Only eIFs that are pertinent to this process are indicated, and individual components of the translation machinery are not drawn to scale

### 1.2.1.3 Upstream open reading frames (uORFs):

Upstream open reading frames locate upstream of the actual ORF in the 5'-UTR with AUG as start codon or alternative starts like CTG. The uORF can appear in several forms, only one or several after one another, they can terminate before the proper ORF or overlap with the gene. After translating a uORF a ribosome has five options. One option of the ribosome is it can remain associated with the mRNA, continue scanning, and reinitiate further downstream, at either a proximal or distal AUG codon (FIGURE 12 option 1 and 2). Another option is to stall during either the elongation or termination phase of uORF translation, creating a blockade to additional ribosome scanning (FIGURE 12 option 3). The uORF may effect gene expression by altering mRNA stability (FIGURE 12 option 4). After termination of an uORF the ribosome has again more options, it can remain associated with the mRNA (FIGURE 12 option 1 and 2) or it can dissociate (FIGURE 12 option 5) (DR Morris, 200).

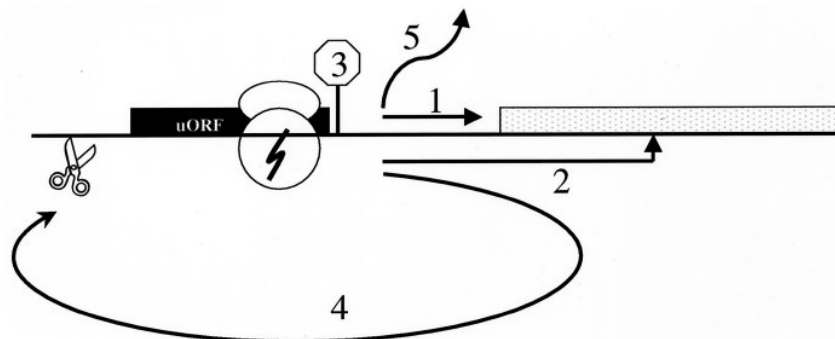


FIGURE 12 | Alternative fates available to a ribosome after translating an uORF (DR Morris, 200).

#### 1.2.1.4 Terminal oligo-pyrimidine tract (TOP) as translational regulator:

TOP mRNAs carry a TOP adjacent to the cap structure in their 5' untranslated region. The oligo-pyrimidine tract probably serves as a protein binding site and this protein binding inhibits then translation. TOP mRNAs normally encode proteins of the translational apparatus (including ribosomal proteins, elongation factors and PABP) which are not translated in resting cells and shift into polysomes when cells are stimulated to grow. This structural motif comprises the core of the translational element of these mRNAs and invariably consists of a cytosine at the cap site, followed by an uninterrupted stretch of 4-15 pyrimidine bases. The translational control of TOP mRNAs is manifested by a selective unloading of these mRNAs from polysomes (translational repression) when progression through the cell cycle is blocked at the G<sub>0</sub>, G<sub>1</sub>/S or G<sub>2</sub>/M phase and when cells are deprived of amino acids. Conversely, TOP mRNAs are recruited into polysomes (translational activation) when resting cells are induced to proliferate or to grow (increase in size), or when cells starved of amino acids are re-fed.



### 1.2.2 Regulatory elements of the 3'-UTR

The three prime untranslated region (3'-UTR) is a particular section of mRNA. It follows the coding region and can be over 1kb long, it. Alternative poly(A) sequences and binding sequences for miRNAs can be found in 3'-UTRs which regulate the stability of the RNA. Strong secondary structures in the 3'-UTRs can act as binding sites for regulatory factors, or complexes like the GAIT structure. All these regulatory mechanisms are able to contribute to the over all translational regulation by the 3'-UTR.

#### 1.2.2.1 Micro RNAs as translational regulator:

microRNAs (miRNAs) are predicted to control the activity of approximately 30% of all protein-coding genes, and have been shown to participate in the regulation of almost every cellular process investigated so far. Most miRNAs form imperfectly complementary stem-loop structures, pair imperfectly with sites in the 3'-UTR of their target mRNAs, and can apparently act by decreasing target messenger RNA levels or by directly inhibiting translation (FIGURE 13). In some cases miRNAs have been proposed to act relatively promiscuously and to inhibit multiple targets. Many genes have predicted target sites for several different miRNAs in their 3'-UTRs, indicating the possibility for combinatorial action of multiple miRNAs to maximize inhibition of gene activity, although for most genes these predictions have not yet been tested (Boyd SD, 2008; Filipowicz W, 2008).

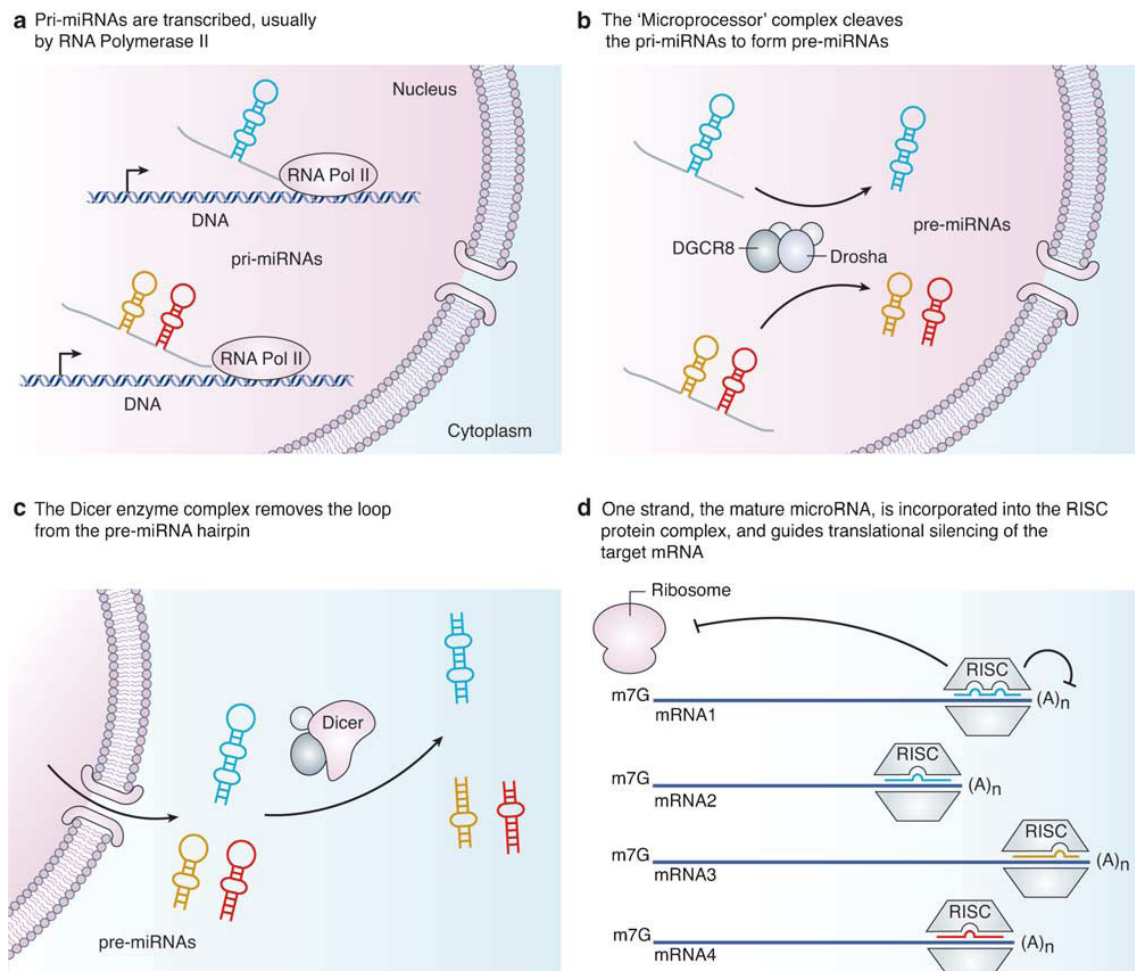


FIGURE 13 | miRNA synthesis and function (Boyd SD, 2008).

Polyadenylation is the synthesis of a poly(A) tail at the end of an RNA molecule. The poly(A) tail consists of a stretch of RNA where all the bases are adenines. This is part of the route in eukaryotes to produce mature mRNA for translation. At the end of transcription, the last bit of the newly made RNA is cleaved off by a complex of proteins, this complex then synthesises the poly(A) tail at the RNA's 3' end. Polyadenylation can result in more than one RNA variant of a gene (similar to alternative splicing), depending on which polyadenylation site is used for the gene in a particular cell. The poly(A) tail is important for the stability of mRNA, and when the tail is shortened the mRNA is soon enzymatically degraded by exonucleases. Roughly half of all protein-coding genes have more than one polyadenylation site, so a gene can code for several mRNAs that differ in their 3' end. For some genes there are several polyadenylation sites on the last exon, and for some genes they are spread over several exons. The vast majority of poly(A) sites are found in the 3'-UTRs, but some sites are found in introns, coding sequences and 5'-UTRs. The different 3'-UTRs resulting from alternative polyadenylation can cause different regulation for different polyadenylation variants, since it can influence which binding sites for miRNAs the 3'-UTR contains.

A new mechanism of translational control was found in monocytes; it is called IFN $\gamma$  activated inhibitor of translation (GAIT). IFN $\gamma$  activates the translation of ceruloplasmin (Cp) in these cells but after some time the protein synthesis stops despite the presence of abundant transcript. This translational silencing is mediated by GAIT. The GAIT element is a structural element consisting of an apical loop, an asymmetric internal bulge and a distal stem (FIGURE 14). Beside the precise structure, the identity of two loop nucleotides (A84 and U87) are essential for binding activity (Ray PS, 2007).

**FIGURE 14** | Secondary structure of human Cp GAIT element (Ray PS, 2007).

The assembly of the *GAIT* complex occurs in two temporally distinct steps. During the first step, a pre-*GAIT* complex of proteins is formed that does not bind the *GAIT* element. In the second step, L13a is phosphorylated and released from the large ribosomal subunit. The released L13a joins GAPDH and the pre-*GAIT* complex to form the functional *GAIT* complex that binds the 3'-UTR *GAIT* element of Cp mRNA and blocks its translation by inhibiting the assembly of the translational initiation complex (FIGURE 15) (Kapasi P, 2007; Ray PS, 2007).

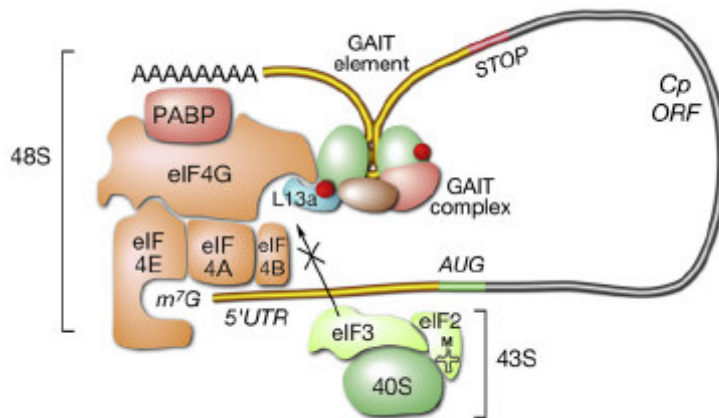


FIGURE 15 | 3'-UTR bound GAIT complex represses translation (Kapasi P, 2007).

### 1.3 The ILEI mRNA

The genomic organization of ILEI, has been performed by BLAST search, Northern blot analysis and RT-PCR amplification (Pilipenko VV, 2004). Two EST sequences (BC009086 and AX424275) were found and assembled together generating a transcript with a total length of 2738bp. Sequence analysis has revealed that in transcript BC009086 the polyadenylation signal sequence (AATAAA) is located 11bp upstream from the poly(A) tail. in transcript. The long transcript AX424275 also contains a polyadenylation signal sequence (ATATAA) only 19bp upstream from the transcript termination, indicating that both short and long transcripts exist as mature mRNA. This prediction for two ILEI mRNA isoforms has been confirmed by Northern blot analysis (Pilipenko VV, 2004) (FIGURE 16).

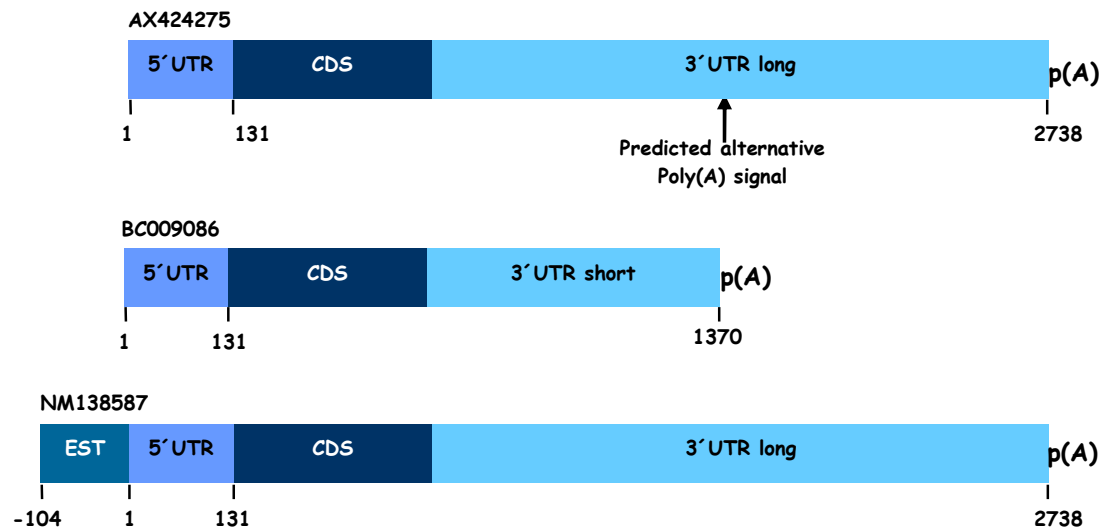


FIGURE 16 | The genomic organisation with alternative poly(A) tail of ILEI (Pilipenko VV, 2004).

The ILEI gene encompasses over approximately 50kb at chromosome 6A3.1 and has ten exons, nine introns. The coding region starts in exon two and ends in exon 10. The alternative poly(A) site in the 3' -UTR is used to generate a shorter ILEI mRNA isoforms, which encodes the same protein product as the long mRNA isoforms. (FIGURE 17) (Pilipenko VV, 2004).

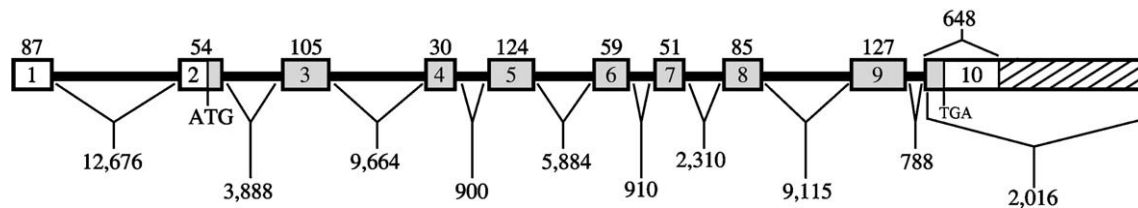


FIGURE 17 | The genomic organisation of the mouse ILEI gene (Pilipenko VV, 2004). Schematic representation of the general structure of ILEI. The ILEI gene has ten exons (numbered) and nine introns (black bars), the coding region (light grey) starts in exon two and ends in exon 10. The alternative poly(A) site in the 3' -UTR is hatched.

### **1.3 Aim of this work**

The first aim of this diploma thesis was to establish an inducible overexpressing setup in the Eph4 cell system in general. Secondly, our protein of interest, ILEI, was to be studied in three different cell lines with and without induction. Another aim was to study the translational regulation of ILEI.

## 2 MATERIALS AND METHODS

### 2.1 DNA techniques

#### 2.1.1 Design of oligonucleotides

Oligonucleotides were used for PCR amplification and DNA sequencing. For site specific hybridisation, oligonucleotides must have 16 to 18 base pairs. For stringent annealing there should be Cs or Gs at the end of every sequence. Primers should also not have secondary structures meaning no complement sequences in itself. Also when primers were used together in the same experiment they should not be complementary to each other to avoid heterodimerisation. A melting temperature between 50°C and 60°C is desirable. The primers were dissolved in H<sub>2</sub>O to a concentration of 100µM. Storage is at -20°C.

#### 2.1.2 PCR (Polymerase Chain Reaction)

Standard reaction of 50µl:

5µl	PCR buffer (10x)
3µl	MgCl <sub>2</sub> (25mM)
0,2µl	Taq Polymerase (5U/µl)
2µl	DMSO
1µl	primer mix (5mM each)
1µl	DNA

Up to 50µl with ddH<sub>2</sub>O

Standard program for the PCR was started with an initial denaturation step at 94°C for 5'.

Then the following 35 cycles consisted a short denaturation step at 94°C for 30'', an annealing step with a primer dependent temperature of 30'', an elongation step at 72°C with approximately 1' for 1kb. A final elongation step for 5' at 72°C was applied for extending some unfinished elongation products and the reaction was hold on 4°C. 10x Orange G was to the PCR product added and loaded directly onto an agarose gel.

Primers for UTR cloning:

ILEI 5' UTR forward

ACGTAAGCTTCGCGATCGGCGCTCGGGAGG

ILEI 5' UTR reverse

ACTGCCATGGATTTTTGCCTTCTCACTCTCTAGCAC

ILEI 3' UTR forward

TATCTAGACGGGAAGGAGCGAGAGGC

ILEI 3' UTR reverse SHORT

TTGGCGCGCCTTGTTGTAACATTTTATTTCTGG

ILEI 3' UTR reverse LONG

TTGGCGGCCCCAGTAAGTGAGCACTGTTCCAC

Agarose gel electrophoresis

Depending on the size of DNA fragments to be separated, the Agarose concentration varied between 1% and 2%. The Agarose was suspended in 1x TAE buffer and boiled in the microwave until it dissolved completely. After cooling down the solution a 0,5µl Ethidium Bromide (10mg/ml) was added. The mix was poured into a gel tray with a comb of choice. When the gel was hardened the comb was removed and the gel tray was put into a gel camber containing 1x TAE. The gel was run at 3V/cm<sup>2</sup>.

### 2.1.3 Determination of the concentration of nucleic acids

The concentration of nucleic acids was determined by measuring the optical density of the sample that was diluted 1:200 in TE at 260nm in a spectrometer. As a blank 1x TE was used. Nucleic acid  $\mu\text{g/ml} = \text{OD}_{260} * 50$

### 2.1.4 Recovery of DNA from agarose gels

The gel extraction was performed using GFX PCR DNA and Gel Band Purification Kit (Amersham Biosciences) according to the manufacturer's instructions. Briefly, the gel band of interest was cut out of the Agarose gel and put in a pre-weighed tube. To 10mg of gel 10 $\mu\text{l}$  of capturing buffer was added, and incubated at 60°C for 15' under shaking. The dissolved sample was transferred into a GFX column in a collection tube and incubated 1' at room temperature. Centrifuge at 13000rpm for 30''. Flow-through was discarded. The Sample was washed with 500 $\mu\text{l}$  wash buffer and centrifuged again. To elute the DNA from the column 40 $\mu\text{l}$  of ddH<sub>2</sub>O was added to the column, incubated for 1' at room temperature and spined for 1' at full speed. The flow trough was collected.

### 2.1.5 Purification of DNA from a PCR reaction

The purification was performed using GFX PCR DNA and Gel Band Purification Kit (Amersham Biosciences) according to the manufacturer's instructions. The PCR reaction was transferred onto a GFX column containing 500 $\mu\text{l}$  of capture buffer. Sample was mix by pipetting up and down. Centrifuge at 13000rpm for 30'' and discard the flow-through. The Sample was washed with 500 $\mu\text{l}$  wash buffer and centrifuged again. To elute the DNA from the column 40 $\mu\text{l}$  of ddH<sub>2</sub>O was added to the column, incubated for 1' at room temperature and spined for 1' at full speed. The flow trough was collected.

### 2.1.6 Restriction digestion of DNA

The restriction digest reactions were performed with enzymes and buffers from Roche and New England Biolabs. The reactions were always incubated at 37°C for 3 hours with a negative control. The enzymes were diluted at least 10 times in the reaction mix and 3U enzymes were calculated for 1 $\mu\text{g}$  of DNA.

Standard reaction of 20 $\mu\text{l}$ :

2 $\mu\text{l}$	restriction buffer (10x)
3U	restriction enzyme I per $\mu\text{g}$ DNA
3U	restriction enzyme II per $\mu\text{g}$ DNA
X $\mu\text{g}$	DNA

Up to 20 $\mu\text{l}$  with ddH<sub>2</sub>O

### 2.1.7 Ligation of DNA

All DNA ligations were carried out using T4 DNA ligase (Roche). They were carried out over night at 16°C always with a negative control in which was no Insert present to see if the vector has religated. The amount of vector to insert was near a 1 : 5 molar ratio.

Standard reaction of 10 $\mu\text{l}$ :

1 $\mu\text{l}$	ligation buffer (10x)
1 $\mu\text{l}$	BSA (1mg/ml)
0.5 $\mu\text{l}$	T4 DNA ligase
X $\mu\text{mol}$	Vektor DNA
5*X $\mu\text{mol}$	Insert DNA

Up to 10 $\mu\text{l}$  with ddH<sub>2</sub>O

### 2.1.8 Heat-Shock transformation of DNA into competent bacteria

For each transformation one vial (50 $\mu$ l) of heat shock competent cells of *E. coli* DH5 $\alpha$  strain (stored at -80°C) were thawed on ice. 1 $\mu$ l of ligation mix was pipetted to the cells and mixed by gently tipping followed by a 30' incubation on ice. Then the cells were put in 37°C warm water for 30'' for the heat-shock, plated out on an LB-Amp plate and incubated over night at 37°C. At the same time, negative control in which only the cut vector without insert was used.

### 2.1.9 Transformation of DNA into competent bacteria by electroporation

For each transformation one vial (40 $\mu$ l) of electro competent *E. coli* cells JA226 strain (stored at -80°C) were thawed on ice. 1 $\mu$ l of the ligation mix was pipetted to the cells and mixed by gently tipping. At the same time, negative control in which only the cut vector without insert was used. Electroporation was performed at a voltage of 2,5kV. Cells were plated out on an LB-Agar plates containing the appropriate antibiotic and incubated over night at 37°C. For later storage parafilm was wrapped around the edges and the plate was put aside at 4°C.

### 2.1.10 Small scale plasmid preparation (Mini-Prep)

The plasmid preparations were made on the QIAGEN SPIN MINIPREP kit. After plates single bacterial colonies were grown out over night, they were picked and grown a another night in 5ml LB medium with the appropriate antibiotics. 1,5ml of this culture were spun down at 13000rpm for 3'. The bacterial pellet was resuspended with 250 $\mu$ l of buffer P1 and then mixed by inverting 4 times with 250 $\mu$ l buffer P2. Afterwards 350 $\mu$ l buffer N3 were added and mixed by inverting again. The reaction mix was centrifuged 10' at 13000rpm and supernatant was applied onto the QIAprep spin columns by pipetting. After the vacuum drawn the solution through the columns, column was washed with 500 $\mu$ l of buffer PB and 750 $\mu$ l buffer PE. Transferred the columns to a microfuge tube and centrifuged 1' full speed to remove all wash buffers. To elute the DNA the columns were placed in a clean tube and eluted with 40 $\mu$ l of ddH<sub>2</sub>O after incubating for 1' at room temperature by spinning for 1' at 13000 rpm.

### 2.1.11 Large scale plasmid preparation (Maxi-Prep)

The plasmid preparations were made with the QIAGEN SPIN MAXIPREP kit. The bacterial cells were harvested after growth for one night in 200ml LB medium with the appropriate antibiotics by centrifuging at 3500 rpm for 8'. The bacterial pellet was resuspended with 10ml of buffer P1 and then mixed by inverting 4 times with 10ml buffer P2 and incubate at room temperature for 5'. Afterwards 10ml buffer N3 was added and mixed by inverting again, incubated for 20' on ice. The reaction mix was spinned for 15' at 3500rpm. A QIAGEN-tip 500 column was equilibrated with 10ml of QTB buffer and the supernatant was applied. After the supernatant was flown rough the column was washed wit 60ml of buffer QC. DNA was precipitated by adding 10,5ml isopropanol at room temperature and centrifuged at 7000rpm for 30' at 4°C. The supernatant was discarded and the pellet washed wit 5ml 70% ethanol for another 10' at 4°C and 7000rpm. The pellet was air-dried until it turned white but not longer otherwise one would not get it dissolved again. The pellet was dissolved in an appropriate amount of ddH<sub>2</sub>O (100 $\mu$ l - 500 $\mu$ l depending on the dimension of the pellet).

### 2.1.12 Bac clone DNA isolation

The Bac-plasmid preparations were made with the QIAGEN SPIN MAXIPREP kit. The bacterial cells were harvest after one night in 1000ml LB medium with the appropriate antibiotics by centrifuging at 6000 rpm for 10'. The bacterial pellet was resuspended with 45ml of buffer P1. The cells were divided up to 15ml per falcon (50ml) tube and 15ml buffer P2 was added to every tube followed by incubation at room temperature for 15'. Afterwards 15ml buffer N3 was added, mixed by inverting and incubated for 20' on ice. The reaction mix was centrifuge 30' at 3500 rpm. A QIAGEN-tip 500 column was equilibrated with 10ml of QTB buffer and the supernatant was applied. After the supernatant was flown rough the column was washed wit 60ml



of buffer QC. DNA was precipitated by adding 10,5ml isopropanol at room temperature and centrifuged at 7000rpm for 30' at 4°C. The supernatant was discarded and the pellet washed with 5ml 70% ethanol for another 10' at 4°C and 7000rpm. The pellet was air-dried until it turned white but not longer otherwise one would not get it dissolved again. The pellet was dissolved in an appropriate amount of ddH<sub>2</sub>O (100µl - 500µl depending on the dimension of the pellet).

## 2.2 Cloning strategies

### 2.2.1 The inducible Tet-On system

In general, vector and insert were digested with the same two enzymes, separated on agarose gel, gel extracted and ligated.

pcDNA™4/TO was cut with BamH I and Xho I to insert the DNA fragment containing the coding sequence (CDS) for the Tet-On-ILEI construct and the FFL CDS for the pcDNA4/TO-FFL reporter construct (FIGURE 18).

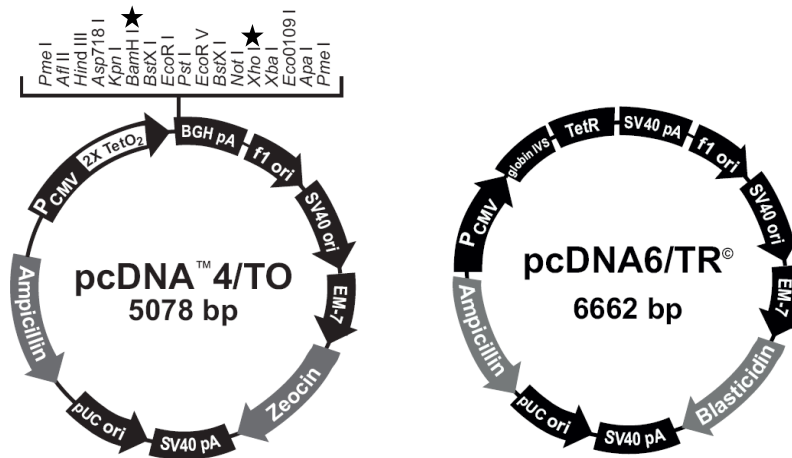


FIGURE 18 | pcDNA™4/TO and pcDNA6/TR® vectors from Invitrogen.

### 2.2.2 The UTR constructs

The UTR constructs were cloned after amplifying the insert via PCR . The primer sequence and the procedure is noted under 2.1.2. After the PCR the fragments were purified (2.1.6) and digested (2.1.7) with the same enzymes as the vectors in which they were inserted.

The pGL3-Control-MCS vector is a derivative of the pGL3-Control vector (FIGURE 19) were after the Xba I site a small multi cloning site (MCS) was inserted with restriction sites EcoR V and others (kindly provided from G. Obernosterer).

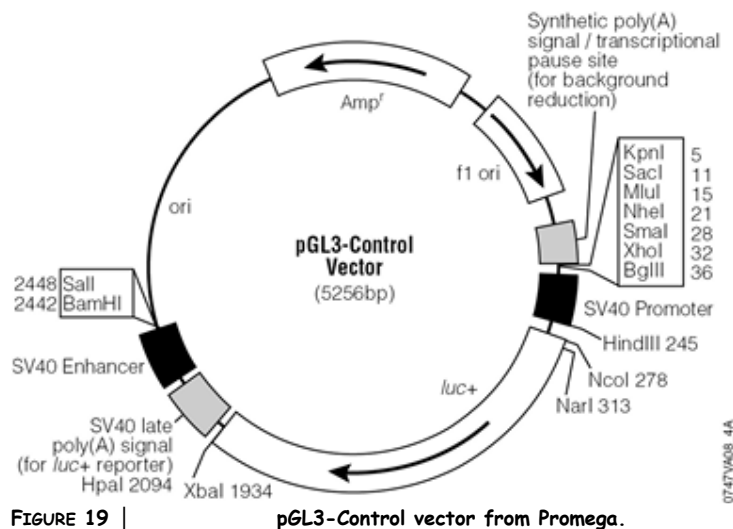


FIGURE 19 | pGL3-Control vector from Promega.

To generate the ILEI 5'-UTR construct the pGL3-Control-MCS vector was digested with Nco I and Hind III.

The vectors ILEI 3'-UTR short and long were generated by digesting the pGL3-Control-MCS vector with Xba I and EcoR V.

For the ILEI 5' and 3'-UTR short and long vector both digests mentioned above were carried out.

The pGL3-Enhancer vector lacking the SV40 promoter served as negative control (FIGURE 20).

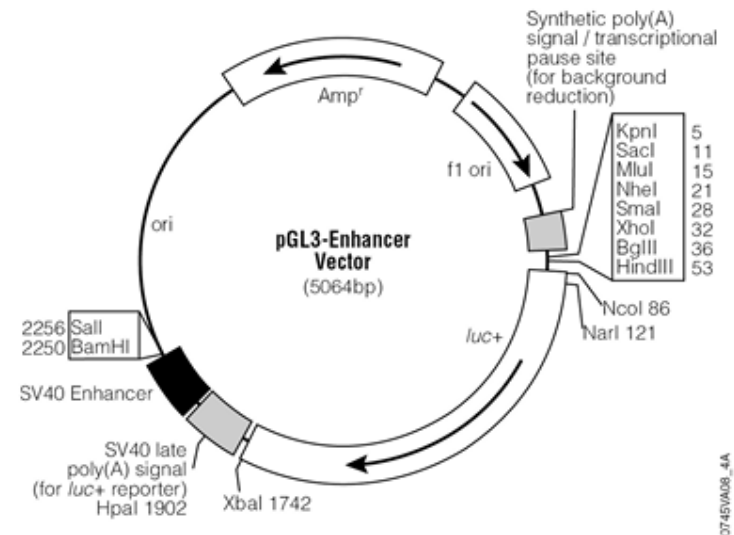


FIGURE 20 | pGL3-Enhancer vector from Promega.

## 2.3 RNA techniques

### 2.3.1 Isolation of RNA

#### 2.3.1.1 TRIZOL Reagent Invitrogen

Tissue samples (50 to 100mg) were homogenized in 1ml of TRIZOL reagent with a Polytron homogenizer (Kinematica). Cultured cells were trypsinised and washed with PBS before 1ml of TRIZOL agent was added. Homogenized samples were incubated for 5' at room temperature to permit complete dissociation of nucleoprotein complexes. 200 $\mu$ l of chloroform was added and the tubes were shaken vigorously by hand for 15' and incubated for 3' at room temperature. The samples were centrifuged at 13000rpm at 4°C for 15'. Upper aqueous phase was transferred into a fresh tube and precipitate the RNA by adding 500 $\mu$ l 2-propanol. By incubating at 4°C for 10' and followed by centrifugation at 13000rpm at 4°C. Supernatant was removed and the RNA pellet was washed with 1000 $\mu$ l 70% ethanol. The pellet was air-dried until it turned white and dissolved in 15 $\mu$ l of ddH<sub>2</sub>O.

#### 2.3.1.2 Quiagen RNeasy® Mini Kit

Fresh RLT buffer was prepared by adding 10 $\mu$ l  $\beta$ -meraptoethanol to 1ml RLT solution. Cells from culture dishes were trypsinised and washed. 350 $\mu$ l RLT buffer was added to disrupt the cell membranes and vortexed 1'. 350 $\mu$ l of 70% ethanol was added and mixed well by pipetting. The sample was transferred into a RNeasy spin column and vacuum was applied until transfer was complete. The column was washed with 700 $\mu$ l RW1 buffer. 10 $\mu$ l DNase I stock solution were added to 70 $\mu$ l RDD buffer and mixed by inverting. This mix was pipetted on the column and incubated 15' at room temperature to digest the DNA completely. Then another 350 $\mu$ l of buffer RW1 was added and centrifuged at 13000rpm for 15'. Flow-through was discarded. The column was washed twice with 500 $\mu$ l Buffer RPE. The column was removed from the vacuum manifold and placed in a tube, centrifuged at full speed for 1' to get rid of all the buffer. The column was placed in a new tube and the RNA was eluted with 30 $\mu$ l of RNase-free water by centrifugation for 1' at full speed.

### 2.3.2 RNA clean up

Fresh RLT buffer was prepared by adding 10 $\mu$ l  $\beta$ -meraptoethanol to 1ml RLT solution. The sample volume was adjusted to 100 $\mu$ l with RNase-free water, 350 $\mu$ l RLT buffer was added and mixed well. 250 $\mu$ l pure ethanol was pipetted to the sample and it was placed in an RNeasy Mini spin column. The column was centrifuged for 15' at 13000rpm and the flow-through was discarded afterwards. The column was washed twice with 500 $\mu$ l RPE buffer. The column was removed from the tube and placed it in a new tube, centrifuged at full speed for 1' to get rid of all the buffer. The column was placed in a new tube and the RNA was eluted with 40 $\mu$ l of RNase-free water by centrifugation for 1' at full speed.

### 2.3.3 RNA nano chip

The gel was prepared by putting 550 $\mu$ l of RNA 6000 Nano gel matrix (marked in red) into a spin filter and centrifugating at a bench centrifuge at full speed for 10'. RNA 6000 Nano dye concentrate (marked in blue) was vortexed (room temperature) and 1 $\mu$ l was added to 65 $\mu$ l of the filtered gel. The mix was vortex and spinned for 10' at full speed. A RNA chip was put on the Chip Priming Station and 9 $\mu$ l gel-dye mix was pipetted in the well marked with **G**, the Chip Priming Station was closed and the plunger pressed until it was held by the chip. After waiting for exactly 30' the chip was released. 9 $\mu$ l of gel-dye mix were pipetted in the well marked **G** and 5 $\mu$ l of RNA 6000 Nano Marker (marked in green) in all 12 sample wells and in the well marked with a ladder. In the well marked with a ladder also 1 $\mu$ l of RNA 6000 Nano ladder was pipetted. To each sample well 1 $\mu$ l of sample was added and the chip was vortexed for 1'. The chip was run in the Agilent 2100 bioanalyzer within the next 5' using the program: "eukaryote Total RNA Nano".

### 2.3.4 Isolation of polysome bound RNA on Sucrose-Gradient

From the two basic sucrose solutions (15% and 40% (w/v)) two more solutions with 23.3% and 31.6% (w/v) sucrose were prepared (by mixing the 15% solution with the 40% stock at ratios of 2:1 and 1:2, respectively). 2.5 ml of complete 40% (w/v) sucrose mix were pipetted into RNase-free polyallomer tubes for SW41 (Beckman) or equivalent swing-out rotor. These tubes are 14mm in diameter and 89mm in length, and have a total capacity of 11 ml. In vertical position the tubes were quick-frozen in liquid nitrogen. 2.5 ml of 31.6% solution were pipetted on to the still frozen 40% layer, quick-frozen again and the same procedure repeated with the 23.3% and 15% solutions. Gradients were stored at -70°C until use. In the evening before the actual experiment, the required number of frozen sucrose gradient tubes were put into the cold room to thaw slowly overnight. Through convection the concentration steps formed a smooth, linear gradient by the next morning.

Cells were harvested by trypsinising and washing the cells ( $5 \times 10^7$  per gradient). in 1131 $\mu$ l of cold NP-40 lysis buffer supplemented with 14.4 $\mu$ l RNasin Plus (40U/ $\mu$ l), 18 $\mu$ l cyclohexamid (10mg/ml), 24 $\mu$ l DTT (1M) and 12 $\mu$ l PMSF the cells were lysed for 15' on ice. The lysate was centrifuged at 3300rcf for 3' at 4°C in a microcentrifuge tube to pellet the nuclei. the supernatant was transferred to a new microcentrifuge tube containing 30 $\mu$ l heparin (50mg/ml), together it was centrifuged at full speed for 10' at 4°C, in a microcentrifuge tube to pellet the mitochondria and membrane particles. 1ml of the supernatant was pipetted on the sucrose gradient, and was centrifuged at 38000rpm, for 120' at 4°C in an ultracentrifuge using an SW41Ti rotor. The acceleration was set to 5 (medium) and brake were switched off. The gradient was harvested in about 20 fractions of 550 $\mu$ l each into tubes containing 30 $\mu$ l of 20% (w/v) SDS, 12 $\mu$ l EDTA (0.5M) and 10 $\mu$ l proteinaseK (10mg/ml). This mixture was incubated for 30 min at 37°C. Each fraction was extracted with 300 $\mu$ l Tris buffered phenol and 300 $\mu$ l chloroform : isoamylalcohol 24:1. Phases were separated by centrifugation for 5' in a microcentrifuge at 13000rpm. 600 $\mu$ l of upper aqueous phase were recovered. 1ml of ethanol was added to precipitate the RNA at -80°C for 60'. Samples were centrifuged 30' at full speed, supernatant was removed carefully, the pellet rinsed once with 500 $\mu$ l 70% ethanol; spinned for another 10' at full speed and air dried. The pellet was dissolved in 15 $\mu$ l of RNAase-free water and stored at -70°C until use.

### 2.3.5 Northern blot

Gel trays (14,5cm x 21cm) and combs were made RNase-free by incubating in 100mM NaOH for 30' followed by washing with RNase-free H<sub>2</sub>O. An appropriate amount of agarose was weighed for a 1,2% gel in 1x MOPS buffer. It was taken into account that formaldehyde (5,1ml/100ml) was added after boiling the agarose. By boiling, the agarose was dissolved and then cooled down to 50°C while stirring. In a fume hood, 5,1 ml of 37% (v/v) formaldehyde per 100ml of agarose solution and ethidium bromide (1,0mg/l) were added. After careful stirring the gel was poured immediately. The gel hardened for at least 45'. To 14µl of RNA solution 32,7µl denaturation buffer was added and incubated at 56°C for 15', then 4,7µl of sample buffer was pipetted to the samples. The hardened gel was put into the electrophoresis chamber and filled up with 1x MOPS running buffer to cover the gel. The samples were loaded and run at 110V until the bromophenol blue was migrated about 2/3 of the gel length (about 4 hours). After the run was complete, a photograph of the gel under UV irradiation (302nm) was taken.

Nylon membrane were cut to the same size as the gel. Thick Whatman papers soaked with RNase-free Na<sub>3</sub>PO<sub>4</sub> (50mM). The surface of the Whatman papers had to be larger than the gel. The level of blotting buffer had to remain below the top surface of the sponge. Two pieces of filter paper (Whatman 3MM), of the same size as the sponge were wetted in the buffer and placed on top of the sponge. On top of this the gel with slots facing downwards on the filter paper were placed and the spacers inserted (e.g., parafilm strips, at least 3cm wide) along each side of the gel. The equilibrated nylon membrane was put on top of the gel. It was made sure that no air bubbles were trapped between gel and membrane. One piece of wet Whatman paper and two additional pieces of dry paper (cut to the same size as the gel) were placed on top of the membrane. Over that a stack of absorbent paper towels (50-75mm high) or further Whatman papers cut to the same size as the gel were put on top of the papers. A glass plate and a weight (500-1000g) were set on top of the paper towel stack. The transfer from the gel to the nylon membrane happened over night. In the morning the towels and filter paper were removed without lifting the nylon membrane. Mark the position of the slots and orientation of the filters were before. The slots on the gel were marked on the membrane with a soft pencil and lifted away from the gel. The gel was baked in an 80°C oven for 1 hour to dry the membrane completely. For a covalent fix of RNA to the membrane a UV cross-linker (such as Stratagene) was used.

### 2.3.6 Northern blot probe labelling

A PCR of the fragment according to 2.1.2 was made and purified according to 2.1.5 then digested with the proper enzymes according to chapter 2.1.7. A Northern blot membrane was pre hybridised at 65°C for 1 - 2 hours in 20ml of church buffer. In a tube were 1 - 5µg of the DNA probe and up to 25µl ddH<sub>2</sub>O mixed with 10µl random primers. This mix was heated for 5' at 99°C and spinned down briefly. 10µl dCTP buffer (10x) and 5µl P32-dCTP and 1µl Exo(-)Klenow (5U/µl) were added and incubated for 30' to 60' at 37°C. 2µl stop mix were pipetted to the reaction as well as 3µl yeast tRNA (10ng/µl) plus 25µl of a NH<sub>4</sub>Ac solution (7,5M). The sample was mixed and left 5' at room temperature, then spinned down at 13000rpm for 5' and the supernatant was discarded. The probe was washed with 70% ethanol and dissolved in 100µl 1x TE. The radioactivity of the probe was checked with a GM-counter. For hybridization the radioactive probe was denatured at 95°C for 5' and put right afterwards on ice. A change the church buffer (4ml) was made and the probe was pipetted directly into the fresh buffer in the tube with the membrane. Over night at 65°C the probe was hybridised. In the morning the membrane was washed 3 times in wash buffer at room temperature for 5' and once at 65°C for 30'. The membrane was wrapped in a thin foil and exposed to auto radiographic films (Kodak Bio MAX X AR Film) at -80°C for minimum 2 days. If the membrane was needed for being probed a second time it was stripped with stripping buffer for 30' at 80°C. After stripping there was no need for pre-hybridization.

### 2.3.7 Reverse transcription of RNA into cDNA

Standard reaction of 20 $\mu$ l:

2 $\mu$ l	PCR buffer II (10x)
4 $\mu$ l	MgCl <sub>2</sub> (25mM)
2 $\mu$ l	dGTP (10mM)
2 $\mu$ l	dATP (10mM)
2 $\mu$ l	dCTP (10mM)
2 $\mu$ l	dTTP (10mM)
1 $\mu$ l	RNase inhibitor
1 $\mu$ l	MuLV reverse transcriptase (50U/ $\mu$ l)
1 $\mu$ l	random hexameres (50mM)
1 - 5 $\mu$ g RNA	

Up to 20 $\mu$ l with RNase-free water H<sub>2</sub>O

The negative control was the standard reaction without reverse transcriptase.

The standard programme for making cDNA was 10' at room temperature than 60' at 42°C followed by 10' at 94°C. To the reaction mix 30 $\mu$ l of ddH<sub>2</sub>O were added

#### $\beta$ -Actin PCR

Standard reaction of 50 $\mu$ l:

5 $\mu$ l	PCR buffer (10x)
3 $\mu$ l	MgCl <sub>2</sub> (25mM)
1 $\mu$ l	dNTPs mix (10mM each)
0,2 $\mu$ l	Taq Polymerase (5U/ $\mu$ l)
1 $\mu$ l	$\beta$ -Actin primer mix (10mM each)
1 $\mu$ l	DNA
38,8 $\mu$ l	ddH <sub>2</sub> O

Standard program for the  $\beta$ -Actin PCR was started with an initial denaturation step at 94°C for 5'. Then the following 25 cycles consisted a short denaturation step at 94°C for 30'', an annealing step at 55°C for 30'' an elongation step at 72°C for 45'. There was a final elongation step for 5' at 72°C was there for extending some unfinished constructs then the reaction was hold on 4°C. To the PCR product 10x OrangeG was added and loaded directly onto an agarose gel.

## 2.4 Protein chemistry

### 2.4.1 Determination of protein concentration (Bradford assay)

From a BSA stock solution with 1mg/ml a standard concentration row was prepared 2,5 - 15µg/ml. The BioRad Bradford solution was diluted 1:5 with ddH<sub>2</sub>O. In a plastic cuvette 1ml of the diluted Bradford reagent was mixed with 1µl of a protein sample by covering the cuvette with a piece of parafilm and vortexing it briefly. After an incubation time of 5' the extinction at 595nm was measured in a spectrophotometer.

### 2.4.2 Cell lysis for SDS-PAGE

A total protein preparation from eukaryotic cells growing in 6 well plates was made. The supernatant from the cells was collected and stored for later experiments. The cells were washed once with 1x PBS and trypsinised in 10x Trypsine. When they detached from the plate they were taken up in fresh FCS containing medium. At 2400rpm they were centrifuged for 3' and the medium was discarded. The cells were washed again with 1x PBS and then lysed with 60µl lysis buffer. The lysing cells were incubated for at least 30' on ice before centrifuging them at 4°C for 30' at 13000rpm. The supernatant was collected in a fresh tube and the protein concentration was measured with the Bradford method (2.4.1.).

### 2.4.3 Supernatant preparation for SDS-PAGE

From cells which were collected to be lysed for SDS-PAGE and Western blots the supernatant was taken and also loaded on a gel. For Ultra-filtration of a protein solution in Ultracel YM-10 filters with a nominal weight limit of 10.000Da were used. The supernatant was collected in a tube and spined for 5' at full speed on 4°C to sediment all cell debris that would clog the filter columns. 500µl of the supernatant were placed in a MICROCON centrifugal filter device and centrifuged at 4°C for 30' at 12300rpm. The tube with the filtrate was emptied and the column was put back in the tube. Another 500µl were put into the column and spined again at 4°C and 12300rpm for 15'. To get the concentrate the column was flipped up side down in a fresh tube and centrifuged for 1' at room temperature, full speed. The volume of the supernatant concentrate was measured with a pipette.

### 2.4.4 SDS-PAGE

Protein samples were loaded on 10% PAGE gels with 1,0mm or 1,5mm thickness. PAGE running buffer was used and the gel ran at 200V and 40mA for about 2 hours.

### 2.4.5 Western blot analysis (semi dry)

For semi-dry Western blotting two filter papers Watman 3MM were soaked in blotting buffer, the PVDF membrane was soaked briefly in methanol and then in blotting buffer. The gel was moistened in the blotting buffer too and then the blotting sandwich was assembled. Filter paper - membrane - gel - filter paper. The transfer from gel to the membrane was performed in a Pharmacia Biotech Multiphor II unit at 20V and 56mA. For a mini gel (5,5cm x 8,5cm) with 1mm 1 hour and a 1,5mm gel 1,5 hours at room temperature. After the transfer the gel was blocked 1 hour at room temperature or over night at 4°C with a blocking buffer. The 1<sup>st</sup> antibody was incubated 1 hour at room temperature or over night at 4°C in blocking buffer. The membrane was washed 3 times for 10' in wash buffer and followed by 1 hour at room temperature or over night at 4°C in incubation with the 2<sup>nd</sup> antibody in blocking buffer. Finally the membrane was washed again 3 times for 10' in washing buffer. For detection the membrane was moistened with ECL plus Western blotting Detection solution and under safe light conditions a high performance chemoluminescence film was put on it. After an incubation time that can range from 1'' to 1' the film was developed.



## 2.5 Cell culture

### 2.5.1 Cultivation of adherent mammalian cells

All cell lines were grown in the appropriate media in plastic culture dishes in an incubator at 5% CO<sub>2</sub> level and 95% humidity at 37°C. The cells were split when they were 95% confluent mostly 1:4 every second day.

Cell line	medium
EpRas	4% FCS in EAGL
EpC40	10% FCS in EAGL
EpH4	10% FCS in EAGL
XT	15% FCS in DMEM F12

The EAGL medium was supplemented with an antibiotic and Hepes.

Penicillin	100U/ml
Streptomycin	0,1mg/ml
Hepes pH= 7,3	0.02M

### 2.5.2 Freezing of adherent cells

Cells were trypsinised and pelleted (1200rpm for 5') and resuspended in 1,5ml FCS containing 10% DMSO. The cells were frozen to -80°C in cryogen micro tubes (Nalgene) and after at least 49 hours transferred into liquid nitrogen at -192°C. Normally one 10cm dish was frozen in one cryo tube.

### 2.5.3 Thawing of adherent cells

Cells were thawed quickly at 37°C in a water bath and then transferred in fresh media. The cells were centrifuged at 1200rpm for 5' the medium was discarded. Then the cells were resuspended into new media and plated out on the appropriate dish.

### 2.5.4 Liposome based transfection of adherent mammalian cells

The day before transfection of the cells were plated out with 400.000 cells per 6 well. For the transfection two tubes (A and B) were prepared. In tube A were 2µg of the DNA for the transfection mixed with 125µl Optimem. In tube B were 10µl Lipofectamin™ 2000 mixed with 240µl Optimem. Both tubes were incubated for 5' at room temperature. Then tube A was pipetted into tube B, they were mixed thoroughly and incubated for 20' at room temperature. 750µl Optimem were added to tube B and mixed. The mixture was put to the cells on a 6 well plate and the cells were incubated for 5 hours. After that the media was changed to the suitable one for the cells. At the next day cells could be harvested to be used either for SDS-PAGE gels, Luciferase assays or for sub cloning.

### 2.5.5 Subcloning of cell lines via single cell sort

Transfected cells were selected with an suited antibiotic for as long as the control dish without the protective construct needed to die. After that the cells were trypsinised and resuspended into media with Ciproxin (2mg/ml) and EDTA (20µg/ml) for sorting in a FACS machine into 96 well plates, one cell per well or two cells per well. The media was changed one week after the sort and the well were checked under the light microscope for grown colonies. When the colonies were 80% confluent the cells were successively expanded. To guarantee, that the cells keep the transfected construct the cells media was supplemented from time to time with antibiotics.

### 2.5.6 Establishing stable transfected cell lines

pcDNA6/TR<sup>®</sup> TetR cells:

EpH4-TetR, EpC40-TetR and EpRas-TetR cells were selected with Blasticidin (25µg/ml). As control there was always one plate of the corresponding parental cell lines selected as well. The selection was ended when the parental cells were dead.

pcDNA4/TO<sup>®</sup>-ILEI Tet-On-ILEI cells:

EpH4-Tet-On-ILEI, EpC40-Tet-On-ILEI and EpRas-Tet-On-ILEI cells were selected with Zeocin (2mg/ml) and Blasticidin (25µg/ml) at the same time. As control there were always one plate of the corresponding parental cell lines selected as well. The selection was ended when the parental cells were dead.

### 2.5.7 Dox induction (Tet-ON system)

To induct the Tet-ON systems the cells were plated out and when they adhered they were treated with Doxycycline hyclate (5µg/ml) for 24 hours. After that, the cells were harvested and the total protein was checked on a SDS-PAGE gel or used for luciferase assays.

### 2.5.8 TGFβ induction

To induced the cells systems the cells were plated out and when they adhere they were treated with TGFβ (5ng/ml) for 24 hours. After that cells were harvested and the total protein was checked on a SDS-PAGE gel or used for luciferase assays.

### 2.5.9 Renilla FFL reporter assays

Transfected cells (2.5.4) were grown on 96well plates and induced with Dox as described in 2.4.7. The firefly luciferase activity (FFL) was measured by adding a volume of Dual-Glo Luciferase Reagent equal to the culture medium to each well and mixed. For a 96 well plate it was typically 100µl. The plate was incubated at room temperature at least for 10' before measuring the firefly luminescence. To measure the *Renilla* luciferase activity a volume of Dual-Glo Stop & Glo Reagent equal to the culture medium was added to each well and mixed. 10' the mix was incubated and the *Renilla* luminescence was measured. The ratio of luminescence from *Renilla* to FFL was calculated. This ratio was normalised to the ratio of a control well into which no DNA was transfected. The calculations were performed in Excel.

### 2.5.10 *In vitro* cell assays in collagen gels

To allow three-dimensional growth of the cells *in vitro* they were seeded in collagen gels. The day before pouring the gels the cells were splitted to 50% confluence. The collagen stock solution (concentration varies with batch) was diluted with the 10% FCS media to an end-concentration of 1,6 mg/ml. Cells (in their appropriate media) and collagen were pre-cooled on ice and pipetted careful the cells into the collagen. To get a uniform mixture it was pipetted up and down to avoid bubbles. The mixture of cells and collagen was pipetted onto a planar working place 100µl per well (24 well plate) forming a drop. The gel polymerised at room temperature in 10' then the plate was placed in a humid chamber at 37°C for approximately 90'. The gels were fed afterwards and put back on 37°C. Next day, the feeding was repeated with fresh media. The next feeding with freshly prepared media was every other day until the cells formed structures. Depending on the cells 1000- 2000 cells per well were seeded.

Serum free collagen gel medium: DMEM-F12

+ BPE	13µg/ml	Bovine pituitary extract
+ DEX	1µmol/l	Dexamethasone
+ IP	10nM	Isoproterinol
+ TGFα	5ng/ml	
+ Insulin	0,04 I.E./ml	

**2.5.11 *In vitro* cell assays on filters**

For the filter experiments 50.000 cells were plated out per filter (Falcon 3090). Every other day Dox (5µg/ml) was added to the medium in cases of + Dox treatment. On every 2<sup>nd</sup> day the cells were trypsinised and from these cells 50.000 were plated out on fresh filters. Underneath a 6 well filter were 2,7ml of medium and above the filter 1,5ml. For long term exposure to Dox cells were grown on filters for more than 8 days.

**2.5.12 Proliferation curve**

On 6cm dishes 250.000 cells were plated out. From each clone triplicates were made with and without Dox treatment. Every other day Dox (5µg/ml) was added to the medium in cases of +Dox treatment. On every 2<sup>nd</sup> day the cells were trypsinised and counted with CASY®1 (Scharfe System) cell counter. The range of living cells was in this case 10 - 30µm in diameter. After the cell counting 250.000 cells were plated out again. This Procedure was done over 8 days.

## **2.6 Mouse work**

### **2.6.1 Mammary gland fat pad injection of tumor cells**

The cells for injection were trypsinised, counted and washed in PBS. The cells were set up so that 100.000 cells were in 30 $\mu$ l PBS. The mice were narcotised with a mixture of Ketamine (5mg/ml) and Xylazine (0,8mg/ml) 0,2ml per 10g body mass of the mouse. The narcotic was injected intra peritoneal. In every fat pad 30 $\mu$ l of cell suspension were injected. Tumor growth was measured with the calliper ruler. To calculate the Volume of the tumor this equation was used:  $(width^2 \times length)/2$ .

### **2.6.2 Tail vein injection of tumor cells**

The cells for injection were trypsinised, counted and washed in PBS. The cells were set up so that 100.000 cells were in 100 $\mu$ l PBS. The mice were secured in a special apparatus where they could not move. The tail was put under a infra red light so that the tail vein expanded under the warmth. In every tail vein 100 $\mu$ l of cells suspension were injected.

## 2.7 Histology

### 2.7.1 Preparation of frozen tissue samples

The exgrafted tumors from mice were washed in 1x PBS to clear them from blood. In a plastic cubicle a layer of Tissue-Tec was given and put onto dry ice until the underside froze a bit, then the tumor was embedded in Tissue-Tec. After the whole cube was frozen solid the embedded tissue was stored at -80°C.

### 2.7.2 Preparation of PFA-fixed and paraffin embedded tissue sections

The exgrafted tissue was washed once in PBS so that all blood was removed and then fixed in a 4% PFA solution over night at 4°C. The tissue was dehydrated in Tissu-Tek VIP machine.

Dehydrations protocol:

<b>Solution</b>	<b>how long</b>	<b>temperature</b>
Ethanol 70%	2 hours	37°C
Ethanol 80%	1 hour	40°C
Ethanol 96%	1 hour	40°C
Ethanol 100%	1 hour	40°C
Ethanol 100%	1 hour	40°C
Xylol	1 hour	40°C
Xylol	1 hour	40°C
Paraffin	1 hour	60°C

After that the exgrafts were put in a cage with hot paraffin and cooled until they were solid. The paraffin blocks were stored at room temperature.

4µm sections of -10°C pre-cooled paraffin-embedded tissue samples were obtained by cutting with a microtome (HM 355s) and applied on super frost+ glass slides in a warm water bath. For deparafinisation the slides were baked in an oven at 65°C for 1 hour.

## 2.8 Immunocyto- and Immunohistochemistry

### 2.8.1 Staining of Collagen gels

The gels were fixed in -20°C cold acetone : methanol 1:1 mixture for 10' at -20°C. To rehydrate them they were washed with a series of ethanol water mixtures (100%, 70%, 50%, and 25% ethanol), once with PBS then three times with PBST. To block the gels a solution of PBST with 0,2% gelatine and 1:1000 bovine IgG was piped on them. The 1<sup>st</sup> antibody was diluted in blocking solution and put on the gels for 1 hour. The gels were washed three times rapidly with PBST and three more times slowly in PBST. The 2<sup>nd</sup> antibody was also applied in blocking solution and incubated for 1 hour. To obtain a background as low as possible the gels were washed three times rapidly with PBST and three times slowly with PBST. After that the gels were put on glass slides and mounted with Prolong Gold (Promega) in which DAPI was already present. The slides were kept at room temperature for one night to dry and were sealed with nail polish on the edges the next day. After that the slides were stored at 4°C.

### 2.8.2 Staining of PFA-fixed paraffin-embedded tissue sections

#### 2.8.2.1 Hematoxylin and Eosin staining

Staining protocol in Shandon Thermo machine at room temperature:

<b>Solution</b>	<b>how long</b>
2x Xylol	10'
2x Ethanol 100%	2'
Ethanol 90%	30''
Ethanol 80%	30''
Ethanol 70%	30''
Ethanol 30%	30''
H <sub>2</sub> O	1'
Hematoxylin 0,4%	5'
H <sub>2</sub> O	2'
HCl 4,4mM	6''
H <sub>2</sub> O	2'
H <sub>2</sub> O	1'
H <sub>2</sub> O	5'
Ethanol 30%	30''
Ethanol 70%	30''
Ethanol 80%	30''
Eosin 0,5%	20''
Ethanol 90%	30''
Ethanol 100%	30''
2x Xylol	2'

#### 2.8.2.2 Cleaved caspase 3 staining

This stainings were taken in Ventana Discovery with the ChromoMap™ DAB kit in combination with UltraMap™ kit.

#### 2.8.2.3 Ki67 staining

This stainings were taken with the DABMap™ DAB kit in in Ventana Discovery machine. From every tumor three frames were photographed at different sites. For the evaluation of the stainings the number of blue and brown stained nuclei was counted manually in every frame. The total number of nuclei served as 100% for calculations.

## 2.8.2.4 ILEI staining

Memo kindly stained this glass slides for me.

Solution	how long	temperature
Deparaffination		
3x Xylene	7'	RT
Ethanol 100%	1'	RT
Ethanol 100%	1'	RT
Ethanol 50%	1'	RT
Ethanol 50%	1'	RT
3x H <sub>2</sub> O	1'	RT
Retrieval buffer <sup>∞</sup>	20'	99°C

The slides were removed from the retrieval buffer and air-dried at RT. Tissues were encircled with a PAP pen.

The following drop reactions (\*) were obtained in a wet chamber.

1x PBS	8'	
Goat serum 29%	15' (*)	
Rabbit anti ILEI antibody <sup>#</sup>	60' (*)	
1x PBS	10''	
1x PBS	2'	
1x PBS	2'	
Blocking endogenous peroxidise		
H <sub>2</sub> O <sub>2</sub> / 1x PBS 0,3%	20'	
Goat anti rabbit antibody	30'' (*)	
1x PBS	10''	
1x PBS	2'	
1x PBS	2'	
Streptavidine-biotine <sup>§</sup>	30' (*)	
1x PBS	10''	
1x PBS	2'	
1x PBS	2'	
Coulour development in AEC <sup>Δ</sup>	6' to 8'	
H <sub>2</sub> O	1'	
Hematoxylin 1g/l	2' to 3'	
H <sub>2</sub> O	every 30'' over 8'	

The slides were dried at RT for about 15', mounted with Aquatex solution and covered with slides.

<sup>#</sup> Rabbit anti ILEI polyclonal antibody. Dillution 1:300, pre-incubated with a pool of 8ng/ml of momologous peptides Fam3A and Fam3D to avoid cross reactions.

<sup>∞</sup> EDTA1mM/Tween20 0,05% pH=8

<sup>§</sup> Streptavidin-biotin complex. 1ml 1x PBS was mixed with 10μl solution A, and 10μl solution B. The mixture was incubated at RT for 30' after that 1ml 1x PBS and 20μl horse sera was added.

<sup>Δ</sup> AEC Solution 3,3-amino-9-ethyl carbazole in 100ml N,N-dimethylformamid. For working solution 7ml stock were added to 200ml sodium-acetate buffer (20mM, pH=4,9) and filtered. Finally 22μl H<sub>2</sub>O<sub>2</sub> were added.

## **2.9 Microscopy**

### **2.9.1 Light and fluorescence microscopy**

For light microscopy pictures of histological stainings the Axioplan 2 from Zeiss was used with Image Access software. The light microscopy cell pictures were taken with a Leitz Laborvert FS microscope with Scion Image software. For the pictures of the collagen gels the Zeiss Axiovision microscope with metamorph software was used.

### **2.9.2 Confocal microscopy**

All pictures of stained collagen gels are single Z-stack photos made with a Zeiss LSM510 confocal microscope with LSM510 software.



### 3 RESULTS

#### 3.1 Generating the TetR clones

To learn something about the relevance of ILEI levels in tumor progression and growth we decided to generate inducible ILEI over-expressing clones in the EpH4 cell system.

For the transfection of the cells with the two constructs of the T-Rex inducible expression system a stepwise approach was used (FIGURE 21). Clones were selected and characterised for an unchanged phenotype after each step.

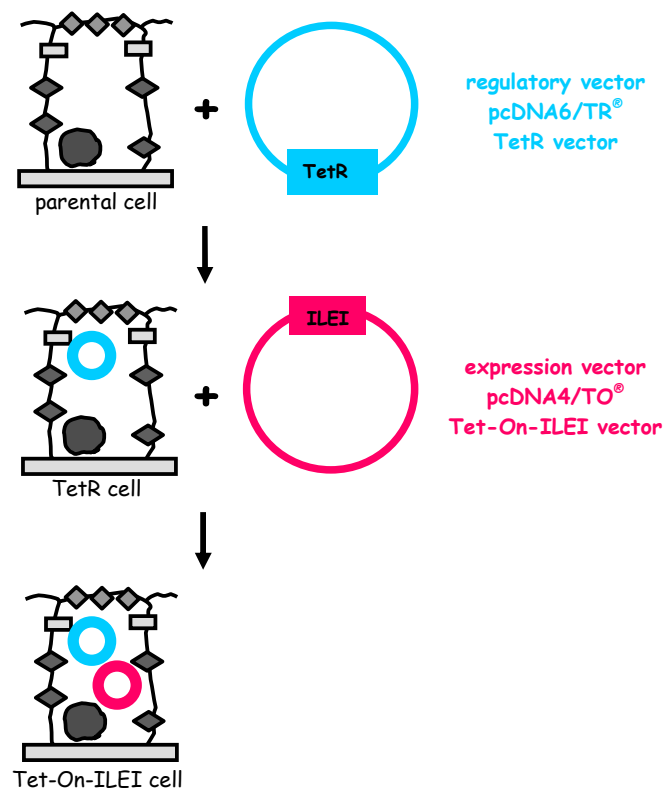
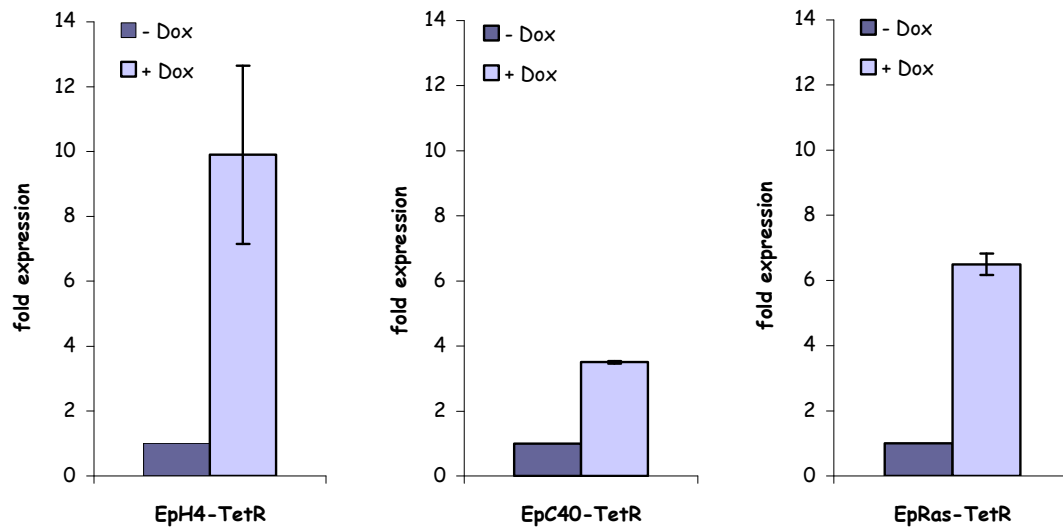


FIGURE 21 | Cloning strategy and stepwise approach for transfection.

For the generation of TetR clones EpH4, EpC40 and EpRas parental cells were transfected with the pcDNA6/TR® vector. The transfected TetR cells were selected with Blasticidin (25µg/ml) (for minimum 5 days) followed by isolation of single cell clones. TetR-clones with epithelial phenotype were elected for further studies were following transiently transfected with the pcDNA4/TO-FFL reporter and the pRL-TK2-Renilla control vector. To test the inducibility of the TetR-clones, they were cultured in the presence and absence of Doxycycline (Dox) (5µg/ml) for 24 hours. A combined FFL Renilla dual luciferase reporter assay pointed out the high expressing clones of each cell line (FIGURE 22).



**FIGURE 22 | Inducibility of the best TetR clones from each cell line.**  
 EpH4-TetR clone expresses 9,7 times more FFL upon Dox induction than the uninduced one. The induced EpC40-TetR clone expresses 3,5 times more of the reporter gene than the uninduced control. In case of the EpRas-TetR cells the induction with Dox increases the FFL expression by 6,2 fold. The error was calculated with standard deviation (SD).

Some of the single cell clones were excluded from further studies based on slow growth rate or loss of epithelial morphology. From all the clones only a few had an induction capability of over two fold (TABLE 2). Statistically 50 to 100 clones had to be analysed in order to get a clone with reasonable inducibility.

	EpH4-TetR		EpC40-TetR		EpRas-TetR	
	No.	%	No.	%	No.	%
Clones transferred from 96 to 24 well plates	557		506		166	
Clones grown on 24 well plates after expansion	463	83,1	470	92,9	143	86,1
Clones tested in the luciferase reporter assay	170	30,5	235	50,0	92	55,4
Clones with induction capacity < 1 fold	28	16,5	115	48,9	39	42,4
Clones with induction capacity of 1 - 1,5 fold	88	51,8	112	47,7	49	53,3
Clones with induction capacity of 1,5 - 2,0 fold	49	28,8	5	2,1	2	2,2
Clones with induction capacity > 2,0 fold	5	2,9	3	1,3	2	2,2

**TABLE 2 | Statistics of tested Tet-R clones.**  
 The number of clones transferred to 24 well plates is 100% to the next two rows. For the calculations of induction capacity the number of luciferase tested clones was taken as 100%.

### 3.1.1 *In vitro* characterisation of the TetR-clones

It was necessary to characterise the TetR-clones with reference to the parental cell lines so that further experimental data with the over expressed gene of interest are comparable to the original cell lines. First, the morphology on plastic was determined (FIGURE 23).

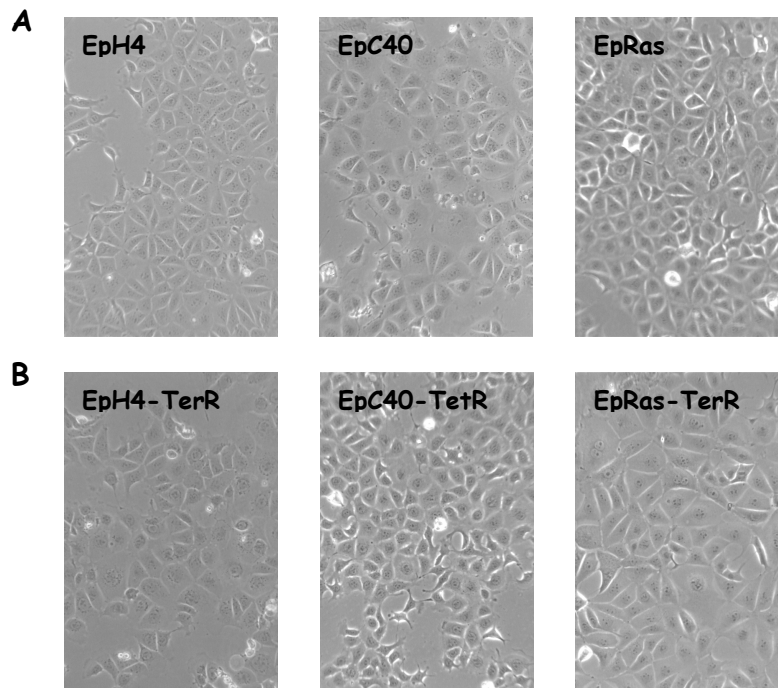


FIGURE 23 | Epithelial morphology of the parental cell lines and the TetR clones on plastic culture dishes.  
A) parental cell lines B) TetR clones

There were no differences in morphology between the parental cell lines and the TetR clones to observe when cells were grown on plastic culture dishes.

The morphology of parental cell lines and TetR-clones was also tested in collagen gels upon TGF $\beta$  treatment (FIGURE 24). In all cases the parental cells and the TetR clones grow in their typical structures and reacted as expected to TGF $\beta$  treatment.

Eph4 and Eph4-TetR cells form both hollow, organotypic structures and die upon TGF $\beta$  treatment (FIGURE 24 A and B).

EpC40 and EpC40-TetR cells form hollow structures without TGF $\beta$  and undergo scattering when TGF $\beta$  is added. Scattering cells move out of the collective structures and are spindle shaped (FIGURE 24 C and D).

EpRas and EpRas-TetR cells form hollow spheres of cells without TGF $\beta$  and undergo EMT upon TGF $\beta$  treatment which can be seen in the spiky, invasive outgrowths (FIGURE 24 E and F).

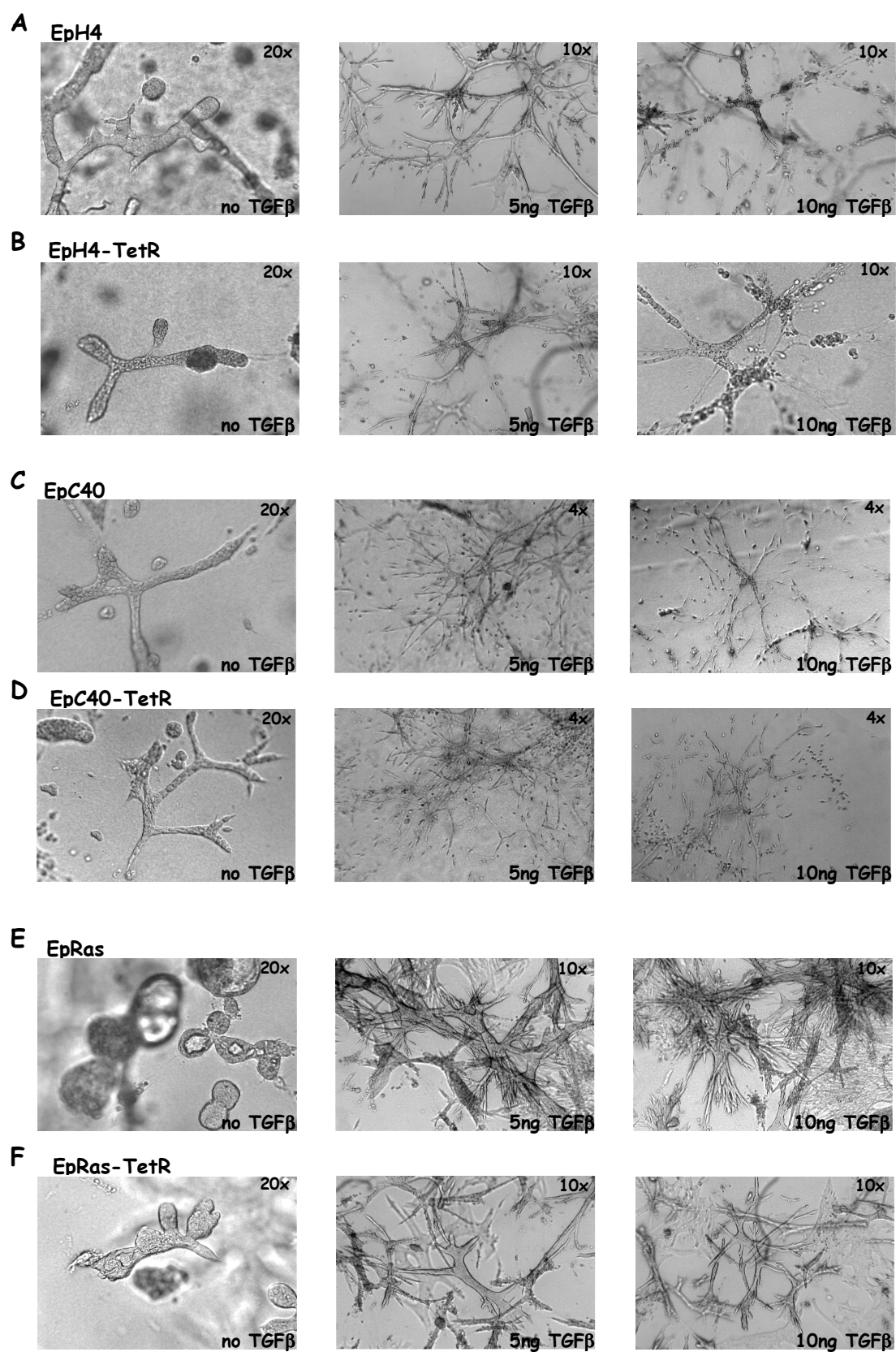
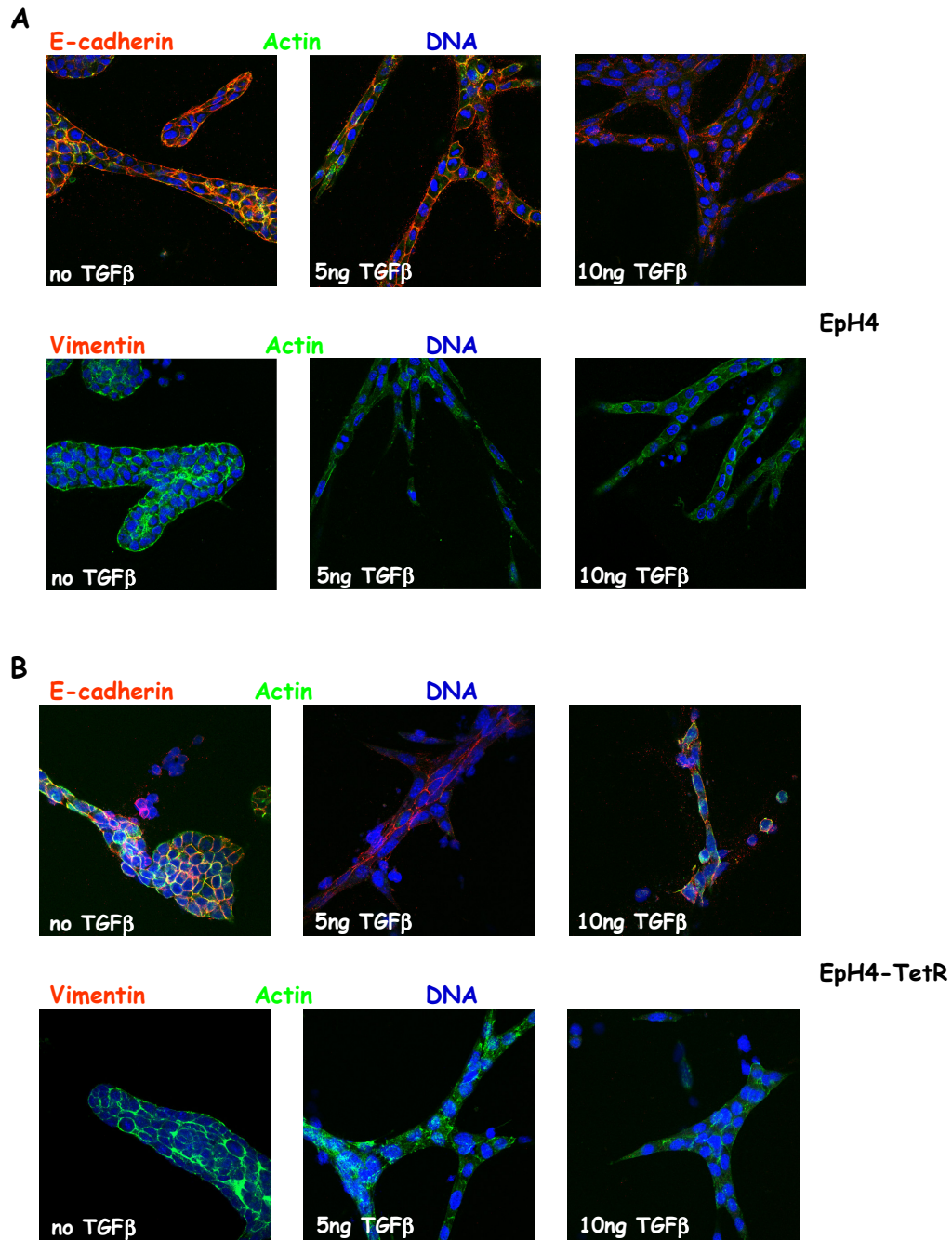


FIGURE 24 | Comparison of the parental cell lines and the TetR clones in collagen gels upon TGF $\beta$  treatment.

The changes in marker expression upon TGF $\beta$  treatment was checked in collagen gels (FIGURE 25 to 27).



**FIGURE 25 |** Marker staining of Eph4 and Eph4-TetR cells in collagen gels upon TGF $\beta$  treatment.  
 A) parental Eph4 cells in the top panel stained for E-cadherin (red), actin (green) and DNA (blue) and in the bottom panel stained for Vimentin (red), actin (green) and DNA (blue).  
 B) Eph4-TetR cells, stained the same way.

Eph4 and Eph4-TetR cells show both strong E-cadherin staining but no vimentin staining (FIGURE 25).

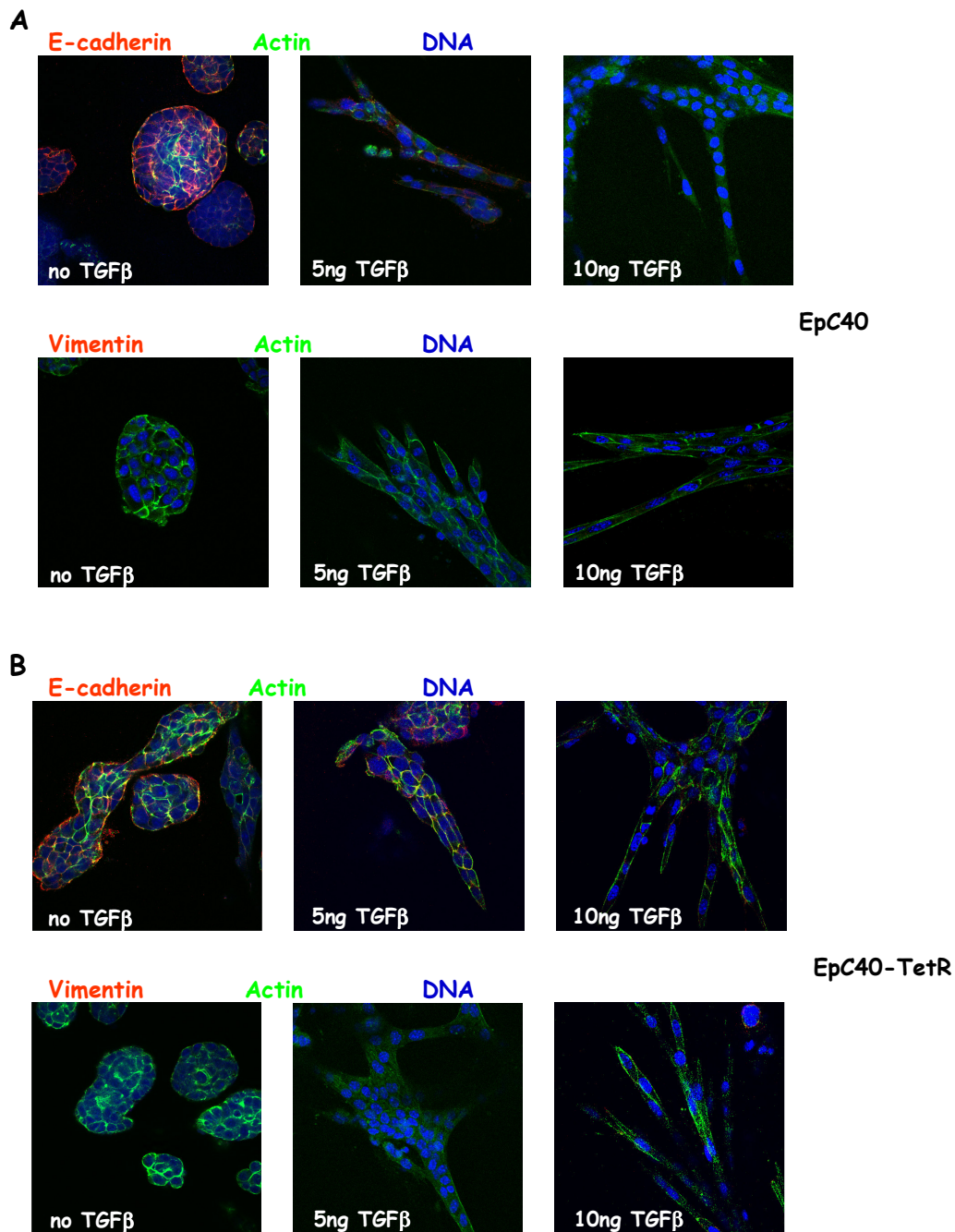


**FIGURE 26 |** Marker staining of EpC40 and EpC40-TetR cells in collagen gels upon TGFβ treatment.

A) parental EpC40 cells in the top panel stained for E-cadherin (red), actin (green) and DNA (blue) and in the bottom panel stained for Vimentin (red), actin (green) and DNA (blue).

B) EpC40-TetR cells, stained the same way.

EpC40 and EpC40-TetR cells show both strong cortical E-cadherin expression, which is down regulated when TGFβ is added. Vimentin staining is not present in EpC40 or EpC40-TetR cells neither with nor without TGFβ treatment (FIGURE 26).



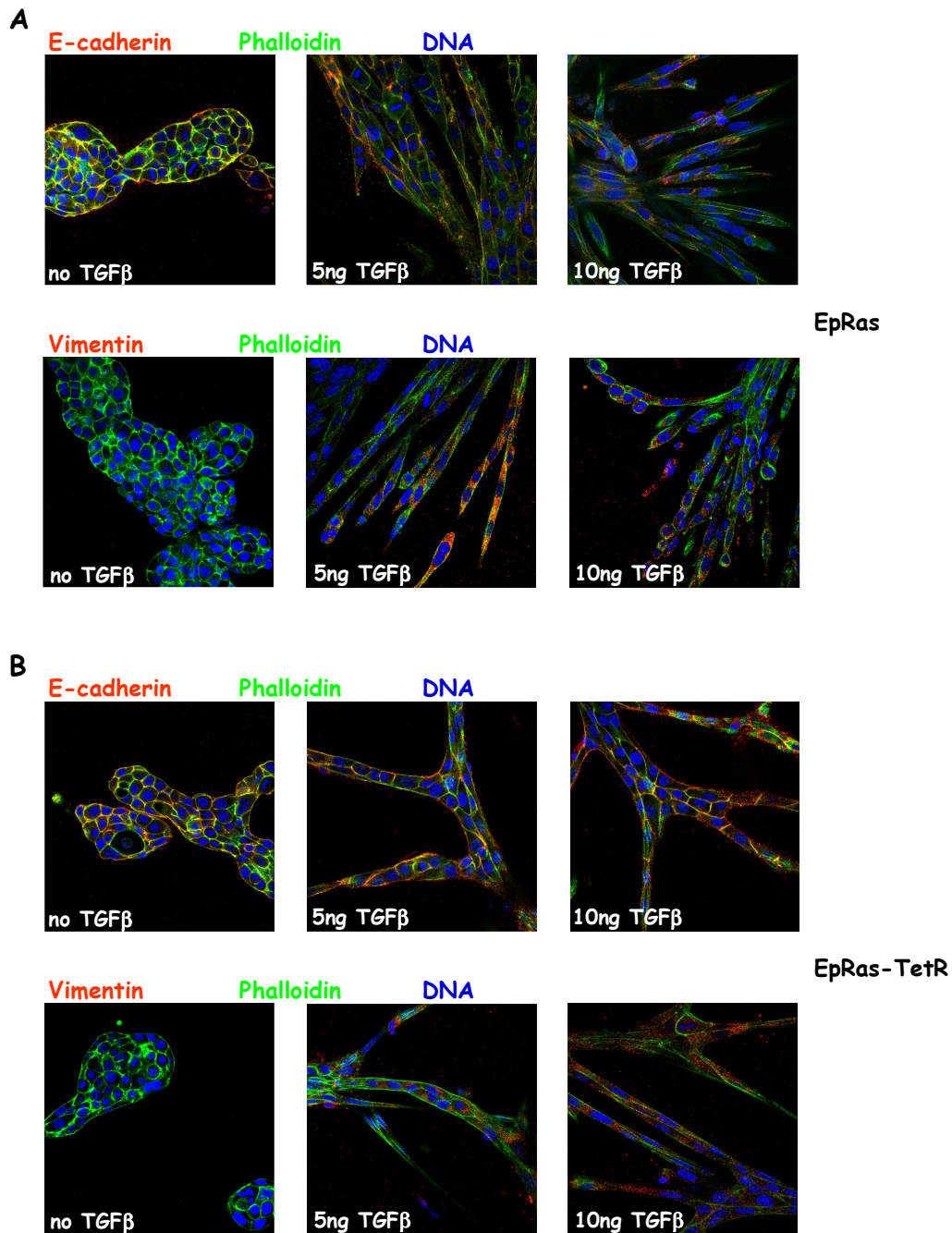


**FIGURE 27 | Marker staining of EpRas and EpRas-TetR cells in collagen gels upon TGFβ treatment.**  
 A) parental EpRas cells in the top panel stained for E-cadherin (red), actin (green) and DNA (blue) and in the bottom panel stained for Vimentin (red), actin (green) and DNA (blue).  
 B) EpRas-TetR cells, stained the same way.

EpRas and EpRas-TetR cells express E-cadherin when no TGFβ is present and down regulate it when TGFβ is added. Vimentin is not present without TGFβ but when cells are treated with TGFβ it is expressed (FIGURE 27).

### 3.1.2 *In vivo* characterisation

After the *in vitro* characterisation mouse experiments were performed to compare the parental cell lines with the generated TetR clones *in vivo*. Tumor growth was tested by injecting 100.000 cells to the mammary gland fat pads of nude mice. The growth was measured for several weeks (FIGURE 28).

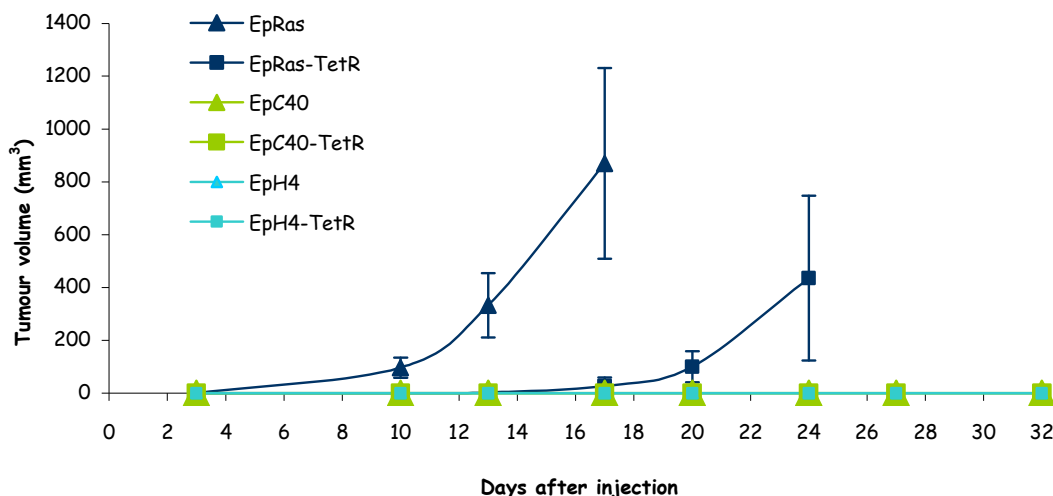


FIGURE 28 | Tumor growth of all parental cell lines and TetR clones in nude mice. The error bars were calculated with standard deviation (SD).

The graph in FIGURE 28 shows that both parental EpRas cells and EpRas-TetR cells formed tumors, in contrast to EpC40 and EpC40-TetR as well as EpH4 and EpH4-TetR cells. In comparison to the EpRas parental cells the EpRas-TetR cells grow slower (FIGURE 28). After a long period EpC40 and EpC40-TetR cells formed nodules as well, indicating a very slow tumor growth of EpC40 and EpC40-TetR cells. This is why in the following experiments a 10 fold higher number of EpC40-TetR cells was used (FIGURE 29).

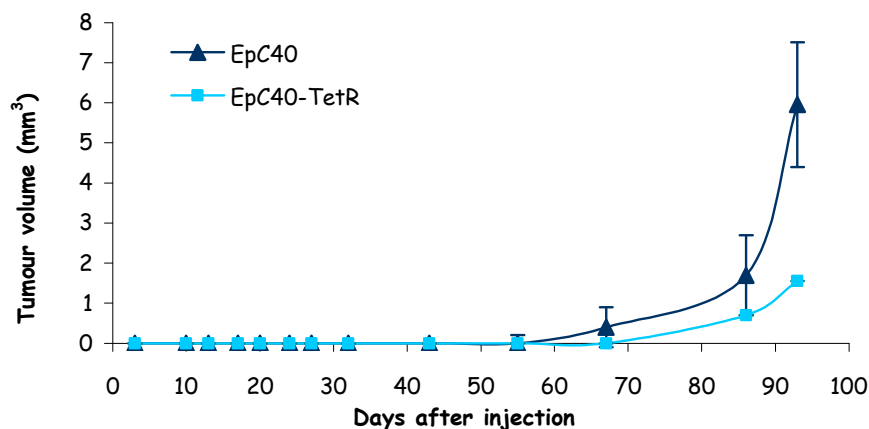


FIGURE 29 | Tumor growth of EpC40 and EpC40-TetR cells in nude mice. The error bars were calculated with standard deviation (SD).



The metastatic capabilities of EpRas, EpC40 and both TetR clones were investigated by tail vein injection. 100.000 cells per mouse were injected intravenously to see if the lung would be colonised by these cells (FIGURE 30). The survival of the mice was monitored after tail vein injection.

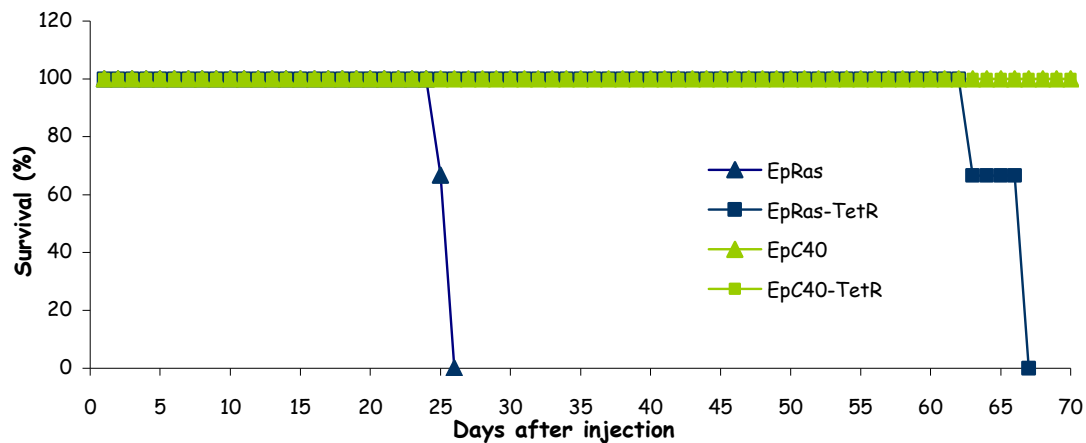


FIGURE 30 | Survival rate of nude mice after tail vein injection of EpRas, EpRas-TetR, EpC40 and EpC40-TetR cells.

The blot shows that parental EpRas cells developed lung metastases faster than the corresponding TetR cells. This agrees with the observation that they showed slower tumor growth. Both, EpC40 and EpC40-TetR cells failed to form lung metastases.

Metastasis formation was confirmed by the analysis of the lungs from the dead mice. The lungs of mice with injected parental and TetR cells were dissected and compared (FIGURE 31).

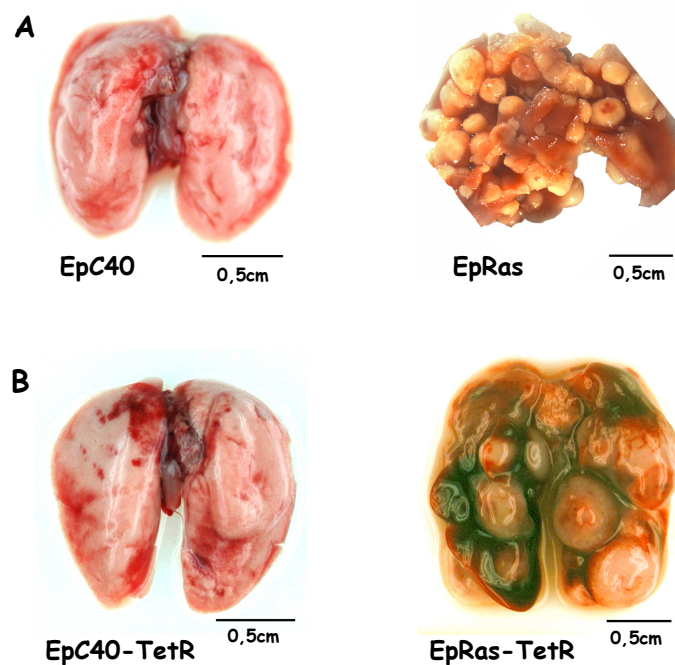


FIGURE 31 | Lung colonisation of parental and TetR cells in nude.

The dissected lungs mirrored the results of the survival statistics. No metastases in EpC40 and EpC40-TetR injected mice and huge metastases in EpRas and EpRas-TetR mice were observed.

### 3.2 Tet-On-ILEI overexpressing clones

ILEI was cloned into the multiple cloning site of the pcDNA4/TO<sup>®</sup> expression vector. For the generation of Tet-On-ILEI clones, EpH4-TetR, EpC40-TetR and EpRas-TetR cells were transfected with the pcDNA4/TO<sup>®</sup>-ILEI vector. The transfected Tet-On-ILEI cells were selected with Zeocin (2mg/ml) followed by isolation of single cell clones. Some of the single cell clones were excluded from further studies based on slow growth rate or loss of epithelial morphology (TABLE 3).

	EpH4-Tet-On-ILEI		EpC40-Tet-On-ILEI		EpRas-Tet-On-ILEI	
	No.	%	No.	%	No.	%
Clones transferred from 96 to 24 well plates	53		61		49	
Clones grown on 24 well plates after expansion	39	73,6	47	77,0	29	59,2
Cells with mesenchymal phenotype	7	17,9	21	44,7	1	3,4
Expanded cells with epithelial phenotype	32	82,1	26	55,3	28	96,6

TABLE 3 | Statistics of tested Tet-On-ILEI clones

The number of clones transferred to 24 well plates is 100% to the next row. For the cells with epithelial and mesenchymal phenotype the expanded cells on 24 well plates were taken as 100%.

#### 3.2.1 *In vitro* characterisation of the Tet-On clones

##### 3.2.1.1 Western blot analysis for inducibility

To test the inducibility of the Tet-On-ILEI-clones they were cultured in the presence or absence of Dox (5µg/ml) for 24 hours. Western blot analysis of concentrated supernatant (SN) and whole cell lysates (IC) was used for each cell line to identify clones with high ILEI inducibility (FIGURE 32 to 34).

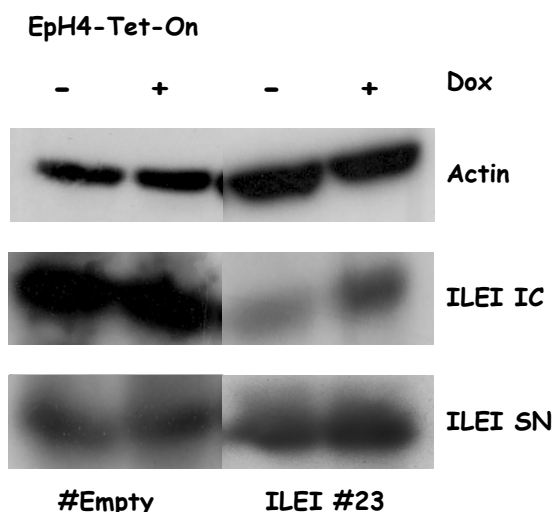
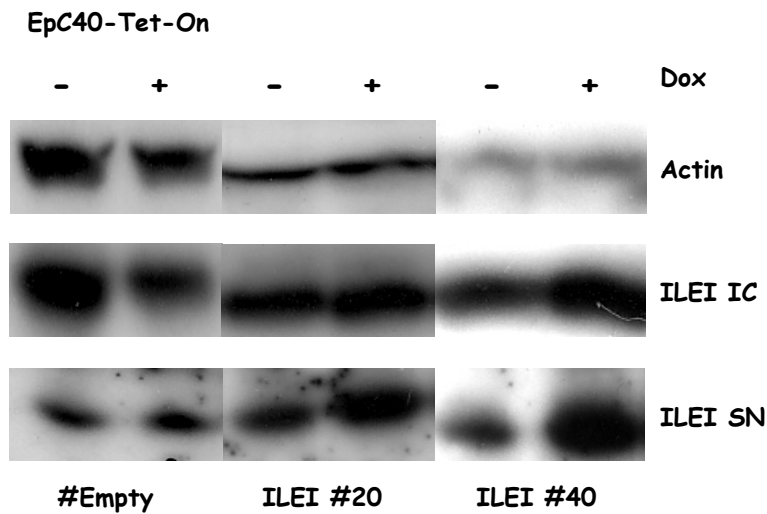


FIGURE 32 | Western blot analysis for ILEI on culture supernatant (SN) and on whole cell lysate (IC) of Eph4-Tet-On-ILEI cells with or without Dox induction.

The analysis on Western blot shows that the Eph4-Tet-On-ILEI clone #23 has slightly elevated ILEI levels in the supernatant and elevated intracellular ILEI levels when treated with Dox in comparison to no Dox treatment. In case of the Eph4-Tet-On-Empty control the ILEI levels were not enhanced with Dox addition.



**FIGURE 33 |** Western blot analysis for ILEI on culture supernatant (SN) and on whole cell lysate (IC) of EpC40-Tet-On-ILEI cells upon Dox induction or without induction.

EpC40-Tet-On-ILEI clone #20 had low levels of ILEI in general but when induced with Dox, the ILEI levels were higher, predominantly in the supernatant. The EpC40-Tet-On-ILEI clone #40 showed generally high ILEI levels with or without induction but when induced with Dox, the supernatant- and intracellular ILEI levels were elevated.

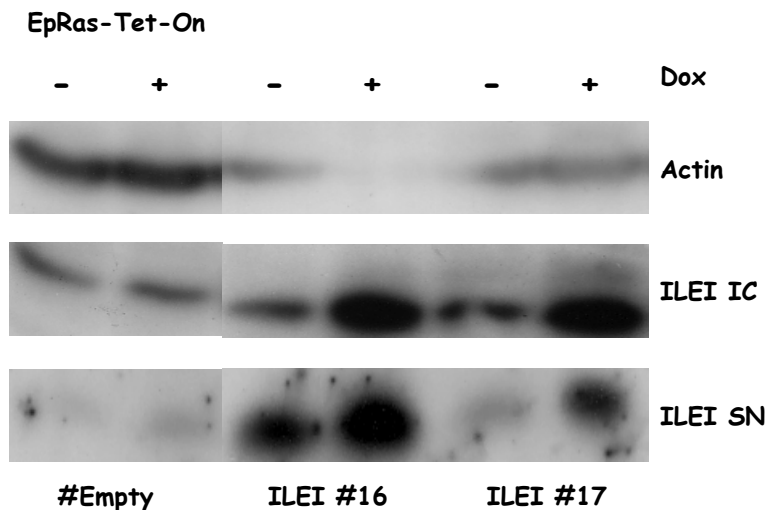


**FIGURE 34 |** Western blot analysis for ILEI on culture supernatant (SN) and on whole cell lysate (IC) of EpRas-Tet-On-ILEI cells upon Dox induction or without induction.

EpRas-Tet-On-ILEI clone #16 had a high basal ILEI level nevertheless showed nicely elevated ILEI levels upon expression with Dox both intracellularly and in the supernatant. The EpRas-Tet-On-ILEI clone #17 had a lower ILEI expression without induction, than the clone #16 but a strikingly high inducibility.

### 3.2.1.2 Proliferation curves

To see if the Dox induction and therefore the higher ILEI concentration in the cells and in the surrounding medium had an effect on growth rate. Proliferation studies were performed (FIGURE 35 to 37).

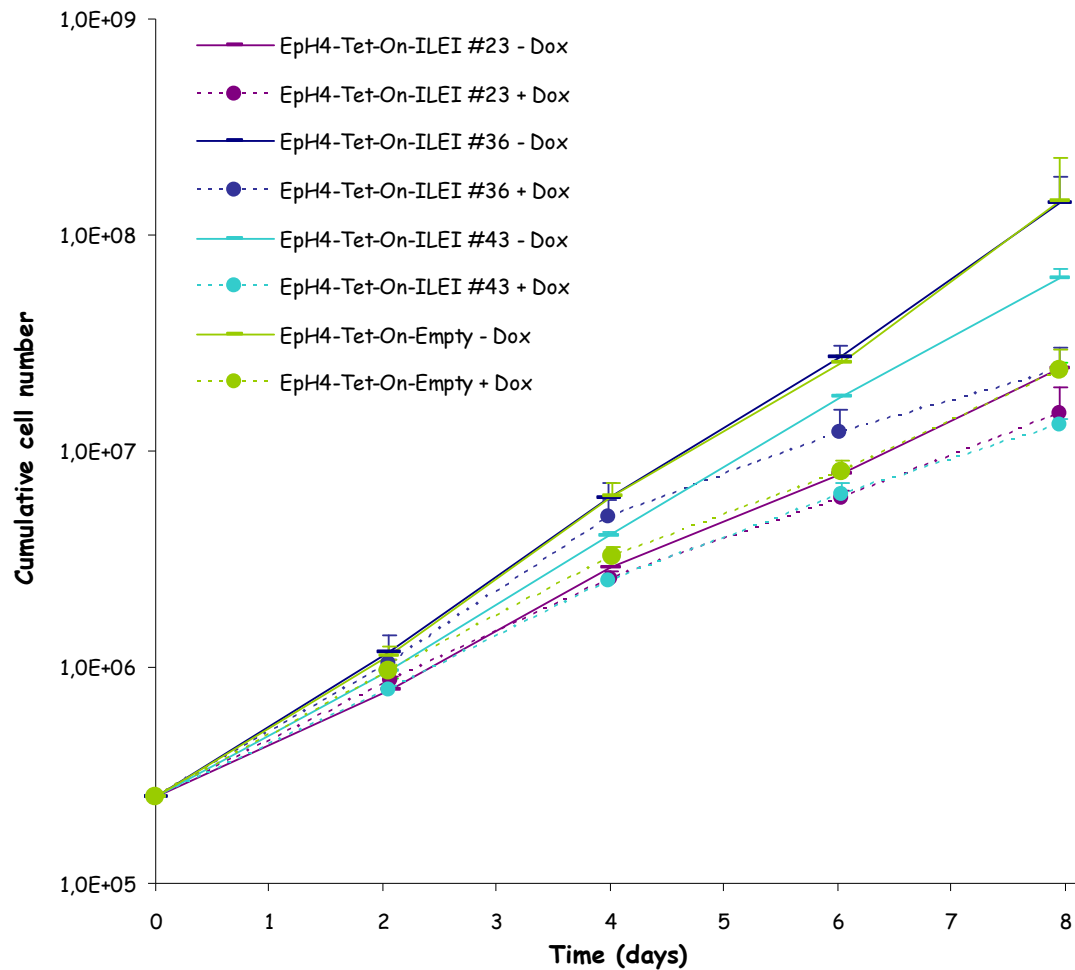


**FIGURE 35 |** Proliferation curve of different Eph4-Tet-On-ILEI clones with and without Dox induction. The error bars were calculated with standard deviation (SD).

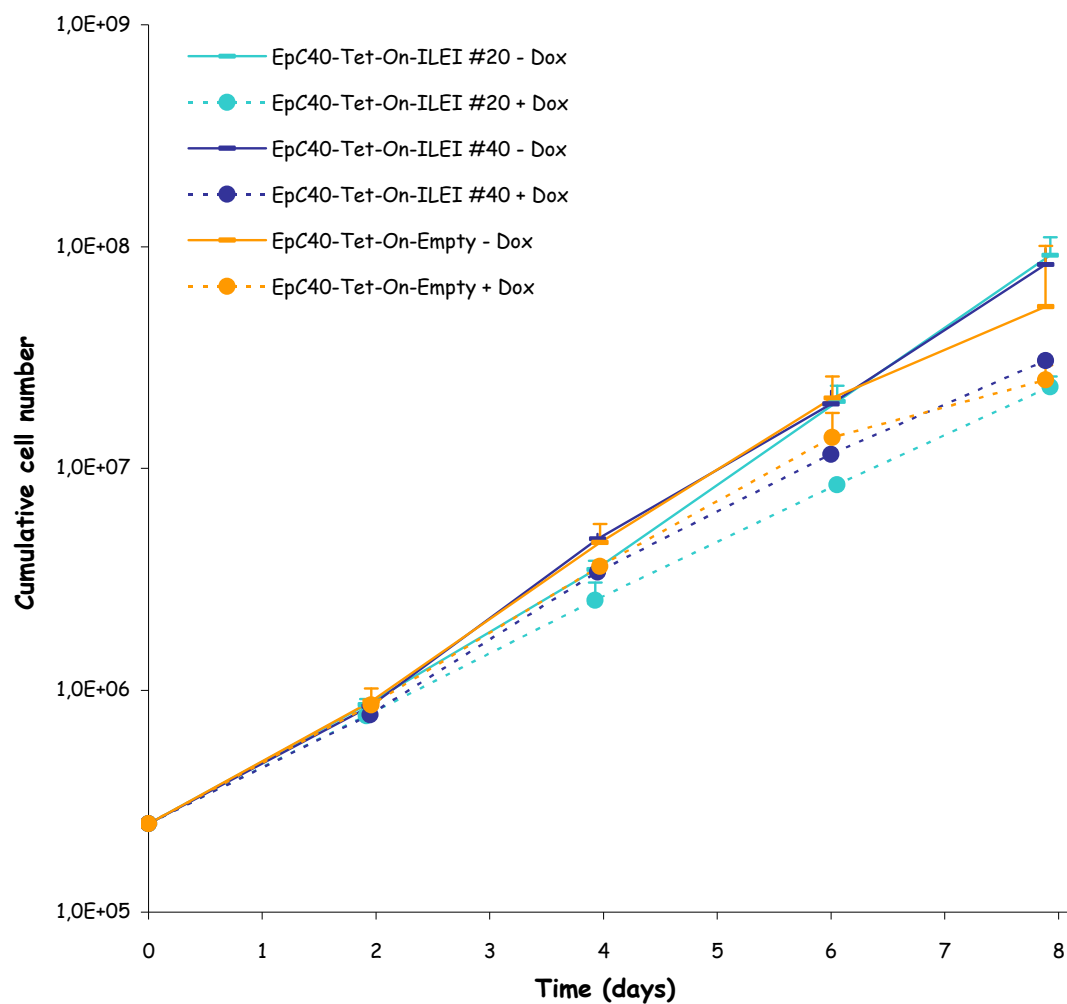
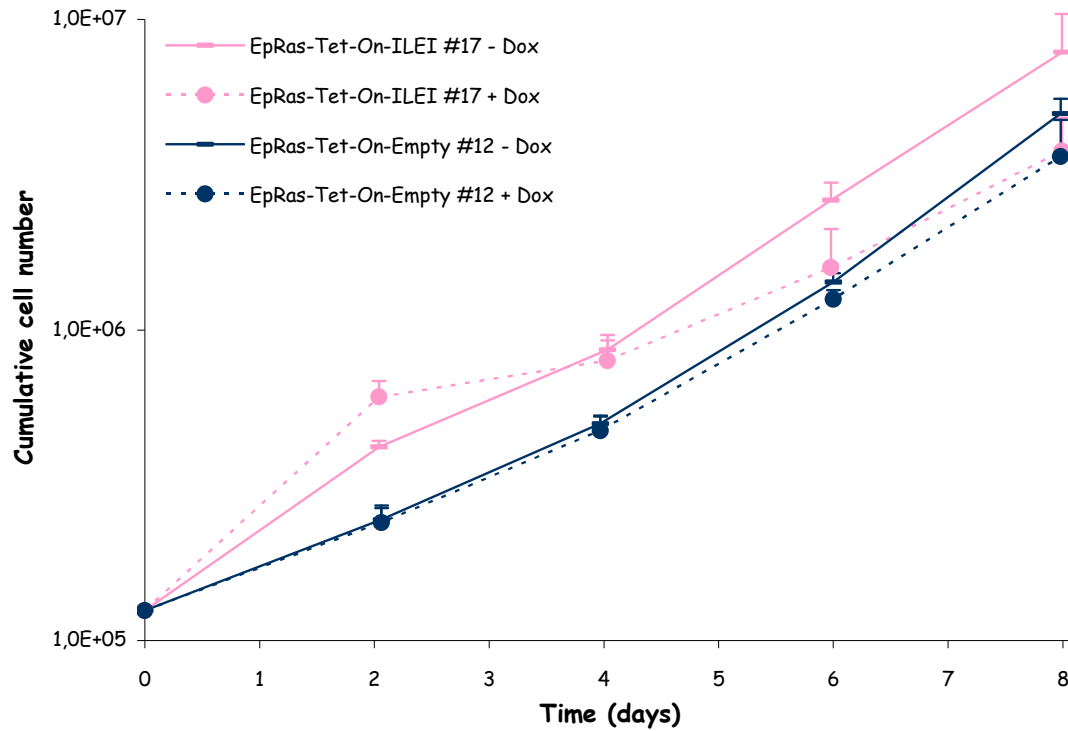


FIGURE 36 | Proliferation curve of different EpC40-Tet-On-ILEI clones with and without Dox induction. The error bars were calculated with standard deviation (SD).



**FIGURE 37 |** Proliferation curve of different EpRas-Tet-On-ILEI clones with and without Dox induction. The error bars were calculated with standard deviation (SD).

For all clones in all cell lines it is true that the uninduced cells grow a bit faster than the ones treated with Dox. However this difference was not significant. This indicates, that ILEI had no effect on cell proliferation.

### 3.2.1.3 Morphology of the Tet-On clones

We tested if there were morphological changes on plastic when Dox was added for a longer period of time (minimum 8 days). On plastic, there were no differences visible in all tested cell lines.

To see if morphological differences were developed when cells are grown on porous supports, EpC40-Tet-On-ILEI cells were treated prolonged with Dox. This way secreted ILEI has not only to the apical membrane but also to the basolateral membrane free access. As a representative example for all cell lines experimental data of EpC40-Tet-On-ILEI cells are shown (FIGURE 38).

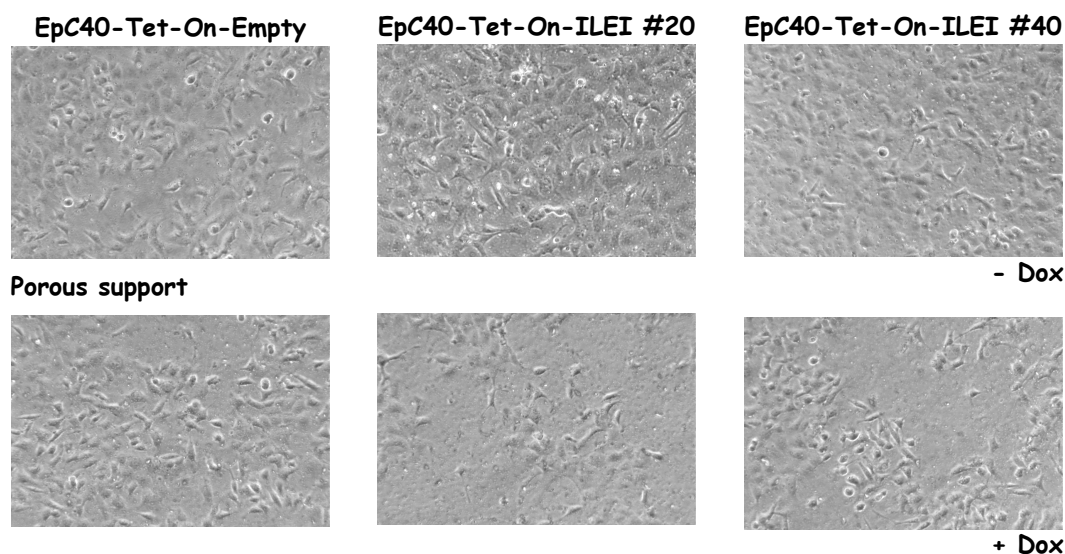
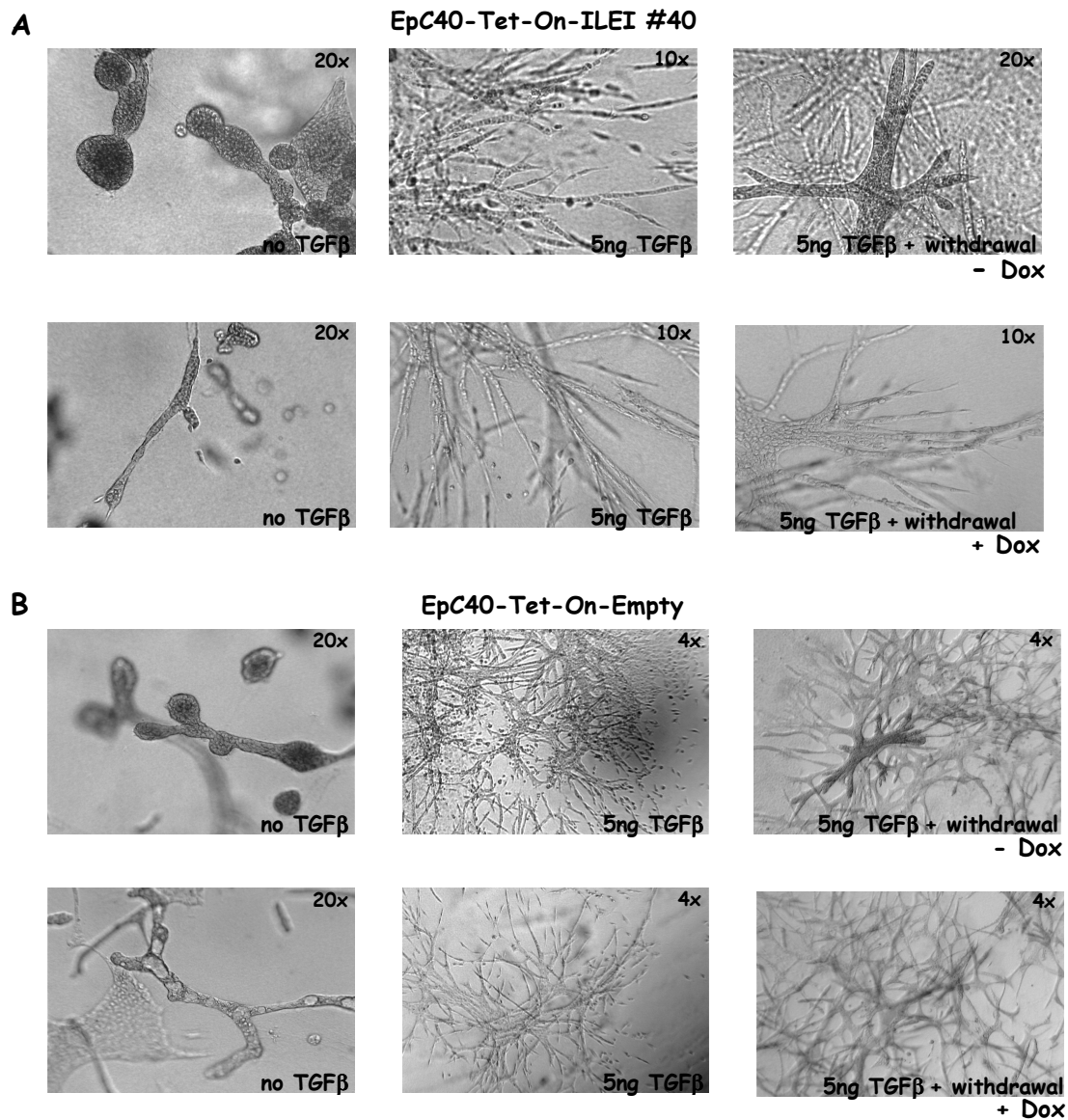


FIGURE 38 | EpC40-Tet-On-ILEI clones grown on porous support.

No morphology changes could be observed by long-term Dox treatment on porous support compared to untreated cells.

In collagen gels, the morphology of EpRas-Tet-On-ILEI and EpH4-Tet-On-ILEI was the same regardless if treated with Dox or not. The only cells showing a slight difference were EpC40-Tet-On-ILEI #40 (FIGURE 39)



**FIGURE 39 |** Collagen gels of EpC40-Tet-On-ILEI empty with different TGFβ concentrations. First slide with no TGFβ treatment, second slide 5ng TGFβ treatment and third slide first a 5ng TGFβ treatment for 2 days and then a 4 to 5 days withdrawal. In the upper panel no Dox, lower panel 1ml/ml Dox over the whole period of the experiment.

Normally, EpC40 cells form tubular, epithelial structures in collagen gels. This changes to a scattering phenotype upon TGFβ treatment in a reversible manner. Thus the TGFβ induced scattering, spindle shaped migrant cells reverted back to more rounded, compact structures if the factor is withdrawn. As expected, EpC40-Tet-On-Empty cells showed exactly this phenotype regardless the addition of Dox. It was the same in case of EpC40-Tet-On-ILEI #40 in the absence of Dox. Addition of Dox had also no effect on the epithelial structure formation and scattering phenotype of EpC40-Tet-On-ILEI cells. However, in the presence of Dox these cells showed a lack of epithelial reversion after TGFβ withdrawal, and kept their spiky morphology.



### 3.2.2 *In vivo* characterisation of the EpRas-Tet-On-ILEI and EpC40-Tet-On-ILEI clones

After the *in vitro* characterisation mouse experiments were done to compare tumor formation and lung colonisation of EpC40-Tet-On-ILEI and EpRas-Tet-On-ILEI cell lines with and without Dox induction.

The tumor growth of the different EpC40-Tet-On-ILEI clones was tested in the same way as in the case of EpRas-Tet-On-ILEI with the exception, that 1.000.000 cells per fat pad were injected (FIGURE 40). The greater number of cells is because the EpC40 cells grow slower *in vivo* than the EpRas cells (see chapter 3.1.4).

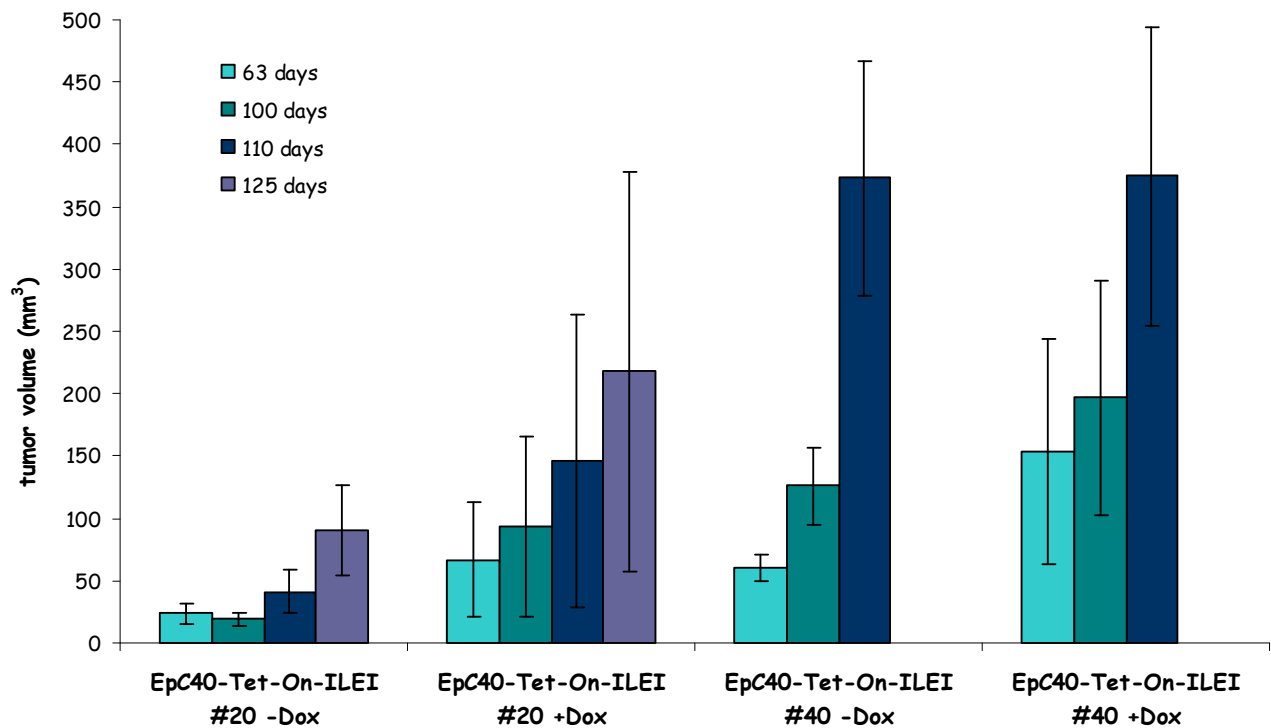
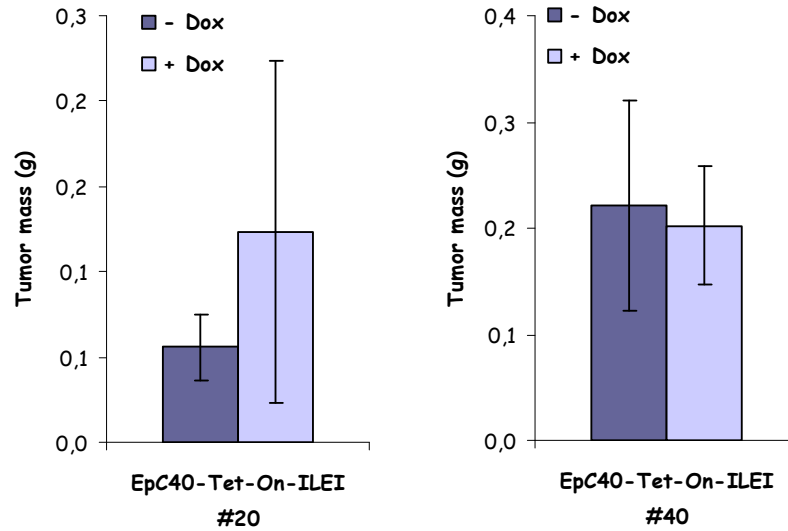


FIGURE 40 | Time course of tumor growth of EpC40-Tet-On-ILEI clones #20 and #40 with or without Dox. The error bars were calculated with standard error of means (SEM).

The EpC40-Tet-On-ILEI clone #20 showed a slight increase in tumor growth when treated with Dox in contrast to the untreated one. The difference is not significant but a tendency is there. The EpC40-Tet-On-ILEI clone #40 shows no difference in tumor volume with or without Dox and has a faster tumor growth in general. These findings are reflected in the Western blots, where the two clones were induced. Clone #20 had a lower basal level of ILEI in comparison to clone #40.

When the EpC40-Tet-On-ILEI tumors #20 and #40 exceeded a certain dimension they were excised after scarification of the mice and weighed (FIGURE 41).



**FIGURE 41 |** Tumor mass of EpC40-Tet-On-ILEI clones #20 and #40 upon Dox induction. The error was calculated with standard error of means (SEM).

The clone EpC40-Tet-On-ILEI #20 shows some differences upon Dox induction in contrary to the EpC40-Tet-On-ILEI clone #40, which showed no differences in growth upon Dox induction. This might be a result of the already higher ILEI levels in the clone #40.

Tumor growth in the EpRas-Tet-On-ILEI cell lines was tested by injecting 100.000 cells in to the mammary gland fat pads of nude mice. The Tumor diameter was measured over several weeks (FIGURE 42). To ensure Dox induction, the drinking water of mice was supplemented with 5% sucrose either with or without 1mg/ml Dox and changed every second day.

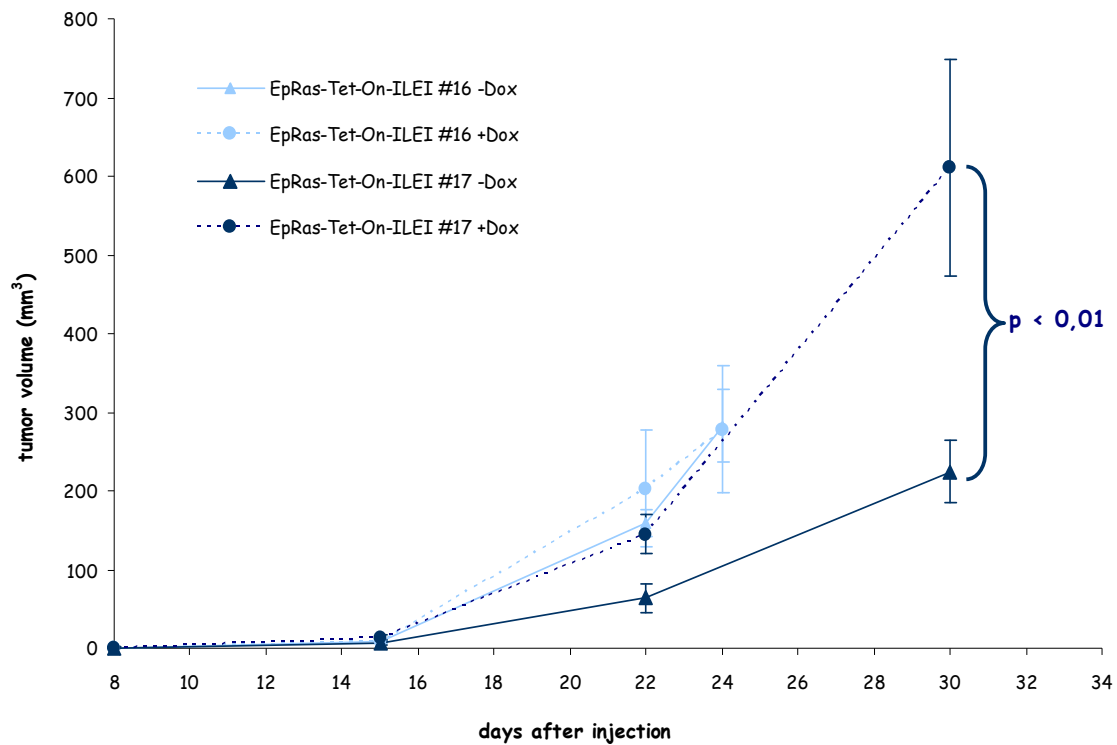


**FIGURE 42 |** Tumor growth of EpRas-Tet-On-ILEI clones #16 and #17 upon Dox induction in nude mice. The error bars were calculated with standard error of means (SEM).

When the EpRas-Tet-On-ILEI tumors #16 and #17 exceeded a certain dimension they were explanted and weighed (FIGURE 43).

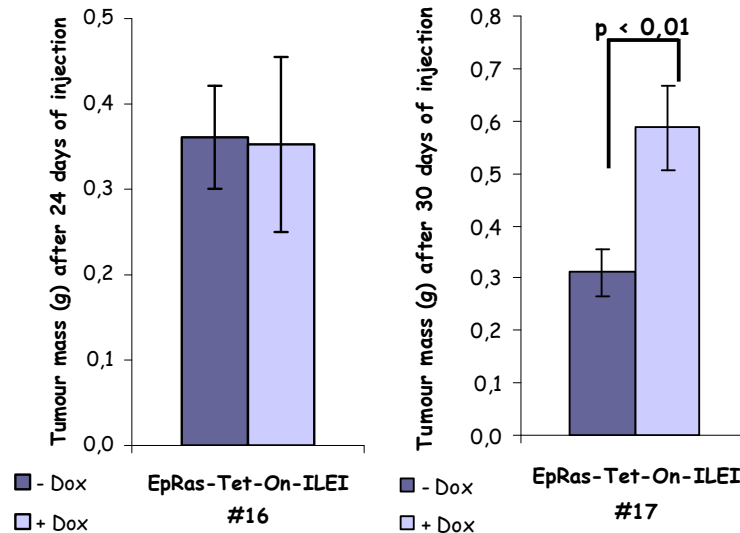


**FIGURE 43 |** Tumor mass of EpRas-Tet-On-ILEI clones #16 and #17 upon Dox induction. The error bars were calculated with standard error of means (SEM).

The EpRas-Tet-On-ILEI clone #16 showed no differences in growth upon Dox induction. This may be a result of the already high ILEI levels without induction. Significant differences between + and - Dox induction were seen in clone EpRas-Tet-On-ILEI #17.

To analyse the metastatic capabilities of the two EpRas-Tet-On-ILEI clones 100.000 cells per mouse were injected into the tail vein. The lungs of the animals were dissected at the same time point to see the metastatic nodules (FIGURE 44).

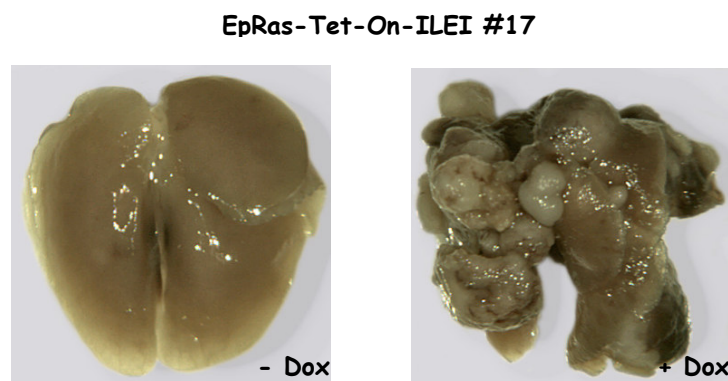


**FIGURE 44 |** Lungs of EpRas-Tet-On-ILEI #17 mice with and without Dox induction.

It is clearly visible that the difference in tumor growth is mirrored in the difference in lung colonisation. The lung without Dox treatment is free of metastases while the lung with Dox treatment was overgrown with partially huge metastases. This was the result of a first pilot experiment. In order to do statistical analysis of the effect of ILEI interaction on lung colonisation, a higher number of mice need to be included. However, such an experiment was outside the time frame of my diploma thesis.

### 3.2.3 Histological analysis of exgrafted tumors

To see if there were different ILEI levels in the induced tumors in comparison to the uninduced ones we performed ILEI stainings (FIGURE 45 and 46).

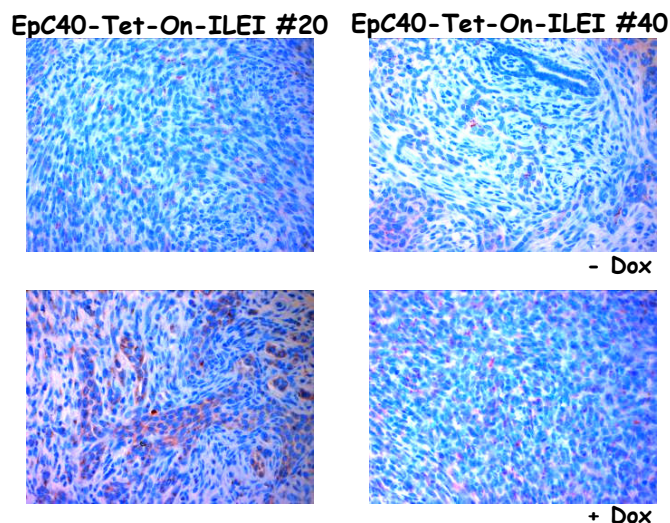


FIGURE 45 | ILEI staining of EpC40-Tet-On-ILEI clones #20 and #40 tumors with and without Dox induction. Red dots mark ILEI nuclei (blue) are the counterstained with Hematoxylin.

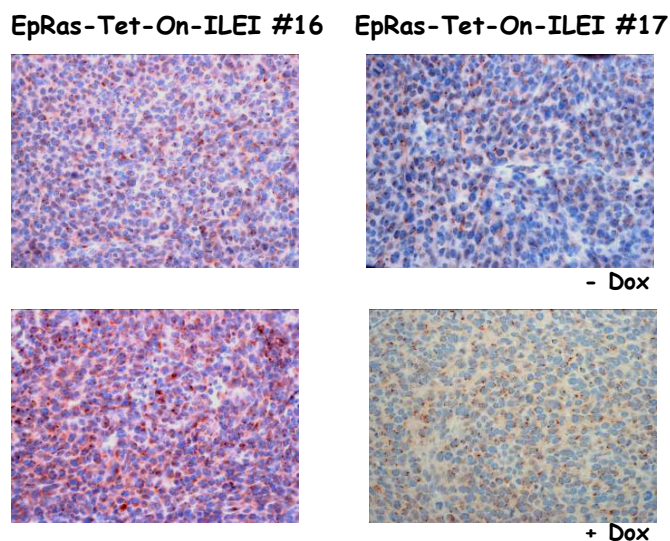


FIGURE 46 | ILEI staining of EpRas-Tet-On-ILEI clones #16 and #17 tumors with and without Dox induction. Red dots mark ILEI nuclei (blue) are the counterstained with Hematoxylin.

The tumors from mice receiving Dox in their drinking water clearly showed elevated ILEI expression.

The next questions were: (i) What is the reason for the increased tumor growth rates and (ii) how did ILEI caused this increased tumor growth.

To test whether the size differences in tumors with or without Dox induction were due to alterations in apoptosis rates, all tumors were subjected to immunohistochemical staining for activated caspase 3 (FIGURE 64 and 65 APPENDIX). There were no significant differences in EpC40-Tet-On-ILEI and EpRas-Tet-On-ILEI tumors concerning apoptosis between Dox-induced and uninduced tumors.

Similarly, the proliferation of different tumors with and without Dox induction was checked using immunohistochemical (IHC) stainings for the proliferations marker Ki67. IHC stainings for the EpC40-Tet-On-ILEI clones #20 and #40 with and without Dox induction (FIGURE 47 and 49). For quantification, several stainings were counted and the percentage of Ki67 stained nuclei over the total number of nuclei was calculated (FIGURE 48 and 50).

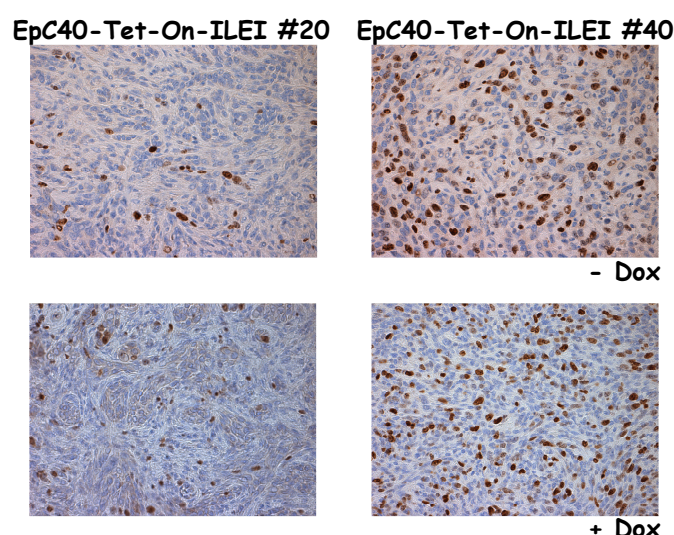


**FIGURE 47 |** Ki67 IHC staining of EpC40-Tet-On-ILEI clones #20 and #40 tumors with and without Dox treatment. Ki67 IHC staining (brown) marks proliferating nuclei, Hematoxylin contra staining (blue) labels all nuclei,

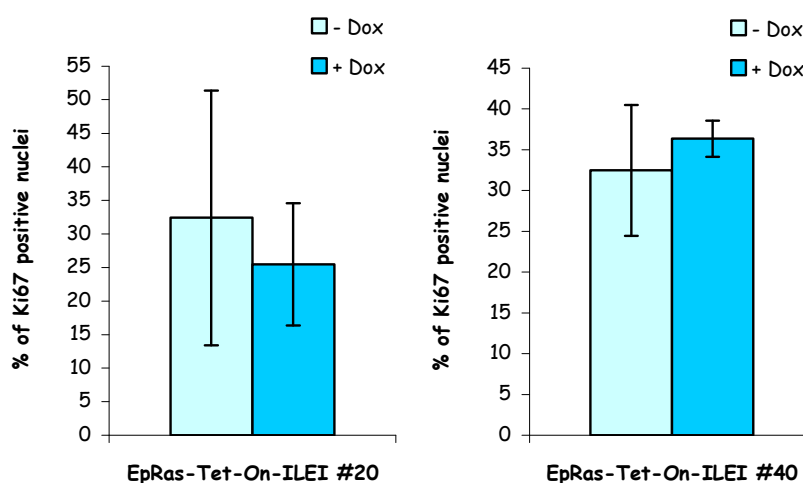


**FIGURE 48 |** Frequency of Ki67 positive nuclei from tumors induced by EpC40-Tet-On-ILEI clones #20 and #40, with and without Dox application to the mice.



The total number of nuclei (Ki67 stained and unstained) served as 100% for calculations. The error was calculated with standard deviation (SD).

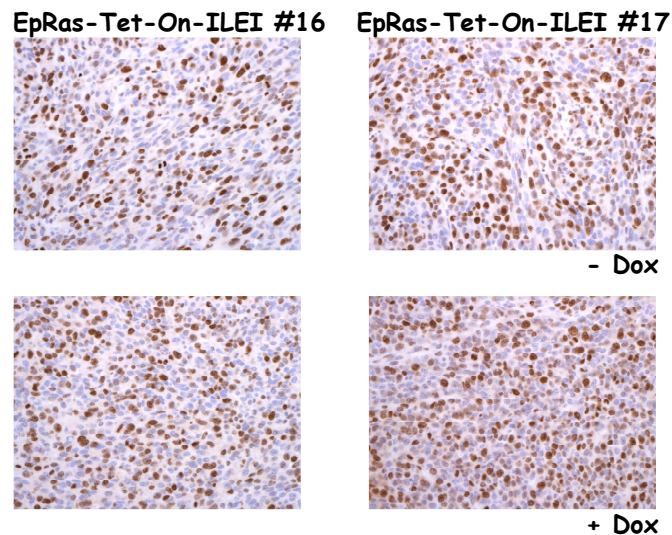


**FIGURE 49 |** Ki67 IHC staining of EpRas-Tet-On-ILEI clones #16 and #17 tumors with and without Dox treatment. Ki67 IHC stainings (brown) marks proliferating nuclei, Hematoxylin contra staining (blue) labels all nuclei,

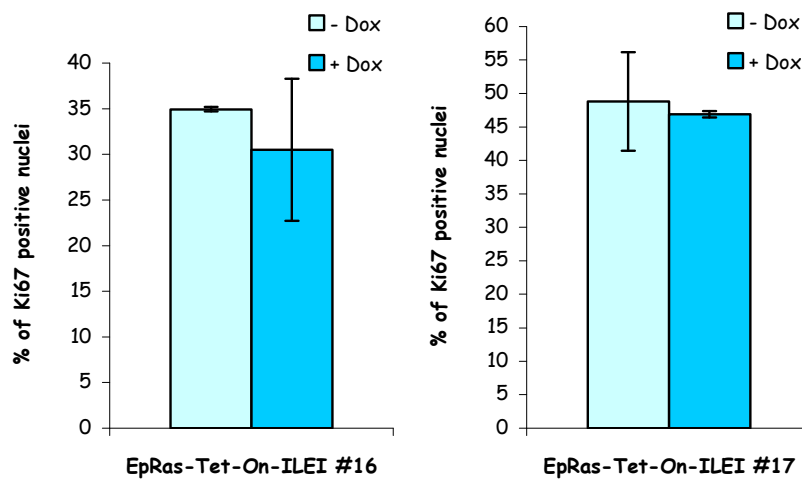


**FIGURE 50 |** Frequency of Ki67 positive nuclei from tumors induced by EpRas-Tet-On-ILEI clones #16 and #17, with and without Dox application to the mice. The total number of nuclei (Ki67 stained and unstained) served as 100% for calculations. The error was calculated with standard deviation (SD).

In summary, there was no difference in proliferation between Dox induced and uninduced tumors. These findings indicate that the ILEI induced increased tumorigenic capacity of the cells is not a consequence of elevated apoptosis protection or proliferation rate.

Hematoxylin and Eosin stainings were performed as well (FIGURE 66 and 67 APPENDIX). Hematoxylin stained DNA (purple) and Eosin is for visualising soft tissue (pink).

### 3.3 Translational control of ILEI

#### 3.3.1 Regulatory motives in the 5'-UTR of ILEI

The aim of these experiments was to find out, how translational regulation of the ILEI gene occurred. Below, the sequence of the predicted, long 5'-UTR is shown. This 5'-UTR of ILEI there is an alternative start codon (CTG) at nucleotide position 43 (FIGURE 51). The uORF starting from this CTG ends before the real start codon (AUG) and ORF begin. If the uORF would be translated the resulting peptide would be 42 amino acids in length. Secondary structure prediction by the program mfold (FIGURE 52) indicated that the alternative start codon might be accessible because it is localized in a loop region.

```

1      CCACGCGTCCGCCCCACGCGTCCGGGGAGGAGGCCTGGGGCGAGCTGGCTTCCTCCTCGGC
1      P R V R P R V R G G L G R A G F L L G
1      H A S A H A S G E E A W G E L A S S A
1      T R P P T R P G R R P G A S W L P P R

61     GCGGGCGGGCGCGCGGCGAAGCCGAGGAGCCGGGGAAAGCCGAGGCGCGATCGGCGCGC
21     A G G R A A K P E E P G K A E A R S A R
21     R A G A R R S R R S R G K P R R D R R A
20     R G R A R G E A G G A G E S R G A I G A

121    TCGGGAGGAGGCGGGCGGGTGGCACCTCCCGTCGGCCTCCGACAGGACTGACGGCGGCG
41    S G G G G G G G T S R R P P T G L T A A
41    R E E A A A V A P P V G L R Q D * R R R
40    L G R R R R R W H L P S A S D R T D G G

181    CGACCGCAGACGGGACCTTCTTTTGGAGACGTGCTAGAGAGTGAGAAGGCAAAAATGA
61    R P Q T G P S F G D V L E S E K A K M
61    D R R R D L L L E T C * R V R R Q K *
60    A T A D G T F F W R R A R E * E G K N

```

**FIGURE 51 | uORFs of the murine ILEI 5'-UTR with two alternative start codons CTG.**  
In blue the uORF is marked and in green the start codon AUG. The bold asterisk labels distinguish the end of the uORF.

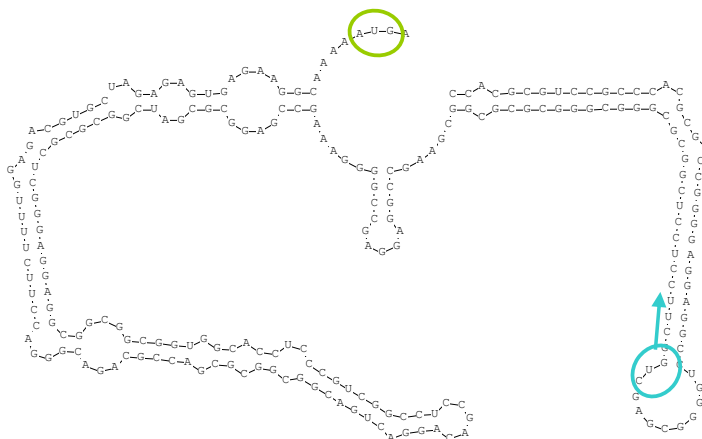


**FIGURE 52 | Secondary structure prediction of 5'-UTR of murine ILEI with mfold.**  
In blue circle the uORF start codon CUG is marked and in green circle the start codon AUG from the ORF.



RegRNA predicted two regulatory motives in the 5'-UTR, a terminal oligo-pyrimidine (TOP) element and an IRES site (FIGURE 53). Till now, TOP elements have been experimentally shown only in mRNAs coding for ribosomal proteins and transitional regulatory proteins. Some exploration of the predicted TOP elements in the ILEI 5'-UTR still needs to be found. The predicted IRES site could have some translational effect on the ILEI gene but no experiments have been done in this direction (FIGURE 54).

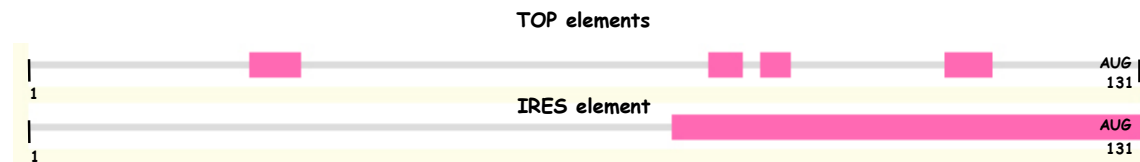


FIGURE 53 | Prediction of regulatory elements in the ILEI 5'-UTR using RegRNA.

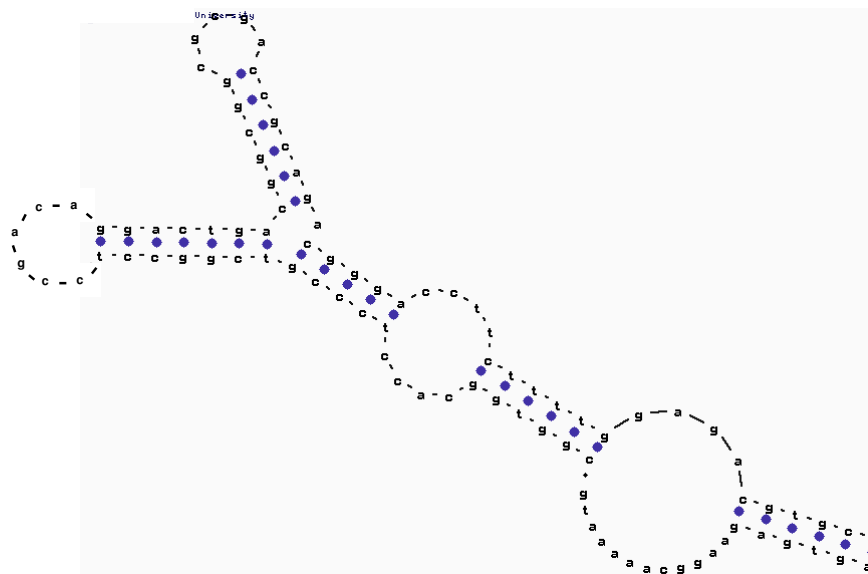


FIGURE 54 | Prediction of the murine ILEI IRES in the 5'-UTR with RegRNA.

### 3.3.2 Regulatory motives in the 3'-UTR of ILEI

Two forms of the ILEI 3'-UTR have been found, which divide the 3'-UTR in a long and a short version. This is the result of an alternative poly(A) signal (FIGURE 55 top panel) located in the 3'-UTR, which has been confirmed by the findings of J. H. Jr. Greinwalds group (see chapter 1.12 and (Pilipenko VV, 2004)). The existence of two different ILEI mRNA isoforms raised the question to what extent the two mRNAs are involved in the translational control of ILEI.

There are nine predicted GAIT elements in the ILEI 3'-UTR (FIGURE 55 bottom panel and FIGURE 56) but only the one marked with the arrow head is predicted in all secondary structure calculations by mfold, indicating a high probability for the formation and stability of this stem-loop structure. No functional studies were done of this predicted structure.

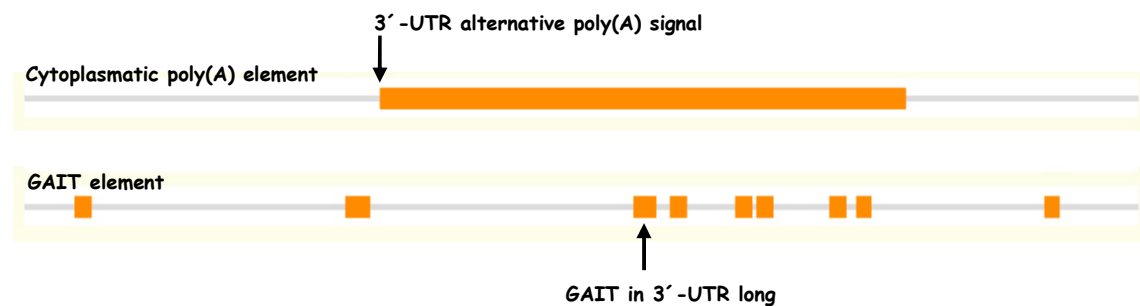


FIGURE 55 | Prediction of regulatory elements in the ILEI 3'-UTR with RegRNA.

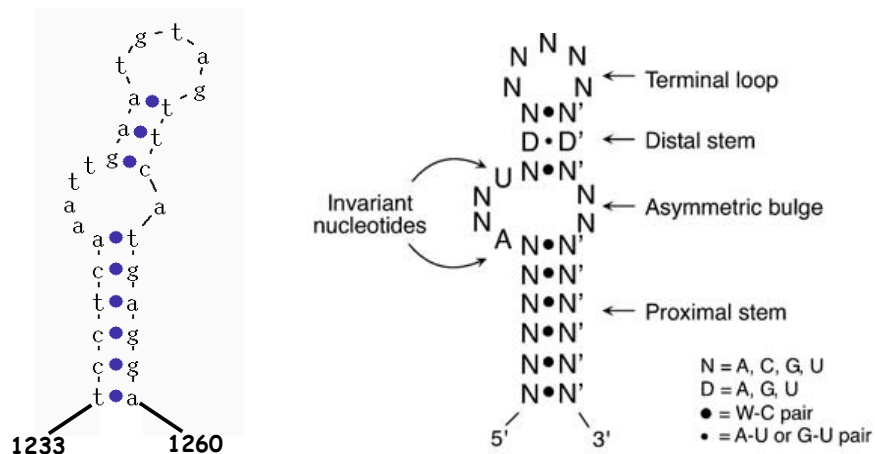


FIGURE 56 | Left side: putative ILEI GAIT prediction with RegRNA. Right side: Consensus sequence of the secondary structure of GAIT elements (Ray PS, 2007).

### 3.3.3 Characterisation of the translation rate of the two ILEI 3'-UTR isoforms

Initial data using RT-PCR showed that low ILEI expressing EpRas cells and high ILEI expressing EpRasXT cells have no difference in the abundance of ILEI mRNA. However, this assay did not distinguish between short and long ILEI mRNA forms (Waerner T, 2006). To examine if different ILEI protein levels correlate with a difference in the relative abundance of long versus short ILEI mRNA Northern blot analysis with four cell lines was performed (FIGURE 57). These four cell lines have naturally unequal intrinsic ILEI levels. The epithelial NMuMG, EpH4 and EpRas cell lines have low amounts of ILEI and the fibroblastoid EpRasXT cell line expresses considerably higher amounts of the ILEI protein. NMuMG cells are normal murine mammary gland cells, often used as an *in vitro* model for EMT related questions, since similarly to EpRas cells they undergo TGF $\beta$  dependent EMT.

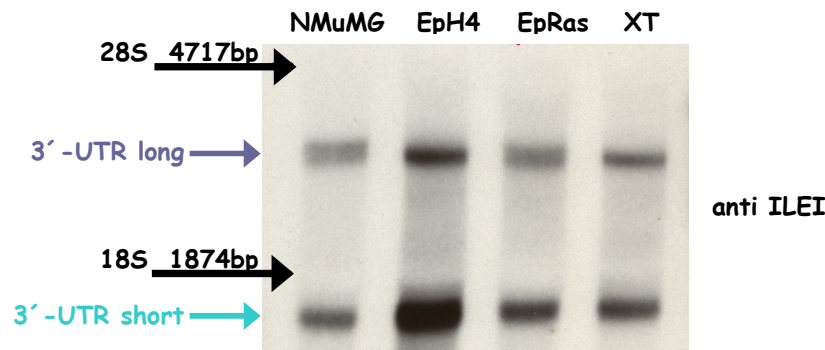


FIGURE 57 | The two isoforms of 3'-UTRs in different cell lines.

There was no difference in the relative abundance of one of the two mRNA isoforms in cells with different ILEI protein levels.

Next, we tried to determine if the translation rate of the two isoforms is different upon TGF $\beta$  induction by analysing the distribution of ILEI mRNA isoforms on polysomes. Sucrose gradient ultracentrifugation was applied to fractionate the total mRNA into polysome bound and free mRNA (FIGURE 58). To check if the mRNA was not degraded and the RNA was fractionated properly a chip analysis was run.

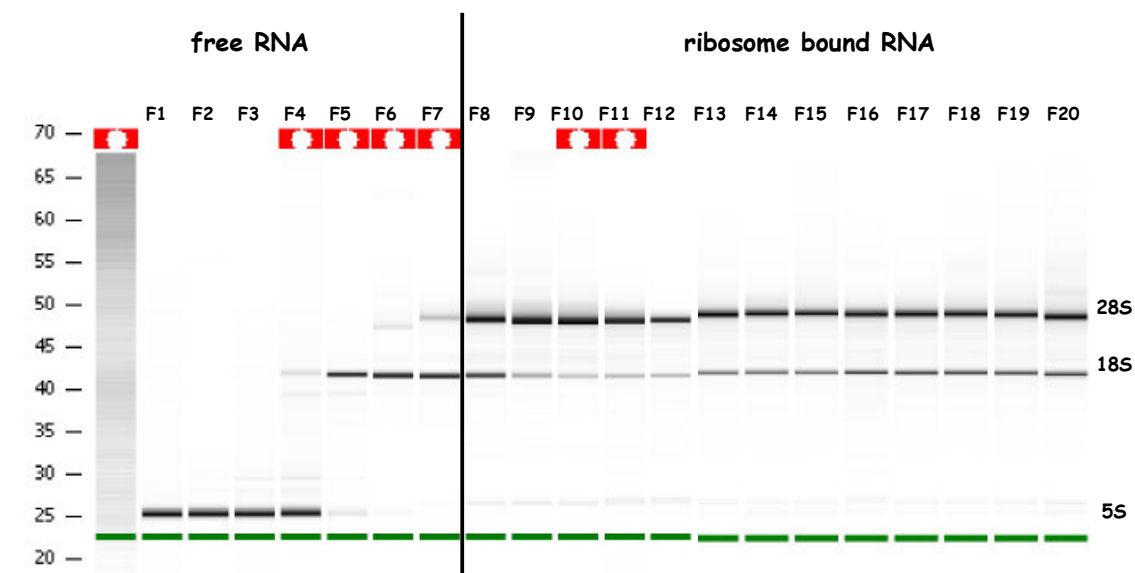
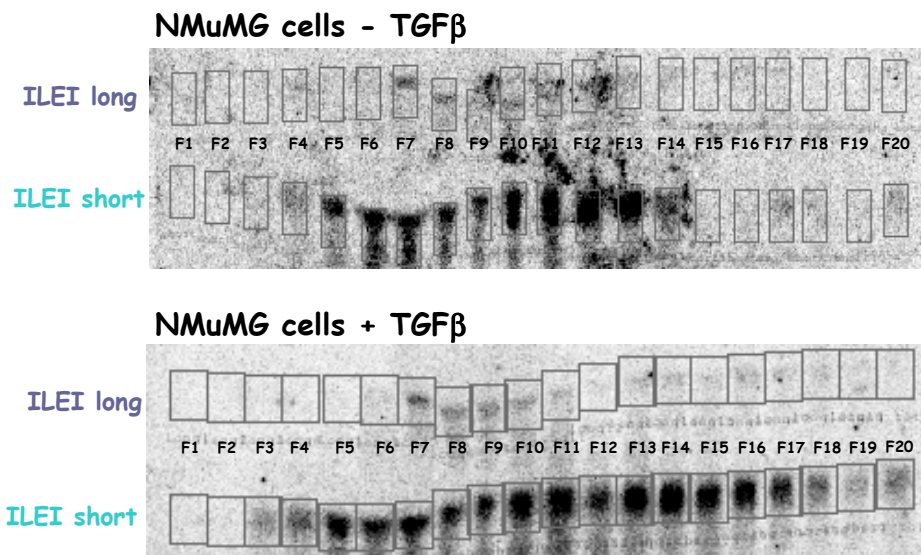
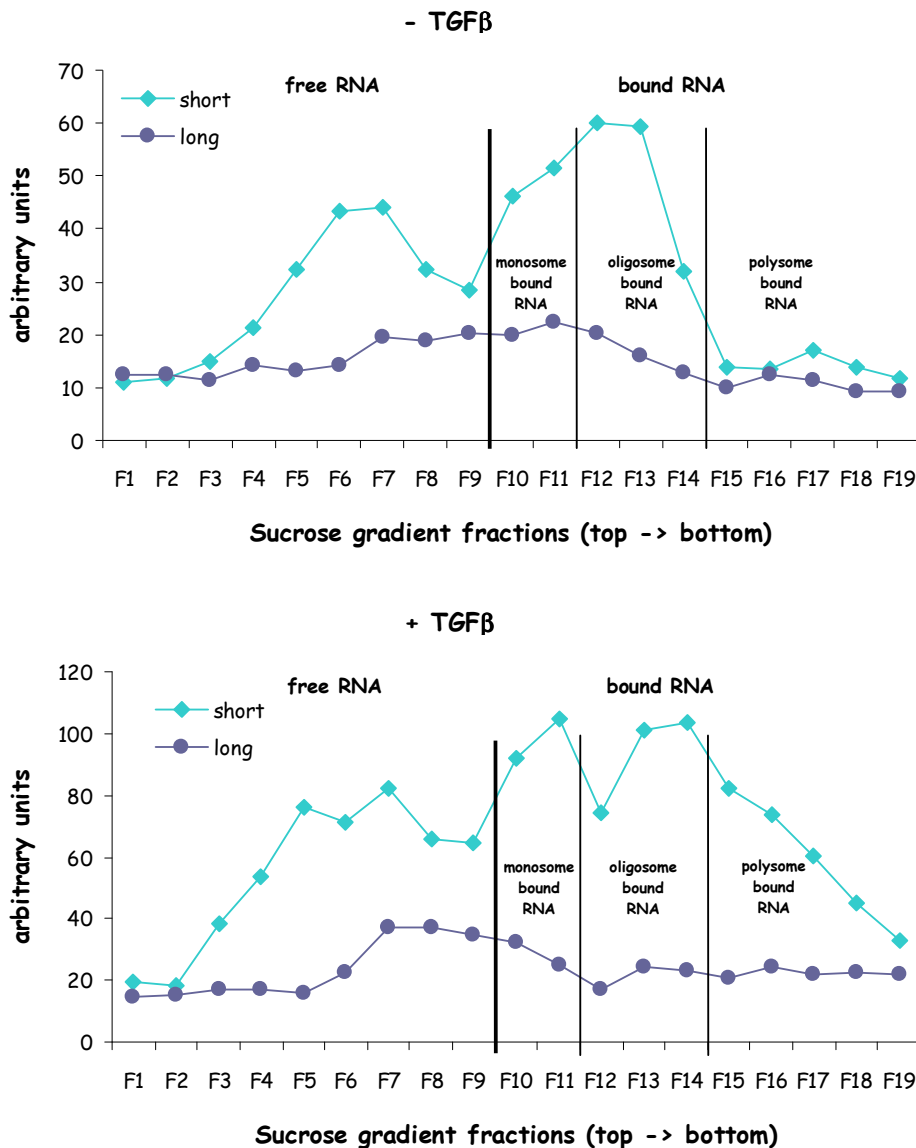


FIGURE 58 | RNA nano chip.

The 18S rRNA is a subunit of the 40S ribosome and the 28S and 5S RNA are subunits of the 60S ribosome. They were used as markers for their corresponding subunits. In the first eight fractions are free mRNA because not all ribosomal subunits are present. From fraction nine on there are actively translated mRNAs found because all components are present to build an intact ribosome. After sucrose gradient fractionation RNA was isolated and Northern blot analysis was used to separate the two isoforms based on their different running velocities in an agarose gel (FIGURE 59). Obviously, the later an mRNA appears in the sucrose gradient fractions, the higher number of ribosomes is bound the transcript ending up in polysome bound mRNA fractions (FIGURE 60). To detect both isoforms an ILEI probe for ILEI ORF was used.



**FIGURE 59 |** Northern blot analysis of ILEI on RNA fractions of a sucrose gradient. Top panel without TGF $\beta$  treatment, bottom panel with TGF $\beta$  treatment. Autoradiogram was generated using a Phosphorimager. Quantification was performed using IMAGEquant. Black boxes mark the quantified regions for long and short ILEI mRNA of the different fractions.



**FIGURE 60** | NMuMG cell fractions on sucrose gradient.  
Top panel without TGF $\beta$  treatment, bottom panel with TGF $\beta$  treatment.

Northern blot analysis showed a shift from free mRNA to bound mRNA when the cells were treated with TGF $\beta$ . This shift was most apparent within the polysome bound fraction of the short ILEI mRNA (TABLE 4). This means, that more ILEI mRNA was translated and so higher amounts of ILEI protein were produced in the TGF $\beta$  treated cells. In conclusion, this experiment shows that all the important regulatory elements of translational control were present in the short mRNA, thus in the first part of the 3'-UTR or in the 5'-UTR. What the 3'-UTR long is doing when treated with TGF $\beta$  is hard to detect so no conclusions can be drawn from these few experiments.

ILEI mRNA short		
	- TGF $\beta$	+ TGF $\beta$
% free RNA	42,9	38,8
% bound RNA	57,1	61,2
% monosome bound RNA	17,5	15,6
% oligosome bound RNA	27,1	22,1
% polysome bound RNA	12,5	23,4

TABLE 4 | Comparison of the 3'-UTR short levels in TGF $\beta$  treated and untreated cells. The free- and bound RNA are combined the total amount of RNA. Monosome-, oligosome- and polysome RNA combined make the bound RNA fraction.

### 3.3.4 Evaluation of the importance of different UTR regions

To evaluate in which UTR part the important regulatory regions are, seven UTR-FFL constructs were cloned using the pGL3-Control-MCS FFL reporter vector. The construct referred to as 5' carried the 5'-UTR in front of the FFL sequence. The vector called 3' short and 3' long carried insertions of the two different 3'-UTR isoforms inserted directly after the STOP codon of the FFL. The two vectors called 5' + 3' short and 5' + 3' long had the 5'-UTR in front of the FFL and the short or the long 3'-UTR after the FFL coding sequence, respectively. As a positive reference the pGL3-Control-MCS vector (MCS) without any ILEI UTR inserts was used, whereas the pGL3-Enhancer vector (Enhancer) lacking the SV40 promoter served as negative control in the luciferase reporter assay (FIGURE 61).

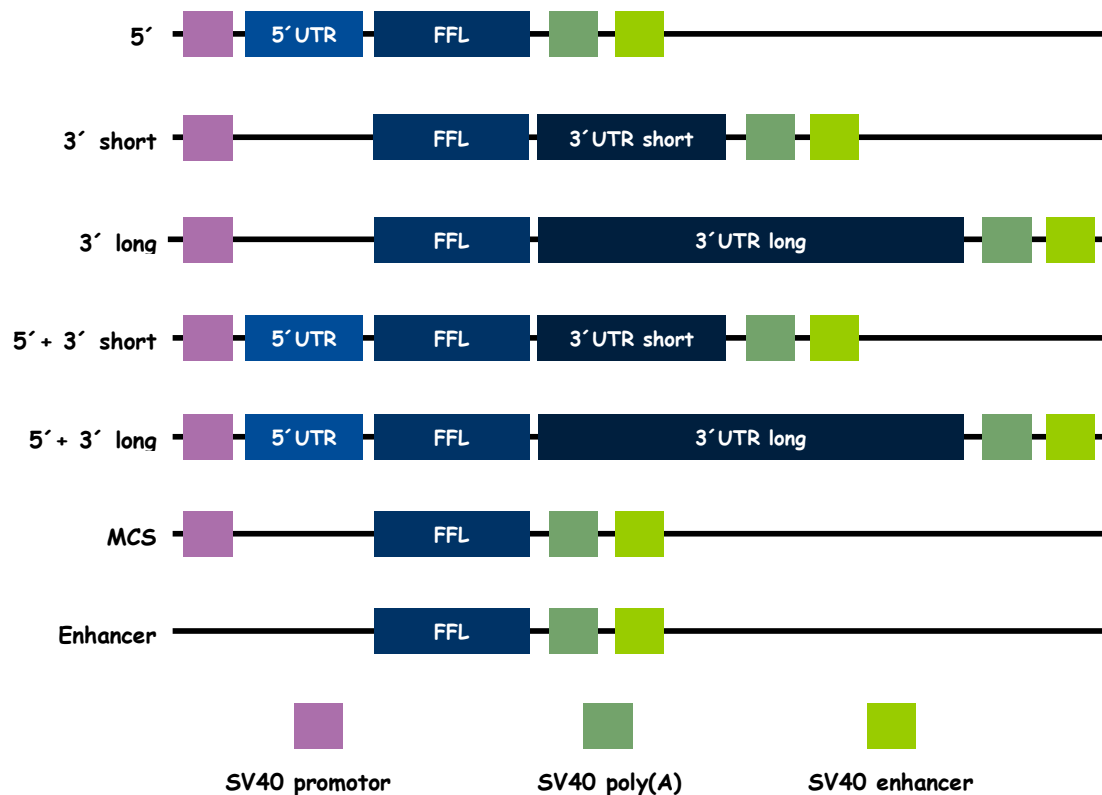


FIGURE 61 | Different UTR-FFL regulator constructs.

The luciferase assays were performed with EpRas and EpRasXT cells. EpRasXT cells show elevated ILEI levels regulated at translational level due to their autocrine TGF $\beta$  signalling

(FIGURE 62). Since EpRasXT cells already have an autocrine TGF $\beta$  loop, treatment with exogenous TGF $\beta$  was not necessary.

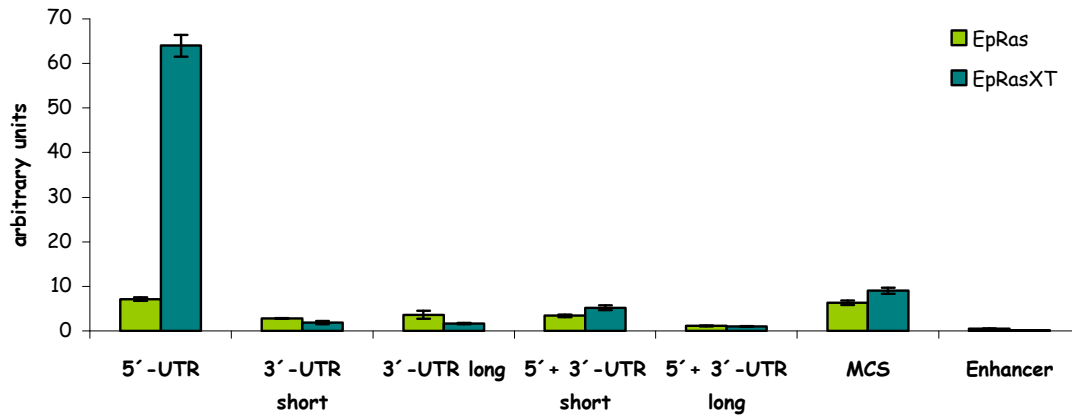


FIGURE 62 | FFL assay with different UTR constructs.

Only the 5'-UTR-FFL construct shows a significant difference in expression between EpRas and EpRasXT. With the other constructs, no clear differences were detectable, thus further experiments were clearly necessary. A very significant, six-fold increase of FFL activity was detected using the EpRasXT cells. 3'-UTR short and long constructs showed at least a 50% decrease in expression compared to the MCS control. Interestingly, constructs in which both the 5'-UTR and 3'-UTR of ILEI were present (5'+3'-UTR short and 5'+3'-UTR long) the inhibitory effect of the 3'-UTRs overcome the activating effect of the 5'-UTR resulting in an inhibition of expression.

## 4 DISCUSSION

A common way to study gene function *in vitro* and *in vivo* is to generate stable cell lines with altered levels of gene expression. However, these systems have the risk to select for clonal effects. In addition, primary effects often can not be set apart from downstream events or might be masked by compensatory mechanisms.

Choosing an inducible system for the manipulation of gene expression level can avoid all this problems. Furthermore, this approach makes it possible to investigate the kinetics of cellular responses after the induction of gene over-expression or knock down.

Although there are some inducible tumor cell lines available to study EMT, there is not a comprehensive model system which would allow studying several stages of tumor formation and progression. The cell lines of our choice provide three different aspects of tumor formation; the non-tumorigenic Eph4 cells, the EpC40 cells which form tumors but are unable to spread and metastasise and the EpRas cells which can form tumors and metastases.



## 4.1 TetR clones

A 2-step approach was taken for cloning the inducible ILEI system. First, a general tool for tumor biology studies (TetR cells) was established, which enables to analyse gene function of any gene of interest *in vitro* and *in vivo* in an inducible manner. In a second step, these TetR clones from EpH4, EpC40 and EpRas, that were selected for good inducibility of the regulatory vector, can be further transfected with the expression vector, in which a variety of genes can be inserted. This way, a broad assortment of genes can be studied in a series of cell lines which represent three stages of tumorigenesis non-tumorigenic (Eph4), tumorigenic but non-metastatic (EpC40) and metastatic (EpRas) cells.

For generating the inducible clones the T-Rex system from Invitrogen was used. According to the manufacturers on clone out of twenty should have a proper induction capability. Our experiments did not reflect these predictions. The average calculated from the transfection of 3 cell lines showed that approximately 50 clones had to be tested to find one with an induction capability over two-fold, and far more clones needed to be analysed to find some with higher induction capabilities.

A very important criteria in the validation of the generated inducible TetR clones is that the introduction of the regulatory vector into the cells does not alter the original characteristics of the cell lines. To test this, several *in vitro* comparative assays were done between the parental cell lines and the TetR clones. In all *in vitro* test we performed the TetR clones behaved exactly like the parental cells. The morphology of all three TetR clones on plastic was identical to their parental cells. In collagen gels the phenotype with and without TGF $\beta$  treatment was equal between parental cell lines and the selected TetR clones. Stainings of these collagen gels were done for E-cadherin and vimentin, two key markers for the distinguish between epithelial cells before and mesenchymal cells after EMT. In all cases the inspected TetR clones showed a similar marker expression as their parental counterparts. This lead to the conclusion that the generated clones behaved *in vitro* similar as the parental cell lines.

The *in vivo* tests, designed to detect possible differences between parental cells and TetR clones consisted tests for tumor growth rate, survival/apoptosis assays and assays for lung metastases (colonisation). EpH4-TetR clones as well as their parental counterparts did not form tumors upon mammary gland fat pad injections. This result was expected since these EpH4-derived clones should be non tumorigenic cells. In case of EpC40-TetR and the parental EpC40 cells, the tumor growth was very slow in both cases in comparison to earlier experiments (FIGURE 63) (Janda E, 2002b). In this earlier experiments two different EpC40 clones were tested EpC40-5 and EpC40-1b. For generation of the TetR clones the EpC40 clone 5 was used (EpC40-5 is referred to as EpC40 throughout my thesis for simplicity) We used this clone since we reasoned that a slower tumor growth rate would make it easier to detect a possible tumor growth enhancement by ILEI. In the published studies, 100.000 cells were injected and after 29 days the EpC40-5 tumors already had a diameter of 5mm. In our tumor growth assay we also injected 100.000 cells but after 30 days there were no tumors visible. More than 90 days were required that tumors reached a size of about 5mm in diameter. This shows that in our examinations the EpC40-5 clone grows only one third as fast as it did in the original experiments.

The growth of the EpRas-TetR clone and the parental EpRas cells after mammary fat pad injections showed distinct differences. The parental EpRas cells formed tumors with comparable size in half the time as the EpRas-TetR clone (FIGURE 28). This slower tumor growth of EpRas-TetR might be a characteristics of the selected subclone. This particular EpRas-TetR clone showed higher sensitivity for TGF $\beta$  than other tested clones. In collagen gels, at a dosage of

10ng/ml TGF $\beta$  the first apoptotic structures appeared despite the cells were undergoing TGF $\beta$  induced EMT. This behaviour might reflect a lower expression level of Ras V12, which was not investigated in detail. The observed slower tumor growth of EpRas-TetR was favourable because a slow growth is a better basis to monitor the effect of a factor with a potential tumor promoting role. The same manner of slow growth was found when the survival rate of nude mice was charted after intravenously injecting cells into the tail vein. Parental EpRas cells killed the mice less than half the time then the EpRas-TetR did (FIGURE 30). This observation correlated with the slower growth rate of the TetR tumors compared to the parental cells. EpC40 as well as EpC40-TetR cells failed to develop lung metastases after tail vein injections which is was consistent with several other experiments (Janda E, 2002b).

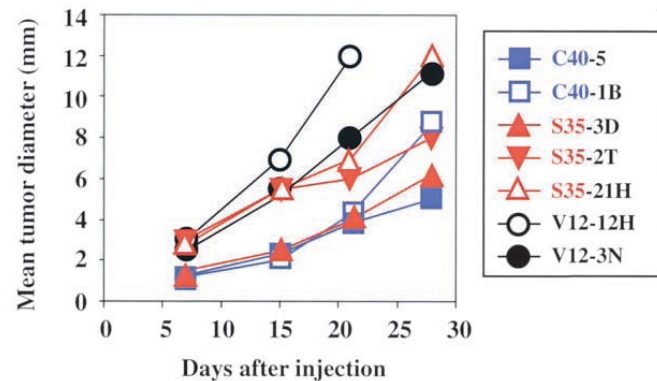


FIGURE 63 | Tumor growth of EpC40 and other cells in nude mice (Janda E, 2002b).

## 4.2 ILEI inducible clones

The second step towards the ILEI inducible clones was to transfect the cells with the Tet-On-ILEI construct. The odds of finding one proper inducible clone was less than 14:1 rendering the selection procedure by Western blot quite time-consuming. In future experiments, this problem could be overcome by cloning an IRES-GFP behind the gene of interest so that one could FACS sort for highly inducible clones. The problem with the clones obtained was that they were only weakly inducible (FIGURES 32 to 34). One or two inducible ILEI expressing clones were found for all three cell lines, however none of these clones showed such a high inducibility as the original TetR clones after the first step. This indicates that either cells might contradict against high ILEI levels or that simply even a higher number of clones should have been tested in order to find good inducibility. This is a common draw-back of strategies of random insertion, where the undesired influence of flanking genomic sequences is not predictable.

EpC40-Tet-On-ILEI clone #20 had low levels of ILEI in general but when induced with Dox, the ILEI level was higher, predominantly in the supernatant. The EpC40-Tet-On-ILEI clone #40 had generally higher ILEI levels with or without induction than clone #20 but when induced, both the secreted and intracellular ILEI level were more significantly elevated. To test the effect of different induced ILEI levels *in vivo*, mammary gland fat pad injections were done. In EpC40-Tet-On-ILEI clone #20 as well as in clone #40 were no eminent differences in tumor size or weight between the uninduced and the induced setup. It has to be mentioned that the EpC40-Tet-On-ILEI clone #20, which had the lower basal ILEI levels showed at least a tendency that the Dox induction resulted in bigger, heavier tumors.

In previous experiments of the Beug group, the analysis of tumor formation by stable over-expressing EpC40-ILEI cells and control EpC40 cells revealed that ILEI strongly enhanced tumor size (3.6-fold increase in mean tumor weight per mouse). Stable ILEI over-expressing EpC40 cells were tested for metastatic behaviour by tail vein injection of nude mice, in comparison to respective control cells. ILEI expression induced strong metastatic capacity in the tumorigenic but nonmetastatic EpC40 cells (Waerner T, 2006). The tumor growth and lung metastases results could not be reproduced in this fashion with the inducible EpC40-Tet-On-ILEI clones.

EpRas-Tet-On-ILEI clone #16 had a high basal ILEI level, but nevertheless showed nicely elevated ILEI levels upon expression with Dox both intracellularly and in the supernatant. The EpRas-Tet-On-ILEI clone #17 had a lower ILEI expression without induction, than the clone #16 but a preliminary high inducibility (FIGURE 43). When fat pad injections were done using these two clones with and without Dox induction the differences in basal ILEI levels might explain the diverse results. The clone #16, which had generally higher basal ILEI levels showed no considerable difference in tumor mass or tumor volume with or without Dox (FIGURE 42 and 43). In case of the EpRas-Tet-On-ILEI clone #17 the basic ILEI level was much lower than of clone #16 and tumor growth of this clone was significant slower than of clone #16. Upon Dox induction, which resulted in higher ILEI levels, tumor mass and volume were significantly increased and become comparable with the growth rate of clone #16. This data might indicate a dose dependent effect of ILEI on tumor growth. However, this does not explain why a further elevation of ILEI in clone #16 did not result in an even higher tumor growth rate. We can only speculate that those levels are above the saturation level of the ILEI receptors expressed in the tumor tissue and therefore could not have any additional effects.

The assay for metastatic behaviour, the lung colonisation assay, was performed only with EpRas-Tet-On-ILEI clone #17. There was a major discrepancy between the lungs of mice supplied or not supplied with Dox in the drinking water (FIGURE 44). The lung without Dox treatment were free of metastases at the timepoint of dissection while the lung with Dox treatment was

overgrown with partially huge metastases. Thus, the difference in tumor growth was mirrored in the difference in lung colonisation, which was mirrored in the difference in ILEI expression levels. This was the result of a first pilot experiment. In order to do statistical analysis on the effect of ILEI induction on lung colonisation, a higher number of mice need to be included.

To analyze, whether ILEI induces EMT in these tumors, we used established procedures to compare EpC40 and EpC40 stable over-expressing ILEI tumors by IHC. In those studies, serial tumor sections were stained for E-cadherin, vimentin, and ILEI expression. The outcome was that EpC40-derived tumors showed strong, membrane-localized E-cadherin expression, while vimentin staining was predominantly detected in only areas presumably representing the stroma. In contrast, the ILEI-positive cells in the EpC40 stable over-expressing ILEI tumors showed no or weak cytoplasmic E-cadherin staining but strong vimentin expression (Waerner T, 2006).

Due to a lack of time, the inducible ILEI over-expressing tumors were IHC stained only for ILEI. The result was that the Dox induced tumors had a stronger ILEI staining than the uninduced ones but the difference was not extremely pronounced. For further examination of this topic it would be sensible to tag ILEI in the transfected cells so that the ILEI and induced ILEI could be distinguishable.

In previous experiments on porous supports (filters, still supporting complete epithelial polarity), stable ILEI over-expression induced complete EMT (Waerner T, 2006). In our experiments regarding this issue we took the Tet-On-ILEI clones from Eph4, EpC40 and EpRas and cultivated them for eight days on filters. Regardless if induced with Dox or not the morphology of the cells was unchanged and remained epithelial (FIGURE 38). No EMT was induced. An explanation might be that the inducible clones have lower ILEI levels and the threshold for inducing EMT was not reached.

In collagen gels, all Eph4, EpC40 and EpRas cells stable over-expressing ILEI underwent complete EMT, forming unordered structures of fibroblastoid cells expressing vimentin but not E-cadherin (Waerner T, 2006). Our experiments with Eph4-Tet-On-ILEI, EpC40-Tet-On-ILEI and EpRas-Tet-On-ILEI cells in collagen gels showed no EMT when treated with Dox. If TGF $\beta$  was added, cells underwent their typical programmes accordingly (Eph4-Tet-On-ILEI cells died, EpC40-Tet-On-ILEI cells underwent scattering and EpRas-Tet-On-ILEI cells underwent EMT) but no differences at all were visible between Dox induced and uninduced cells. After the cells responded to TGF $\beta$ , treatment was stopped. The withdrawal in EpC40-Tet-On-ILEI cells showed that the uninduced cells reverted to more compact and rounder structures while the Dox induced cells maintained their spiky phenotype (FIGURE 39). In conclusion ILEI is not able to induce EMT in the inducible clones, for that TGF $\beta$  is necessary. Nevertheless ILEI is able to maintain the TGF $\beta$  induced mesenchymal phenotype in EpC40 cells.

For all tested clones in all three cell lines including the Tet-On-Empty control clones it was true that the uninduced cells grow a bit faster than the ones treated with Dox. However, this difference was not significant. This indicates, that high Dox concentration might have a slight inhibitory effect, but ILEI had definitely no effect on cell proliferation. Also in IHC of tumor sections for the proliferation marker Ki67, there was no difference in proliferation between Dox induced and uninduced tumors. These findings confirm the *in vitro* growth curve experiments, telling that the ILEI induced increased tumorigenic capacity of the cells is not a consequence of elevated proliferation rate *in vitro* and *in vivo*.

### 4.3 Translational control of ILEI

Translational control is to a big part carried out by structural- and sequential elements in the 5'- and 3'-UTR of a gene. For the well established structural elements, predictions were made for ILEI mRNA using the programmes RegRNA and mfold. It was not possible to investigate any of the predicted elements in experiments during the time course of my diploma thesis.

In the 5'-UTR an IRES motive and a TOP sequence were found (FIGURE 53). To test if this predicted IRES actually induces translation, one would have to perform bicistronic reporter assays. In this type of assays, IRES is located between two reporter open reading frames in a eukaryotic mRNA, so IRES can drive translation of the downstream protein coding region independently of the 5'-cap structure.

The RegRNA prediction showed four TOP sequence elements in the ILEI 5'-UTR. Till now, TOP element has been experimentally shown only mRNA coding for ribosomal- and transitional regulatory proteins. Some exploration of the predicted TOP elements in the unusual context of the ILEI 5'-UTR could reveal new regional sites and functions.

The *in silico* analysis of the 3'-UTR identified an alternative poly(A) site and a GAIT element (FIGURE 55).

The alternative poly(A) signal of the ILEI 3'-UTR was proposed by the group of J. H. Jr. Greinwalds (Pilipenko VV, 2004). We could confirm the existence of a short and a long ILEI mRNA form by Northern blot analysis.

From the predicted nine GAIT elements in the ILEI 3'-UTR it is safe to assume that one of them has a high probability of forming. This one secondary structure is in all calculations with RegRNA equivalent. The ILEI GAIT has the same structure (proximal stem - asymmetric bulge - distal stem - terminal loop) as the consensus sequence motive dictates and also both of the invariant nucleotides are present. Experiments to determine the exact influence of the GAIT element on the ILEI mRNA were not done.

The reporter assay with firefly and *Renilla* was made to inspect in which part of the ILEI UTR the important regulatory regions are. For this tests EpRas and EpRasXT cells were used because EpRasXT cells already have an autocrine TGF $\beta$  loop so that extrinsic TGF $\beta$  treatment was not necessary in order to get cells with high and low TGF $\beta$  levels.

The results of the FFL *Renilla* coupled reporter assays showed that there is a significant difference in EpRas and EpRasXT cells when the 5'-UTR-FFL construct is transfected. In case of all other constructs there was no difference in fluorescence. The interesting thing is that the constructs long or short 3'-UTR in combination with the 5'-UTR showed no difference. One explanation for this discrepancy could be that the 3'-UTR influences the 5'-UTR and renders it inactive. A second explanation could be that the different secondary structures of ILEI mRNA and the FFL 5'-3'-ILEI constructs UTR influence the effectiveness of the regulatory capacity of the 5'-UTR.

The reporter tests only provide data on protein level. As next step it would be sensible to explore the different constructs in q-RT-PCR to assess if the observed effect is exclusively translational.

It has been shown before by semiquantitative RT-PCR that polysome bound, but not total ILEI mRNA, is strongly up regulated in mesenchymal EpRasXT cells when compared to epithelial EpRas cells, clearly showing translational control of ILEI expression (Waerner T, 2006). In conclusion with this we also detected a shift from free ILEI mRNA to bound RNA in Northern blot analysis after sucrose gradient RNA fractionation of NMuMG cells treated with TGF $\beta$  (FIGURE 59 and

60). This shift was apparent most within the polysome bound fraction of the short ILEI mRNA (TABLE 4). It means that more ILEI mRNA was translated and so higher amounts of ILEI protein were produced in the TGF $\beta$  treated cells. In conclusion, this experiment shows that important regulatory elements of translational control are present in the short mRNA, thus in the first part of the 3'-UTR or in the 5'-UTR. From this experiment it is not possible to conclude something about the polysome bound amounts of the 3'-UTR long with or without TGF $\beta$  treatment because the detection was poor.

## APPENDIX

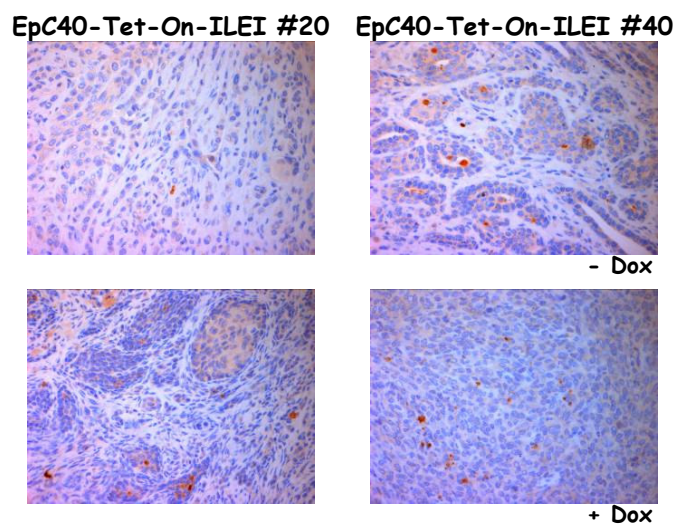


FIGURE 64 | Immunohistochemical stainings for activated caspase 3 (red) of EpC40-Tet-On-ILEI tumors #20 and #40.

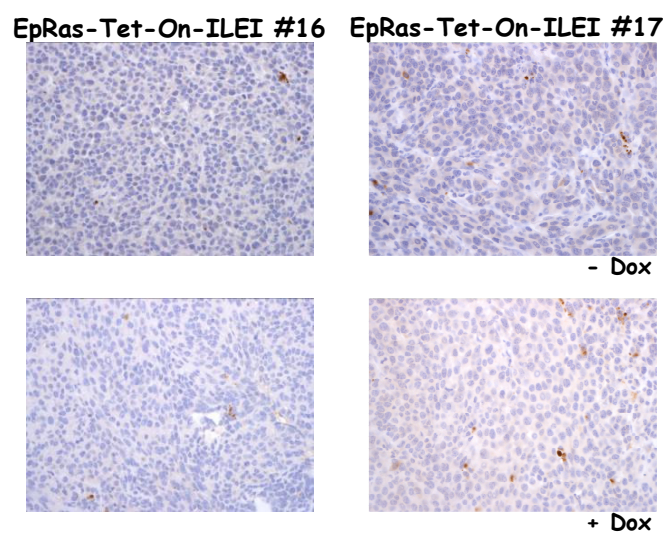


FIGURE 65 | Immunohistochemical stainings for activated caspase 3 (red) of EpRas-Tet-On-ILEI tumors #16 and #17.



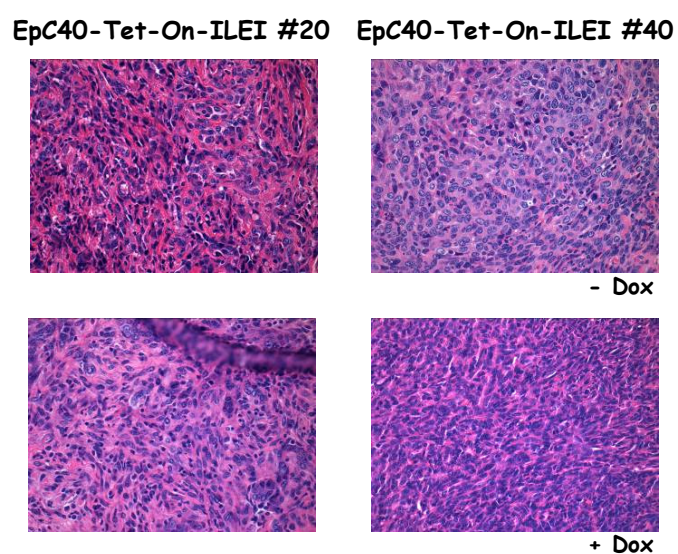


FIGURE 66 | Immunohistochemical stainings for Hematoxylin (purple) and Eosin (pink) of EpC40-Tet-On-ILEI tumors #20 and #40.

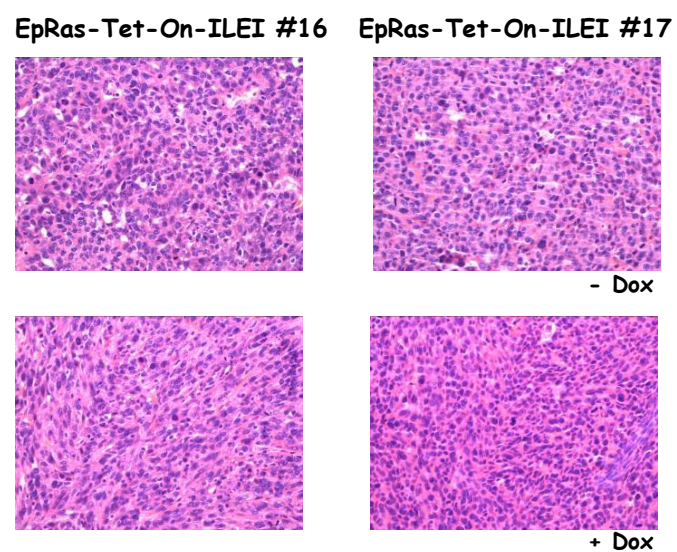


FIGURE 67 | Immunohistochemical stainings for Hematoxylin (purple) and Eosin (pink) of EpRas-Tet-On-ILEI tumors #16 and #17.



## REFERENCES

- AKHURST RJ, B. A. 1999. Genetic events and the role of TGF $\beta$  in epithelial tumour progression. *J Pathol*.
- ANDERSSON S, D. D., DAHLBÄCK H, JÖRNVALL H, RUSSELL DW. 1989. Cloning, structure, and expression of the mitochondrial cytochrome P-450 sterol 26-hydroxylase, a bile acid biosynthetic enzyme. *J Biol Chem*.
- ARIAS AM. 2001. epithelial mesenchymal interactions in cancer and development. *Cell*.
- BERX G, R. E., CHRISTOFORI G, THIERY JP, SLEEMAN JP. 2007. Pre-EMTing metastasis? Recapitulation of morphogenetic processes in cancer. *Clin Exp Metastasis*.
- BOSHART M, W. F., JAHN G, DORSCH-HÄSLER K, FLECKENSTEIN B, SCHAFFNER W. 1985. A very strong enhancer is located upstream of an immediate early gene of human cytomegalovirus. *Cell*.
- BOYD SD. 2008. Everything you wanted to know about small RNA but were afraid to ask. *Lab Invest*.
- CAMPBELL PM, D. C. 2004. Oncogenic Ras and its role in tumor cell invasion and metastasis. *Semin Cancer Biol*.
- CANTLEY LC. 2002. The phosphoinositide 3-kinase pathway. *Science*.
- CHEN RH, E. R., DERYNCK R. 1993. Inactivation of the type II receptor reveals two receptor pathways for the diverse TGF $\beta$  activities. *Science*.
- CHRISTOFORI G, S. H. 1999. The role of the cell-adhesion molecule E-cadherin as a tumour-suppressor gene. *Trends Biochem Sci*.
- CUI. 1996. TGF $\beta$ 1 Inhibits the Formation of Benign Skin Tumors, but Enhances Progression to Invasive Spindle Carcinomas in Transgenic Mice. *Cell*.
- DE CAESTECKER MP, E. P., ANITA B. ROBERTS. 2000. Role of Transforming Growth Factor beta Signaling in Cancer. *Journal of the National Cancer Institute*.
- DERYNCK R, A. R., BALMAIN A. 2001. TGF $\beta$  signaling in tumor suppression and cancer progression. *Nature genetics*.
- DR MORRIS, A. G. 200. Upstream Open Reading Frames as Regulators of mRNA Translation. *Molecular and Cellular Biology*.
- ELENBAAS B, W. R. 2001. Heterotypic signaling between epithelial tumor cells and fibroblasts in carcinoma formation. *Exp Cell Res*.
- FIALKA I, S. H., REICHMANN E, OFT M, BUSSLINGER M, BEUG H. 1996. The Estrogen-dependent c-JunER Protein Causes a Reversible Loss of Mammary Epithelial Cell Polarity Involving a Destabilization of Adherens Junctions. *J Cell Biol*.
- FILIPOWICZ W, B. S., SONENBERG N. 2008. Mechanisms of post-transcriptional regulation by microRNAs: are the answers in sight? *Nature Reviews genetics*.
- FUJIMOTO K, S. H., SHAO J, BEAUCHAMP RD. 2001. Transforming growth factor-beta1 promotes invasiveness after cellular transformation with activated Ras in intestinal epithelial cells. *Exp Cell Res*.
- GORSCH SM, M. V., STUKEL TA, GOLD LI, ARRICK BA. 1992. Immunohistochemical staining for transforming growth factor beta 1 associates with disease progression in human breast cancer. *Cancer Res*.
- GOTZMANN J, M. M., EGER A, SCHULTE-HERMANN R, FOISNER R, BEUG H, MIKULITS W. 2004. Molecular aspects of epithelial cell plasticity: implications for local tumor invasion and metastasis. *Mutat. Res*.
- GRÜNERT S, J. M., BEUG H. 2003. Diverse cellular and molecular mechanisms contribute to epithelial plasticity and metastasis. *Nat Rev Mol Cell Biol*.
- HAHN WC, W. R. 2002. Modelling the molecular circuitry of cancer. *Nat. Rev. Cancer*.
- HANAHAN D, W. 2000. The Hallmarks of Cancer. *Cell*.

- HILLEN W, B. C. 1994. Mechanisms underlying expression of Tn10 encoded tetracycline resistance. *Annual Review of Microbiology*.
- HILLEN W, G. C., ALTSCHMIED L, SCHOLLMEIER K, MEIER I. 1983. Control of expression of the Tn10-encoded tetracycline resistance genes. Equilibrium and kinetic investigation of the regulatory reactions. *J Mol Biol*.
- HOLCIK M, S. N. 2005. Translational control in stress and apoptosis. *Nat Rev Mol Cell Biol*.
- HUBER MA, B., H. WIRTH, T. 2004. Epithelial-mesenchymal transition: NF-kappaB takes center stage. *Cell Cycle*.
- HUBER MA, K., N. BEUG, H. 2005. Molecular Requirements for Epithelial-Mesenchymal Transition During Tumor Progression. *Curr. Opin. Cell Biol*.
- HUGO H, A. M., BLICK T, LAWRENCE MG, CLEMENTS JA, WILLIAMS ED, THOMPSON EW. 2007. Epithelial--mesenchymal and mesenchymal--epithelial transitions in carcinoma progression. *J of Cell Physiology*.
- JANDA E, L., G. GRUNERT, S. DOWNWARD, J. BEUG, H. 2002a. Oncogenic Ras/Her-2 mediate hyperproliferation of polarized epithelial cells in 3D cultures and rapid tumor growth via the PI3K pathway. *Oncogene*.
- JANDA E, L., K. KILLISCH, I. JECHLINGER, M. HERZIG, M. DOWNWARD, J. BEUG, H. GRUNERT, S. 2002b. Ras and TGF $\beta$  cooperatively regulate epithelial cell plasticity and metastasis: dissection of Ras signaling pathways. *J Cell Biol*.
- JECHLINGER M, G., S. BEUG, H. 2002. Mechanisms in epithelial plasticity and metastasis: insights from 3D cultures and expression profiling. *J Mammary Gland Biol Neoplasia*.
- JECHLINGER M, G., S. TAMIR, I. H. JANDA, E. LUDEMANN, S. WAERNER, T. SEITHER, P. WEITH, A. BEUG, H. KRAUT, N. 2003. Expression profiling of epithelial plasticity in tumor progression. *Oncogene*.
- JOAN MASSAGUÉ. 2008. TGF $\beta$  in cancer. *Cell*.
- KAPASI P, C. S., VYAS K, BAUS D, KOMAR AA, FOX PL, MERRICK WC, MAZUMDER B. 2007. L13a blocks 48S assembly: role of a general initiation factor in mRNA-specific translational control. *Mol Cell*.
- KARNOUB AE, W. R. 2008. Ras oncogenes: split personalities. *nature reviews molecular cell biology*.
- KLANN E, D. T. 2004. Biochemical mechanisms for translational regulation in synaptic plasticity. *Nat Rev Neurosci*.
- LAWLOR MA, A. D. 2003. Targeting the PI3K-Akt pathway in human cancer: Rationale and promise. *Cancer Cell*.
- LEE JM, D. S., KALLURI R, THOMPSON EW. 2007. The epithelial-mesenchymal transition: new insights in signaling, development, and disease. *J. of Cell Biology*.
- LODISH H, B. A., MATSUDAIRA P, . 2004. Molecular Cell Biology.
- MACKENZIE NC, R., E. 2006. Found in translation: A new player in EMT. *Dev Cell*.
- MASSAGUE J. 2000. Controlling TGF $\beta$  signaling. *Genes Dev*.
- MAZUMDER B, S. V., FOX PL, . 2003. Translational control by the 3'-UTR: the ends specify the means. *Trends Biochem Sci*.
- McKAY MM, M. D. 2007. Integrating signals from RTKs to ERK/MAPK. *Oncogene*.
- MEIJER HA, T. A. 2002. Control of eukaryotic protein synthesis by upstream open reading frames in the 5'-untranslated region of an mRNA. *Biochem J*.
- MIKULITS W, P.-B. B., HABERMANN B, BEUG H, GARCIA-SANZ JA, MÜLLNER EW. 2000. Isolation of translationally controlled mRNAs by differential screening. *FASEB J*.
- NELSON JA, R.-K. C., SMITH BA. 1987. Negative and positive regulation by a short segment in the 5'-flanking region of the human cytomegalovirus major immediate-early gene. *Mol Cell Biol*.
- OFT M, P., J. RUDAZ, C. SCHWARZ, H. BEUG, H. REICHMANN, E. 1996. TGF $\beta$ 1 and Ha-Ras collaborate in modulating the phenotypic plasticity and invasiveness of epithelial tumor cells.

- PILIPENKO VV, R., A. CHOO, D. I. GREINWALD, J. H., JR. 2004. Genomic organization and expression analysis of the murine Fam3c gene. *Gene*.
- POSTLE K, N. T., BERTRAND KP. 1984. Nucleotide sequence of the repressor gene of the TN10 tetracycline resistance determinant. *Nucleic Acids Res*.
- RAJALINGAM K, S. R., RAPP UR, ALBERT S. 2006. Ras oncogenes and their downstream targets. *Biochim Biophys Acta*.
- RAY PS, F. P. 2007. A post-transcriptional pathway represses monocyte VEGF-A expression and angiogenic activity. *Embo*.
- REICHMANN E, B. R., GRONER B, FRIIS RR. 1989. New mammary epithelial and fibroblastic cell clones in coculture form structures competent to differentiate functionally. *J Cell Biol*.
- REICHMANN E, S. H., DEINER EM, LEITNER I, EILERS M, BERGER J, BUSSLINGER M, BEUG H. 1992. Activation of an inducible c-FosER fusion protein causes loss of epithelial polarity and triggers epithelial-fibroblastoid cell conversion. *Cell*.
- REPASKY GA, C. E., DER CJ. 2004. Renewing the conspiracy theory debate: does Raf function alone to mediate Ras oncogenesis? *Trends in Cell Biology*.
- SCHUBBERT S, S. K., BOLLAG G. 2007. Hyperactive Ras in developmental disorders and cancer. *Nat Rev Cancer*.
- SEMLER BL, W. M. 2007. IRES-mediated pathways to polysomes: nuclear versus cytoplasmic routes. *Cell*.
- SPORN MB. 1969. The war on cancer. *Lancet*.
- THIERY JP. 2002. Epithelial-mesenchymal transitions in tumour progression. *Nat Rev Cancer*.
- THIERY JP, S. J. 2006. Complex networks orchestrate epithelial-mesenchymal transitions. *Nat Rev Mol Cell Biol*.
- WAERNER T, A., M. TAMIR, I. OBERAUER, R. GAL, A. BRABLETZ, T. SCHREIBER, M. JECHLINGER, M. BEUG, H. . 2006. ILEI: a cytokine essential for EMT, tumor formation, and late events in metastasis in epithelial cells. *Cancer Cell*.
- WAKEFIELD LM, R. A. 2001. TGF $\beta$  signaling: positive and negative effects on tumorigenesis. *Current Opinion in Genetics & Development*.
- YAO F, S. T., WINKLER T, LU M, ERIKSSON C, ERIKSSON E. 1998. Tetracycline repressor, tetR, rather than the tetR-mammalian cell transcription factor fusion derivatives, regulates inducible gene expression in mammalian cells. *Hum Gene Ther*.
- ZHAO J, B. R. 1995. Regulation of Transforming Growth Factor  $\beta$ 3Receptors in H-ras Oncogene transformed Rat Intestinal Epithelial Cells'. *Cancer Res*.
- ZHU Y, X., G. PATEL, A. MCLAUGHLIN, M. M. SILVERMAN, C. KNECHT, K. SWEITZER, S. LI, X. McDONNELL, P. MIRABILE, R. ZIMMERMAN, D. BOYCE, R. TIERNEY, L. A. HU, E. LIVI, G. P. WOLF, B. ABDEL-MEGUID, S. S. ROSE, G. D. AURORA, R. HENSLEY, P. BRIGGS, M. YOUNG, P. R. . 2002. Cloning, expression, and initial characterization of a novel cytokine-like gene family. *Genomics*.

**CURRICULUM VITAE**

**Name:** Susanne Sölch

**Geburtstag:** 16.10.1980

**Geburtsort:** München

**Staatsbürgerschaft:** Deutsch

**Ausbildung:**

1987 - 1991	Primary school
1991 - 1993	Hauptschule Glonn
1993 - 1997	Dr. Wintrich Realschule, Ebersberg: Mittlere Reife
1997 - 1999	Dr. Erwin Elhard Chemieschule, München: Abgeschlossene Berufsausbildung als CTA
1999 - 2001	Berufsoberschule, München: Fachhochschulreife und Fachgebundene Hochschulreife
2001 - 2004	Studium der Chemie an der Universität Regensburg: Vordiplom
2004 - 2008	Studium der Chemie an der Universität Wien Hauptfach Biochemie Nebenfächer Analytische Chemie und Organische Chemie
2007	Diplomarbeit am Institut für Molekulare Pathologie (IMP), bei Prof. Dr. H. Beug in Wien Thema: Analysis of the function and translational regulation of ILEI, an essential cytokine in tumorprogression